STATISTICAL MECHANICS FOR WIRELESS SYSTEMS: APPLICATION OF EXCLUSION PROCESSES TO THE MODELING AND ANALYSIS OF MULTIHOP NETWORKS

A Dissertation

Submitted to the Graduate School
of the University of Notre Dame
in Partial Fulfillment of the Requirements
for the Degree of

Doctor of Philosophy

by

Sunil Srinivasa

Martin Haenggi, Director

Graduate Program in Electrical Engineering
Notre Dame, Indiana
September 2011

STATISTICAL MECHANICS FOR WIRELESS SYSTEMS: APPLICATION OF EXCLUSION PROCESSES TO THE MODELING AND ANALYSIS OF MULTIHOP NETWORKS

Abstract

by

Sunil Srinivasa

This thesis focuses on the modeling and analysis of wireless multihop networks, employing a combination of ideas from a well-known tool in stochastic geometry, namely the Poisson shot noise theory and an unfamiliar concept in statistical mechanics, namely the totally asymmetric simple exclusion process (TASEP).

We begin our study by considering the simplest wireless multihop network topology - the line network, where the source, destination and all the relays are located in a collinear fashion. First, we propose a simple buffering and transmission scheme for wireless line networks which not only guarantees packet delivery but also helps keep packet delays small whilst regulating the flow of packets in a completely decentralized fashion. Second, we characterize the end-to-end delay distribution and achievable throughput of the wireless multihop line network for two different channel access schemes, randomized-TDMA and ALOHA. Additionally, we use our results to provide some useful design insights in long line networks.

Next, we consider a more intricate network topology comprising an infinite number of source-destination flows and analyze design-level issues such as determining the optimum density of transmitters or the optimal number of hops along

a flow that maximizes the throughput performance of the network. We also consider several other complex topologies comprising intersecting flows and propose the partial mean-field approximation (PMFA), an elegant technique that helps tightly approximate the throughput (and end-to-end delay) of such systems. We then demonstrate via a simple toy example that the PMFA procedure is quite general in that it may be used to accurately evaluate the performance of multihop networks with arbitrary topologies.

Finally, we identify that when reliable delivery of packets is not very critical, a viable solution towards balancing end-to-end delay and reliability in multihop networks is to have the nodes forcibly drop a small fraction of packets. Based on this principle, we present an analytical framework that helps quantify the throughput-delay-reliability performances of the ALOHA multihop network. We find that while in the noise-limited regime, dropping a small fraction of packets in the network leads to a smaller end-to-end delay at the cost of reduced throughput, in the interference-limited scenario, dropping a few packets in the network can sometimes help mitigate the interference in the network leading to an increased throughput.

We intend to promote TASEPs as a powerful tool to analyze the performance of multihop networks and hope that this introductory work instigates interest in solving other relevant wireless networking problems employing ideas from statistical mechanics.

To the last four years

of hard work and frolic

CONTENTS

FIGURES

ACKNOWLEDGMENTS

There are a number of people I wish to thank for making my experience as a graduate student one of the most rewarding periods of my life. First off, I would like to sincerely thank my advisor Dr. Martin Haenggi for his continual support and guidance over the past six years. His seemingly boundless energy, encouragement, and loyalty to students has been truly inspirational. Dr. Haenggi always showed great faith in my abilities and allowed me to work independently, but at the same time, listened patiently to my ideas and provided invaluable advice at the necessary times. Without his support and guidance, this work could not have been accomplished. Indeed, I couldn't have asked for a better advisor.

I would like to thank Drs. Thomas Fuja, Ken Sauer and Paolo Minero for having found some time out of their busy schedules to be on the committee for my doctoral defense. I also thank them for their feedback, comments and corrections to this thesis.

I would like to thank my labmates, in particular, Sundaram Vanka and Radha Krishna Ganti. All the intellectual discussions we had over the years have helped strengthen the basics of my subject areas, and have been immensely useful towards shaping up this work. I would also like to extend my gratitude to several other groupmates (present and past) – Daniele Puccinelli, Min Xie, Kostas Stamatiou, Chia-han Lee, Peter Vizi, David Tisza, Zhenhua Gong, Xinchen Zhang and Zhen Tong for their helpful criticism and suggestions from time to time during my Ph.D.

Thank you, guys!

I am extremely fortunate to have had a plentiful of close friends at Notre Dame. I thank them all for making my stay here a very memorable and fun-filled one – seems like my six-year stay at Notre Dame passed by in an eyewink. I start off by heartily thanking Darshana Patel, Rashi Talwar, Shashank Maiya and Krishnan Padmanabhan for masterminding the awesom'est 28th birthday that one could have asked for, and making me feel so special. I would also really like to extend my thanks to several other colleagues – Utsaw, Vel, Sachi, Suu, Danny, the Chetwanis, the Chandrahases, the Tiwaris, the Tripathis, the Attarwalas, the Deshlahras, Seemit, Vaibhav, Surya, Suraj, Priyam, Shailaja, Buddika, Jai, Mehrdad, Nikhil, Shyam, Mallu, VJ, Sajid, Sai, Srinath, Sutar, Mahesh, Amit and Amol - for all the fun social times that I have had. Rosemary 1532C, you will be sorely missed :(!

I would like to offer my gratitude to all those who helped me forward my resume during my job-hunting phase. Special thanks to Amaresh Malipatil and Shiva Kotagiri for forwarding my resume at LSI Corporation. I look forward to working with you two. Bay Area, here I come!

Finally, I shall forever be grateful to my parents, Mr. C. S. Srinivasa Murthy and Mrs. Aruna Murthy, and brother, Sudhir Srinivasa. Needless to say, this work could not have been completed without their unconditional support, constant deep love and boundless encouragement. I am really lucky to have you all in my life, and can't thank you enough. Also, thanks to Skype^{TM} and magicJack, I never really felt "away" from home!

CHAPTER 1

INTRODUCTION

1.1 Motivation and Related Work

The past few years have witnessed a surge of revolutionary research developments in the area of wireless communications and networking. Notable contributions include the near-capacity-achieving LDPC and turbo codes, which have now become a standard in the developing market for highly efficient transmission schemes, and technical breakthroughs such as CDMA, OFDM, and MIMO that have brought completely new perspectives on how to intelligently communicate over wireless channels. Such advances in information theory and communication theory have significantly helped further wireless systems' performance in a very short span of time and have provided the thrust for the rapid evolvement of high-rate data communication. Despite these advancements, we are only very gradually evolving from the era of tetherless connectivity predominated by systems with a single-hop architecture such as centralized cellular networks and WLANs to the era of ubiquitous wireless connectivity, that are also expected to subsume systems with multihop architecture such as ad hoc [1] and multihop cellular [2] networks.

Wireless multihop networks are decentralized: they do not rely on pre-existing infrastructure and are typically formed by deploying nodes that possess self-organizing capabilities. In other words, the nodes handle the necessary control

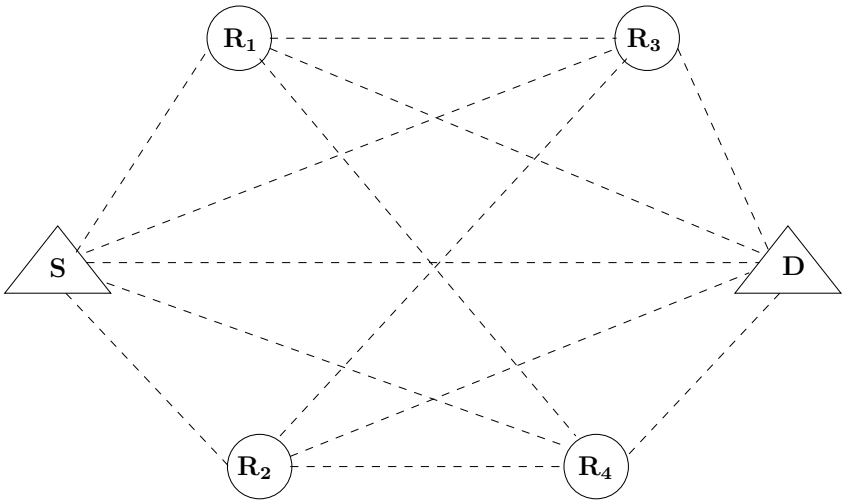

Figure 1.1: A multihop network with a single source S, a single destination D and four potential relays (R_1, R_2, R_3 and R_4).

and networking tasks by themselves (generally via the use of distributed control algorithms), thus facilitating "anywhere, anytime communication". Due to the stringent energy constraint in these devices, a natural communication strategy to conserve battery life is to reduce the range of transmission and employ *multihop routing*[1], wherein relays assist in the delivery of packets from the source to the destination. Thus, in general, multihop networks comprise multiple (concurrent) multihop flows across several source-destination pairs.

A simple multihop network with a single source and a single destination is illustrated in Figure 1.1. One possible route[2] from S to D occurs across relays R_2 and R_3, i.e., S $\rightarrow$ R_2 $\rightarrow$ R_3 $\rightarrow$ D).

Multihop networks are highly appealing for several reasons such as being rapidly deployable and reconfigurable, and lacking single points of failure compared to traditional network architectures, such as cellular networks and WLANs.

[1] And hence the name, multihop networks.

[2] This is an example of a three-hop transmission.

Besides extending network coverage and reducing the per-node power consumption, they also provide other benefits such as simplifying maintenance and decreasing the load off end users. Immediate applications of multihop networks include emergency and battlefield networks, metropolitan mesh networks for broadband internet access, and sensor networks. Unfortunately, however, the lack of a *capacity theory* capable of quantifying the performance of a general multihop network has stunted its development and commercialization [3]. We identify three roadblocks in this regard.

First, while classical information theory has been extremely successful for studying point-to-multipoint links, it is not (and may never be) developed enough to characterize the intricacies of multipoint-to-multipoint networks that arise due to the inherent interactions between nodes – a network with N devices comprises $N(N-1)$ possible one-way connections (not including multicasting). In fact, the capacity of a network with just $N = 3$ nodes is still an open problem, owing to the difficulties in modeling the interactions between the six possible one-way links [4; 5]. In multihop networks, N can be of the order of tens or hundreds or even thousands, and all the links are time-varying. On account of such intricate interactions, multihop networks evade familiar link-based decompositions; studying them using traditional methods such as information theory becomes intractable and hence has yielded little in the way of results.

Second, the multihop nature of packet transmissions causes interweaving of traffic flows, resulting in strong correlations, or interdependencies between the activities of the nodes. For instance, since a traffic flow is relayed across several hops, the packet arrival processes at the nodes (and hence, the departure processes) are coupled with each other. Thus, the end-to-end delay in multihop networks, de-

termined by the joint distribution of the successive delays of a packet traversing multiple nodes may hardly be expressed in a product-form. Likewise, owing to the existence of relay nodes that serve multiple packet flows, the throughputs of the various flows in the network are correlated with each other. Queueing theory has proven to be particularly useful for studying systems with such intricate interactions, but the analysis gets very cumbersome as the network size grows.

Third, in order to optimize the performance of energy-limited multihop networks, a cross-layer design needs to be adopted wherein the interdependencies among the layers of the protocol stack must be taken into account [6]. For example, the most energy-efficient routing protocol in a sensor network may use a centrally-located sensor to forward packets from other sensors. However, the battery of this sensor may then be exhausted quickly, which is undesirable from an application layer standpoint. Likewise, suppose that the physical layer dictates data to be transmitted at a low rate. This will clearly impact the MAC protocol and also the application. Thus, each layer of the protocol stack must respond to local variations and information from other layers, which forms the biggest hurdle in adaptive protocol design. Furthermore, the design approach needs to be adaptive to changes in the environment (which can easily happen due to node mobility) and thus is quite a challenging task.

The development of a novel, accurate and robust capacity theory for wireless multihop networks is one of the most difficult and important problems, and has major ramifications on the field of wireless communications and networking. Meeting this challenge requires new ideas, new tools, and a willingness to think outside the confines of conventional information theory. In view of these challenges, researchers are turning to other branches of study to obtain ideas and

methodologies that help better understand and characterize the dynamical behavior of wireless networks. Using analogous concepts from other subject areas has considerably enhanced our understanding of wireless networks and has helped further the research in the multihop networking community.

Of late, statistical physics has, in particular, captured the attention of the research community since it contains a rich collection of mathematical tools and methodologies for studying interacting many-particle systems, Methodologies such as the mean field theory has been successfully applied to study coding over multiuser MIMO channels [7; 8]. In [9], the authors use ideas such as the replica method to characterize the performance of multiuser detection in CDMA. The statistical mechanics of interfering transmissions in wireless networks has been studied in [10]. Tools from statistical physics have also been successfully applied to study interesting problems in random communication networks such as percolation, connectivity and capacity [11].

Since the performance of wireless networks depends critically on their spatial configuration, stochastic geometry and random graph theory [12]-[15] have also been indispensable tools towards the analysis of multihop networks. They have allowed for analytical results on a number of concrete and important problems. The delay and throughput performances for multihop networks in the presence of a Poisson field of interferers is quantified in [16; 17]. In [18], the authors have introduced the notion of random access transport capacity, which quantifies the bits per second that can be reliably communicated over some distance in the network.

Despite employing such ideas from other subject areas, researchers have however, fallen short of being able to tackle the problem at hand in its generality;

optimal ways of designing and operating multihop networks are known only for a few specific and/or oversimplified cases. Moreover, the analysis is often cumbersome and not scalable with the size of the network[3]. Motivated thus, we employ a combination of tools from stochastic geometry (namely, the Poisson shot noise theory [25]), and statistical mechanics (namely, the totally asymmetric simple exclusion process (TASEP) [26]) to analyze general multihop networks. Our work has the advantage that it allows for a clean, yet rigorous analysis, and provides results that are scalable with the number of nodes in the network; thus it provides useful insights into the design of wireless networks. Also, the framework is quite general in that it may be employed to study multihop networks with arbitrary topologies.

1.2 Organization of the Thesis

The detailed organization of the thesis is as follows.

In Chapter 2, we analyze the simplest type of wireless network topology, namely the multihop line network where the source, destination and relays are all located on a line. First, we propose a simple buffering and transmission scheme for wireless line networks, which not only guarantees delivery and helps keep packet delays in the network minimal but also helps regulate the flow of packets in a completely distributed fashion. We then use a combination of ideas from statistical mechanics and stochastic geometry to characterize the end-to-end delay and achievable throughput of the wireless multihop line network for two different channel access schemes. Additionally, we use our results to provide some useful

[3]An exception in this regard is the myriad of work on scaling laws for wireless networks (see for e.g. [19]-[24]). These, however, only provide a high-level insight on how different networking scenarios and approaches operate, but do not provide exact expressions for the "preconstants", which is where nearlly all the impact of any network design resides.

design insights in line networks. This work has been published in parts, in [27], [28].

In Chapter 3, we consider a more complex network model – a two-dimensional multihop network comprising several source-destination pairs, each communicating wirelessly in a multihop fashion. We then characterize the per-flow throughput and end-to-end delay performances for a typical flow in this 2-D wireless network, for two different channel access mechanisms. Our study offers valuable insights from a system design stand-point such as determining the optimum density of transmitters or the optimal number of hops along a flow that maximizes the system's throughput. We corroborate our theoretical analyses via simulations. This work has been published in [29].

In Chapter 4, we analyze multihop networks with complex topologies. In particular, we consider network models comprising intersecting flows, and propose the partial mean-field approximation (PMFA), an elegant technique that helps tightly approximate the throughput (and end-to-end delay) performance of the system. Moreover, we demonstrate via a simple example that the PMFA procedure is quite general in that it may be used to accurately evaluate the performance of multihop networks with arbitrary topologies. This work has been published in [28].

In Chapter 5, we characterize the throughput-delay-reliability (TDR) tradeoffs of the ALOHA-based multihop network. Specifically, we present an analytical framework that helps quantify the TDR performances of the system. We find that while in the noise-limited regime, dropping a small fraction of packets in the network leads to a smaller end-to-end delay at the cost of reduced throughput, in the interference-limited scenario, dropping a few packets in the network can help

mitigate the interference in the network leading to an increased throughput. We also present some empirical (simulation-based) results which closely match the values obtained analytically. This work has been published in [30].

CHAPTER 2

THE MULTIHOP WIRELESS LINE NETWORK

2.1 Introduction

In this chapter, we begin our analysis by focusing on the simplest type of wireless network topology, namely the multihop line network where the source, destination and relays are all located in a collinear fashion. Our contribution is two-fold:

First, we propose a simple buffering and transmission scheme for multihop wireless line networks, which not only guarantees packet delivery but also helps keep packet delays small whilst helping regulate the flow of packets in a completely decentralized fashion. Second, using a combination of ideas from statistical mechanics and stochastic geometry, we characterize the end-to-end delay and achievable throughput of the wireless multihop line network employing the revised buffering policy for two different channel access schemes. Additionally, we employ our findings to provide useful design insights in long wireless line networks.

The rest of this chapter is organized as follows. Section 2.2 describes the system considered and the channel model. Section 2.3 introduces a novel transmission policy that helps regulate traffic in the line network in a completely decentralized fashion. Section 2.4 introduces the statistical mechanics-based tool that we use for our analysis. Section 2.5 discusses prior work. Section 2.6 characterizes the

throughput and delay for the wireless line network for two different channel access schemes. Section 2.7 concludes the chapter.

2.2 System Model

We consider a multihop wireless line network (see Figure 2.1) with a unidirectional data flow from the leftmost to the rightmost node. The source node S is numbered 0 and generates packets of fixed length at a constant rate. We also take that the source node is backlogged, i.e., it always has packets to transmit. The network contains N relay nodes (numbered 1 through N) and a destination D, numbered $N+1$. Throughout this chapter, we also take that the physical arrangement of nodes is regular (on a lattice grid) with a separation of d between any pair of adjacent nodes. Time is slotted to the duration of a packet, transmission attempts occur at slot boundaries, and each transmitting node transmits at unit power.

We assume that all the nodes in the network use the same channel; thus, simultaneous transmissions cause interference between links. We take the attenuation in the channel to be modeled as the product of a Rayleigh fading component and the large-scale path loss component with exponent γ. The noise in the network is taken to be AWGN with variance N_0. We define the transmission from node i to target node j to be successful if the (instantaneous) signal-to-interference-and-noise ratio (SINR) at j is greater than a predetermined threshold Θ; the probability of successful reception[1] is denoted by $p_s = \Pr[\text{SINR} > \Theta]$. Note, however, that this transmissions can occur only when there is space left in j's buffer. In Figure 2.1, node $N-1$ cannot accept any more packets from node $N-2$ since

[1] In this chapter, we only consider scenarios wherein the reliabilities across each link is the same; we thus drop the dependence of p_s on i or j.

its buffer is full.

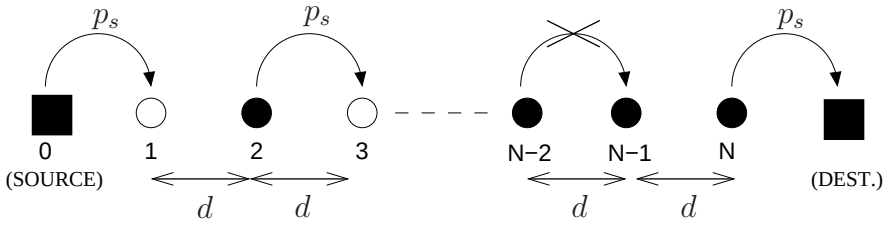

Figure 2.1. A regular linear multihop network topology. The source (node 0) attempts to deliver packets to the destination via N relays. Filled circles indicate filled buffers, while empty circles indicate buffers with room for accepting more packets. The hopping probability across each node is p_s.

2.3 A Revised Transmission Policy for Multihop Networks

Despite being decentralized, multihop networks are not just intended to carry small volumes of data in an energy-efficient manner, but may also be used to provide broadband services under QoS constraints, for example in mesh networks [31]. However, as reported in [32]-[34], existing buffering schemes for multihop wireless networks involving large buffer sizes and a drop-tail policy have certain inherent drawbacks such as buffer overflows, excessive queueing delays and scheduling issues resulting in uncoordinated transmissions. Consequently, the end-to-end delay and throughput performance in such systems is disappointing.

To overcome these shortcomings, we propose the following novel transmission

policy for the linear flow in the network characterized by the following two rules.

1. All the buffering in the network is performed at the source node, while each relay node has a buffer size of unity. Thus, all the queueing occurs at the source node, while relay nodes may hold at most one packet.

2. Transmissions are not accepted by relay nodes if their buffer already contains a packet. Furthermore, packets are retransmitted until they are successfully received. In other words, the network reliability is kept at 100%; packet delivery is guaranteed.

Rule 1 ensures that nodes have at most one packet in their buffer and is favorable for the following reasons.

- First, keeping buffer sizes small can prevent the mean and the variance of the *in-network* end-to-end delay both from getting excessive[2]. Indeed, when buffer capacities are large, several packets may get stacked up, especially when the link quality is poor, thus transportation of packets across the links get delayed. Figure 2.2 plots the empirical mean and variance of the end-to-end delays for CSMA (Carrier Sense Multiple Access)- and ALOHA-based flows for some values of the relays' buffer capacities (denoted by K). In both cases, notice the increase in the mean and the variance of the end-to-end delay with increasing buffer size, in particular at small values of the link reliability p_s. Conversely, the packet delays are much more tightly

[2]In this thesis, we neglect the queueing delay at the source. It is possible that queueing up of packets at the source may lead to a larger *total* end-to-end delay (counted from the time the packet is generated), in particular, when the relays' buffer sizes are small. The advantage of the single-buffer scheme predominates in applications such as sensing and monitoring, wherein the source node can decide to drop older packets, and retain only the most recent packet(s). In such cases, the queueing delay at the source is minimal; the in-network delay is drastically reduced with decreasing buffer sizes (as seen in Figure 2.2).

controlled when the buffer sizes are smaller. Thus, depending on the time a packet spends in its buffer, the source node can judiciously decide whether to drop it (and replace it with a more recent packet).

- Second, employing single-sized buffers can also help lessen estimation errors in networked control systems. This is quite critical in applications such as monitoring physical or environmental conditions, or battlefield surveillance.

  To this end, consider a process evolving as

$$x[k+1] = Ax[k] + w[k], \quad k \in \mathbb{Z}^+,$$

  where $x[k] \in \mathbb{R}^n$ is the process state and $w[k]$ is the process noise assumed to be AWGN with covariance R_w. The process state is observed using a sensor that generates measurements, or observations, of the form

$$y[k] = Cx[k] + v[k], \quad k \geq 0,$$

  where $y[k] \in \mathbb{R}^m$ and the measurement noise $v[k]$ is also AWGN with a positive definite covariance matrix Σ_v. We assume that the pair (A, C) is observable. Considering the optimal encoder and decoder designs described in [36], the estimation error covariance at time slot k becomes

$$\text{Error}[k] = \sum_{m=-1}^{k} \Pr(t_s(k) = m) f_{k-m}(M(m+1)), \tag{2.1}$$

  where $f(S) = ASA^T + R_w$ is the *Lyapunov recursion* [36], and $t_s[k] = m$ denotes the event that $m \leq k$ packets are received by time slot k.

  Figure 2.3 plots the time evolution of the error covariance (of the estimated

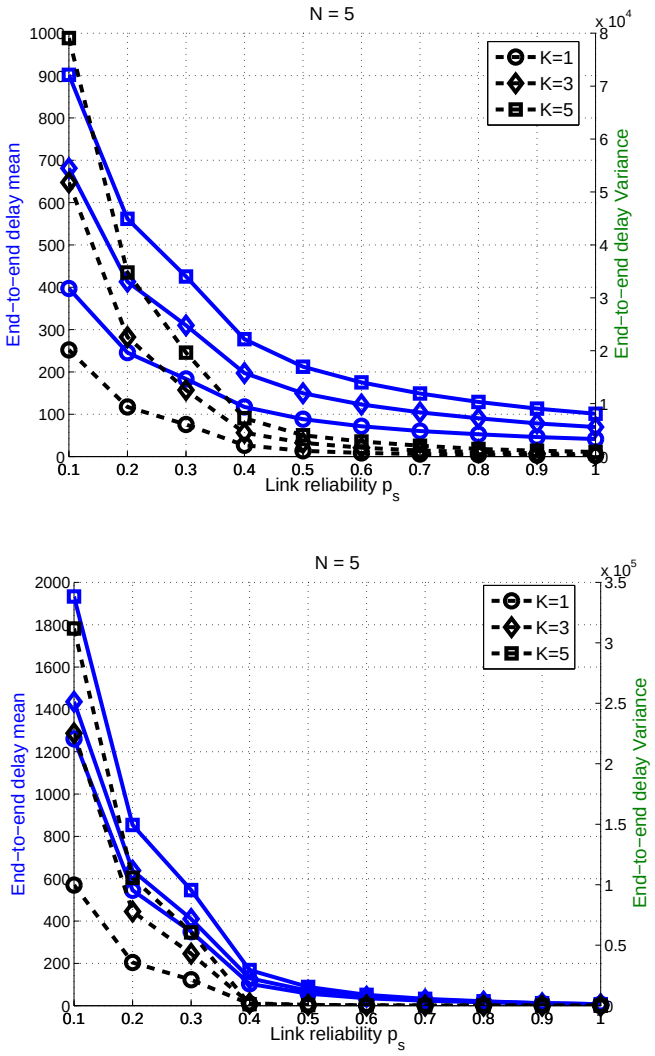

Figure 2.2. Empirical values of the mean (solid lines) and variance (dashed lines) of the end-to-end delay in CSMA-(top) and ALOHA-based (bottom) wireless flows versus the link reliability and buffer size at nodes. In each case, we see that the larger the buffer capacities of the nodes, the higher are the delay mean and variance.

state values) for a CSMA-based flow. We clearly observe that the fastest convergence is obtained for the case $K = 1$; the rate of convergence decreases with increasing buffer size. In essence, the in-network delay for the single-buffer network is the smallest, thus the decoder has access to more observations, and can perform a better estimation of the process states. The same qualitative behavior is expected for the ALOHA-based network as well.

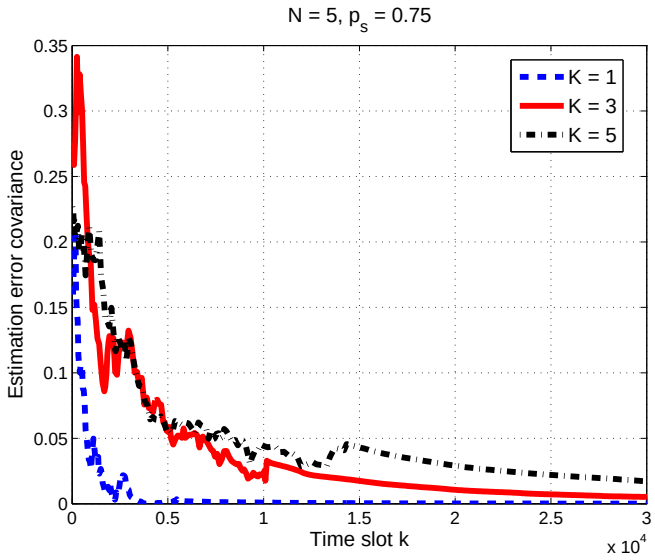

Figure 2.3. Error covariance of the estimates for the CSMA-based flow for different values of buffer sizes K. It is clearly seen that the estimation error converges to its steady state value faster for the single-buffer system.

- Third, large buffers increase hardware cost and energy consumption.

Using Rule 1 alone may lead to a loss in throughput due to dropped packets; Rule 2 is needed mainly to reduce interference and consequently keep the number of failed transmissions small. In fact, Rules 1 and 2 together mean that a successful transmission can occur only when a node has a packet to transmit and its target node has an empty buffer. This is a distributed method to prevent packets from getting too closely spaced and ensure spacing between packets in the network, which is essential for the efficient operation of wireless systems that are subject to interference. Together, the rules help efficiently regulate the flow of traffic in the network in a completely distributed fashion. The revised transmission scheme also intrinsically enforces congestion control and works similar to reactive back-pressure algorithms [35] wherein the load at each server is balanced dynamically based on the states of upstream and downstream queues.

We now introduce the reader to TASEP, a subject area in statistical mechanics which we extensively use for our analysis of multihop wireless networks.

2.4 The Totally Asymmetric Simple Exclusion Process (TASEP)

The TASEP refers to a family of simple stochastic processes used to describe the dynamics of self-driven systems with several interacting particles (such as the kinetics of biopolymerization and traffic) and is a paradigm for non-equilibrium systems [26]. The classical 1D TASEP model with open boundaries is defined as follows. Consider a system with $N + 1$ sites, numbered 0 to N. Site 0 is taken to be the source that injects particles into the system. The model is said to have open boundaries, meaning that particles are injected into the system at the left boundary (site 1) and exit the system on the right boundary (site N). The *configuration* of site i, $1 \leq i \leq N$ at time t is denoted by $\tau_i^{(N)}[t]$ (or simply by

$\tau_i[t]$), which can only take values in $\{0, 1\}$, i.e., each site $1 \leq i \leq N$ may either be *occupied* (denoted as $\tau_i[t] = 1$) or *empty* (denoted as $\tau_i[t] = 0$). The source, however, is taken to be always occupied ($\tau_0[t] \equiv 1, \forall t > 0$). Also, at $t = 0$, all sites other than the source are empty ($\tau_i[0] = 0, 0 < i \leq N$).

In the discrete-time version of the TASEP, the movement of particles is defined to occur in time steps. Specifically, let $(\tau_1[t], \tau_2[t], \ldots, \tau_N[t]) \in \{0, 1\}^N$ denote the configuration of the system in time slot t. In the subsequent time slot $t + 1$, a set of sites is chosen at first, depending on the *updating procedure* (which we describe shortly). Then, for every site chosen, if it contains a particle and the neighboring site on its right has none, then the particle hops from that site to its neighbor with a certain probability (which in general, is site-dependent). This way, the particles are transported from site 0 through the system until their eventual exit at site N. The movement of particles to the right is equivalent to the movement of *holes* (or empty sites) to the left. This *particle-hole symmetry* leads to some interesting system dynamics – as we shall see later, studying only the first $\lceil (N + 1)/2 \rceil$ sites is sufficient to characterize the system completely.

Mathematically, the evolution of the classical TASEP particle flow is defined as follows. Suppose that the i^{th} site is chosen in time slot t.
If $1 \leq i \leq N-1$, the particle on site i (if there is any) jumps to site $i+1$ (provided it is empty) with probability p. Accordingly,

$$\begin{aligned} \mathbb{P}(\tau_i[t+1] = 0) &= 1 - \tau_i[t](1 - p + p\tau_{i+1}[t]) \\ \mathbb{P}(\tau_i[t+1] = 1) &= \tau_i[t](1 - p + p\tau_{i+1}[t]) \end{aligned}$$

and

$$\begin{aligned}\mathbb{P}(\tau_{i+1}[t+1]=0) &= (1-\tau_{i+1}[t])(1-p\tau_i[t]) \\ \mathbb{P}(\tau_{i+1}[t+1]=1) &= p\tau_i[t]+\tau_{i+1}[t](1-p\tau_i[t]).\end{aligned}$$

If $i=0$, site 1 remains occupied at time $t+1$ if it was occupied at time t and gets occupied with probability αp if it was empty. Thus,

$$\begin{aligned}\mathbb{P}(\tau_1[t+1]=0) &= (1-\alpha p)(1-\tau_1[t]) \\ \mathbb{P}(\tau_1[t+1]=1) &= \alpha p+(1-\alpha p)\tau_1[t].\end{aligned}$$

If $i=N$, site N remains empty at $t+1$ if it was empty at time t, and gets emptied with probability βp if it was occupied, i.e.,

$$\begin{aligned}\mathbb{P}(\tau_N[t+1]=0) &= 1-(1-\beta p)\tau_N[t] \\ \mathbb{P}(\tau_N[t+1]=1) &= (1-\beta p)\tau_N[t]\end{aligned}$$

The quantities α, β and p may thus be regarded as the 'influx', and 'outflux' rates and the hopping probability, respectively. A snapshot of the TASEP system model is depicted in Figure 2.4.

The TASEP model is known to exhibit rich non-equilibrium behavior, even at steady state, where the rate of particle flow between any two adjacent sites is a constant. Here, the non-equilibrium nature of the model refers to the fact that the source and destination nodes are never at equilibrium, i.e., data always flows from the source node to the destination node. In this dynamical system, it is of interest to compute the steady state probabilities of the particle configurations,

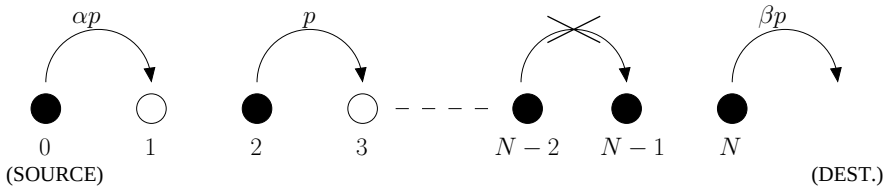

Figure 2.4. Snapshot of a TASEP system model along with the hopping probabilities. The source is numbered 0, and there are N other sites. Filled circles indicate occupied sites and the rest indicate holes. Jumping from site i is possible only if the configuration (τ_i, τ_{i+1}) is $(1, 0)$. In the above example, hopping is not possible between sites $N-2$ and $N-1$.

the occupancies of the sites and the rate of particle flow [37; 38]. The values of the aforementioned quantities, however, explicitly depend on the updating procedure, i.e., the order in which the spatio-temporal hopping, injection and removal of particles is performed. There are four basic and commonly considered TASEP updating procedures:

1. *Random-sequential update*: A site is randomly picked with a uniform probability of $1/(N+1)$ at each time step. Hopping is performed based on rules defined above with probabilities αp, βp and p for particles at sites $i = 0$, $i = N$ and $i \notin \{0, N\}$ respectively.

2. *Sublattice-parallel update*: Assume that the number of sites N is even. We first apply injection/removal rules to sites $0/N$ and also perform hopping on pairs $(2, 3)$, $(4, 5)$, and so on. In the subsequent time step, updating rules are applied to site pairs $(1, 2)$, $(3, 4)$, etc.

3. *Ordered-sequential update*: As the name suggests, this is a procedure where updating is performed in an orderly, sequential fashion. One usually starts

from the right end of the chain and updates the particle at node N. Then, the pairs $(N-1, N)$, $(N-1, N-2)$, and so on are updated until the left end of the chain (node 0) is reached. In this form of updating, a series of adjacent particles can all be transported sequentially, unlike the previous updating schemes.

4. *Parallel update*: The updating rules are simultaneously applied to all the sites, and in each time slot, all particles at sites that have an empty site to their right jump concurrently. This updating scheme is often used to model vehicular traffic flow and is a special case of the well-known Nagel-Schreckenberg model [39].

It is apparent from the description of the TASEP model that it exhibits a similarity to a flow in an multihop network. The sites can be taken to represent the relay nodes and the particles the packets. The hopping probability p is analogous to the link reliability p_s while the exclusion principle models the unit buffer size at the relay nodes. Also, the condition $\tau_0[t] = 1, \forall t$, models the fact that the source node is always backlogged. Figure 2.5 depicts the TASEP-equivalent network flow, wherein we assume that the source has a large buffer and regulates the packet flow into a TASEP model.

2.4.1 The Matrix Product Ansatz Formulation

The starting point for studying the stochastic one-dimensional TASEP model is to write down its *master equation*. Let $P(\boldsymbol{\tau}[t])$ denote the probability of finding the system in the configuration $\boldsymbol{\tau}[t] = (\tau_1[t], \tau_2[t], \ldots, \tau_N[t])$ in time slot t. The master equation describes the evolution of the system with time and takes the

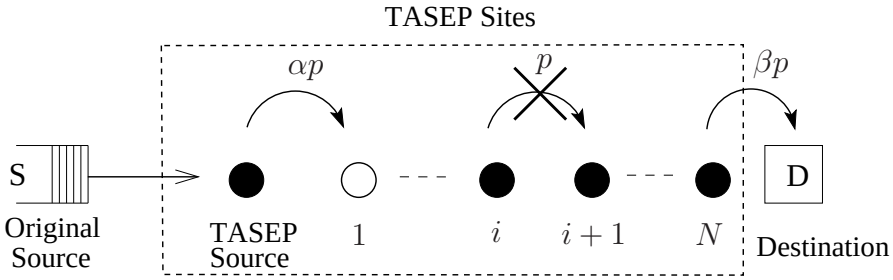

Figure 2.5. TASEP-equivalent network flow along with the (site-dependent) hopping probabilities αp, βp and p. The (backlogged) source node with a large buffer connected to the TASEP particle flow model with $N+1$ sites, each with a buffer size of unity.

form

$$\Delta P(\boldsymbol{\tau}[t]) = \sum_{\boldsymbol{\tau}'[t]} \left[\zeta\left(\boldsymbol{\tau}'[t], \boldsymbol{\tau}[t]\right) P\left(\boldsymbol{\tau}'[t]\right) - \zeta\left(\boldsymbol{\tau}[t], \boldsymbol{\tau}'[t]\right) P\left(\boldsymbol{\tau}[t]\right) \right],$$

where $\Delta P(\boldsymbol{\tau}, t) = P(\boldsymbol{\tau}[t+1]) - P(\boldsymbol{\tau}[t])$, and $\zeta(\boldsymbol{\tau}[t], \boldsymbol{\tau}'[t])$ denotes the rate of transition from $\boldsymbol{\tau}[t]$ to another configuration $\boldsymbol{\tau}'[t]$. For further details on the master equation and its formulation, we refer the reader to [26; 40].

As intuitively expected, in the long time limit ($t \to \infty$), the probability of finding the system in any configuration $\boldsymbol{\tau}$ becomes independent of t, i.e., $\lim_{t\to\infty} \Delta P(\boldsymbol{\tau}[t]) = 0$ (for each of the four updating procedures) [26]. The TASEP flow is then said to have reached a *steady state*. Solving for the steady state configuration probabilities is a formidable task which may be accomplished by considering recursion-based techniques on the system size N (see for e.g. [37; 38]). A more elegant and direct procedure however is to use a matrix product ansatz (MPA) [40], wherein the probability of each configuration at steady state is decomposed

into a product of matrices.

According to the MPA formulation [40], for each of the four updating procedures, the probability of finding the TASEP system in the configuration $\boldsymbol{\tau} = (\tau_1, \tau_2, \ldots, \tau_N)$ at steady state is independent of t and given by

$$P(\boldsymbol{\tau}) = \frac{\langle W| \prod_{i=1}^{N} (\tau_i D + (1-\tau_i)E)|V\rangle}{\langle W|C^N|V\rangle}, \tag{2.2}$$

where D and E are square matrices that operate on occupied and empty sites, respectively, $C = D + E$, and $|V\rangle$ and $\langle W|$ are column and row vectors respectively (represented here by the "ket" and "bra" notation). Evidently, the elements of the matrices and vectors depend strongly on the updating procedure, and in general, they are infinite-dimensional [26]. Nevertheless, the MPA provides an analytical framework for describing the asymmetric exclusion process in a completely algebraic manner. We will employ it extensively for our analysis, in particular in the Section 2.6.

2.5 Related Work

The delay and throughput performances of the classical TDMA, spatial TDMA, ALOHA and several other MAC schemes have been extensively studied for point-to-point links, often using queueing-theoretic approaches (e.g. [41], [42]). Queueing theory has also been used to characterize the throughput and delay performance of flows involving multiple hops (e.g. [43], [44]). However, such analyses are less tractable and often yield only approximate results. In order to circumvent these issues, authors have considered very small [45] or infinitely large [46] networks. Moreover, previous studies have either considered unlimited buffer capacities [47] or neglected queueing delays in the system [48], both of which are not

realistic assumptions. In this chapter, we use existing results from the TASEP literature to derive exact analytical results on the throughput and delay performance of wireless line networks with an arbitrary number of nodes. The TASEP-based framework also has the advantage of obviating the often unwieldy queueing theory-based analysis.

Since we consider relays with unit buffers, the queueing delays at the relay nodes are zero, and we only need to consider access and retransmission delays. The benefits of keeping relay buffer sizes equal to unity has been studied earlier in literature. [49] considers a buffering policy similar to the one described earlier in this chapter, and proposes several amendments to the MAC layer, such as the notion of shadow packets to stabilize the system and achieve the optimal throughput. In [50], the authors show that buffering and network coding implemented at the source node can lead to comparable packet drop rates as to buffering at every intermediate router. In the case of large networks with multiple links, the coding-based scheme can also provide buffer gains. In [51], it is proven that for a line network, the optimal scheduling algorithm that minimizes the end-to-end buffer usage gives preference to serving links closer to the destination. Hence, much of the buffering should occur at the source node.

2.6 Throughput and Delay Analysis for the Wireless Line Network

We study the delay and throughput performances of the wireless line network using ideas from the TASEP literature, for two analytically tractable MAC schemes in this chapter: *randomized TDMA (r-TDMA)* and *ALOHA*. They operate as follows.

- **r-TDMA**: r-TDMA is a modified version of the traditional TDMA MAC

scheme, wherein the transmitting node in each time slot is simply chosen uniformly randomly from the set of *all nodes in the network* instead of being picked in an deterministic fashion (as in conventional TDMA).

The r-TDMA scheme may also be viewed as a time-slotted version of the CSMA protocol since in each time slot, only a single transmitter node gains the right to access the wireless channel (or verifies the absence of other traffic before attempting to transmit over the channel). The only difference between slotted CSMA and r-TDMA is that in r-TDMA, nodes not having packets in their buffers may also be scheduled for transmission in some time slots. This, however, is equivalent to simply "stretching" the time axis. Also, note that the r-TDMA protocol does not entail spatial reuse. However, in small networks, spatial reuse is impractical, and the performance of the r-TDMA-based network is quite good (compared to other MAC schemes).

- **ALOHA**: In ALOHA, in every time slot, each node *having a packet* independently transmits with some (contention) probability q or remains idle with probability $1 - q$.

The r-TDMA and ALOHA schemes may be linked to the TASEP with random sequential and parallel updates. Throughout this thesis, we will only focus on these two updating procedures.

2.6.1 Throughput and Delay Analysis for the r-TDMA-based Line Network

In this section, we characterize the throughput and delay performances of the r-TDMA-based wireless line network. Additionally, we analytically derive (i) the probability mass functions (pmfs) of the delays incurred by packets at each node along the flow and (ii) the joint pmfs of the packet delays across adjacent nodes in

the line network. We also apply our findings to studying the interesting short-hop versus long-hop routing problem.

Since there is no interference in the r-TDMA-based network and the fading power is exponentially distributed, we obtain

$$p_s = \Pr[\text{SNR} > \Theta] = \exp\left(-\Theta N_0 d^\gamma\right). \tag{2.3}$$

Also, since the links are spaced equally, the success probability across any link is the same. This is equivalent to taking $\alpha = \beta = 1$, and $p = p_s$ in the corresponding TASEP model. Incidentally, at the operating point $\alpha = \beta = 1$, the network accepts as many packets as it can (when the first relay node's buffer is empty), and also provides the highest possible service rate[3].

We now provide some useful results from the TASEP literature with random sequential update. The first step is to establish the forms of the square matrices and vectors in (2.2). It is known [40] that in general, the matrices D, E and vectors V, W in (2.2) are all infinite-dimensional[4]. A convenient choice of the matrices and vectors (assuming $p > 0$) is [26]

$$D = \frac{1}{p}\begin{pmatrix} 1/\beta & \gamma_1 & 0 & 0 & \dots \\ 0 & 1 & 1 & 0 & \dots \\ 0 & 0 & 1 & 1 & \dots \\ 0 & 0 & 0 & 1 & \dots \\ \vdots & \vdots & \vdots & \vdots & \ddots \end{pmatrix},$$

[3]Equivalently, the rate of packet flow across the r-TDMA-based network is maximized when $\alpha = \beta = 1$.

[4]The only case for which the matrices are finite-dimensional (in fact, scalars) is when $\alpha+\beta = 1$ [40].

$$E = \frac{1}{p}\begin{pmatrix} (1-\alpha p)/\alpha & 0 & 0 & 0 & \dots \\ \gamma_2 & 1-p & 0 & 0 & \dots \\ 0 & 1-p & 1-p & 0 & \dots \\ 0 & 0 & 1-p & 1-p & \dots \\ \vdots & \vdots & \vdots & \vdots & \ddots \end{pmatrix} \tag{2.4}$$

with

$$\langle W| = (1,0,0,\dots) \quad \text{and} \quad |V\rangle = (1,0,0,\dots)^T,$$

where $(\cdot)^T$ denotes transpose. Here, γ_1 and γ_2 may be chosen so as to satisfy

$$\gamma_1\gamma_2 = \frac{1}{\alpha\beta p}[1-p-(1-\alpha p)(1-\beta p)].$$

When $\alpha = \beta = 1$ and $p = p_s$, we may take $\gamma_1 = 1$, and $\gamma_2 = 1 - p_s$ in (2.4) so that

$$D = \frac{1}{p_s}\begin{pmatrix} 1 & 1 & 0 & 0 & \dots \\ 0 & 1 & 1 & 0 & \dots \\ 0 & 0 & 1 & 1 & \dots \\ 0 & 0 & 0 & 1 & \dots \\ \vdots & \vdots & \vdots & \vdots & \ddots \end{pmatrix}, \quad E = D^T.$$

For these forms of matrices D and E, and vectors W and V, the following two properties hold:

$$C = D + E = p_s DE \tag{2.5a}$$

$$p_s^N \langle W|C^N|V\rangle := \eta(N) = \frac{(2N+2)!}{(N+2)!(N+1)!} \tag{2.5b}$$

While (2.5a) is straightforward to establish, (2.5b) is a consequence of [40, Eqns. 80,81]. We use these results in the remainder of this section.

2.6.1.1 Steady State Probabilities

Using (2.2) along with the forms of matrices and vectors discussed earlier, the steady state probabilities can be computed in a straightforward manner, in particular for small values of N. As examples, we have for $N = 1$,

$$P(0) = \frac{\langle W|E|V\rangle}{\langle W|C|V\rangle} = 1/2, \text{ and } P(1) = \frac{\langle W|D|V\rangle}{\langle W|C|V\rangle} = 1/2.$$

Likewise, using (2.5a) and (2.5b), one can also show for $N = 2$,

$$P(0,0) = P(0,1) = P(1,1) = 1/5, \text{ and } P(1,0) = 2/5.$$

2.6.1.2 Steady State Occupancies

Next, we compute the steady state *occupancy* of each node $0 \leq i \leq N$, defined as the probability that it is occupied at steady state, i.e., $\mathbb{P}(\lim_{t\to\infty} \tau_i[t] = 1)$. Hereafter, we use the simplified notation $\tau_i :\triangleq \lim_{t\to\infty} \tau_i[t]$ to denote the configuration of node i, $0 \leq i \leq N$ at steady state. From (2.2), we obtain the occupancy of node i to be

$$\mathbb{P}(\tau_i = 1) = \frac{\langle W|C^{i-1}DC^{N-i}|V\rangle}{\langle W|C^N|V\rangle}, \quad 0 \leq i \leq N.$$

Now, since τ_i can take values only in $\{0,1\}$, $\mathbb{P}(\tau_i = 1) = \mathbb{E}\tau_i$ and $\mathbb{P}(\tau_i = 0) = 1-\mathbb{E}\tau_i$. In other words, the occupancy of node i is the same as the average number of packets at the i^{th} node's queue. From [37, Eqn. 48], we have for $0 \leq i \leq N$,

$$\mathbb{E}\tau_i = \frac{1}{2} + \frac{1}{4}\frac{(2i)!}{(i!)^2}\frac{(N!)^2}{(2N+1)!}\frac{(2N-2i+2)!}{[(N-i+1)!]^2}(N-2i+1). \tag{2.6}$$

In particular, the values at the end nodes are

$$\mathbb{E}\tau_1 = \frac{3N}{2(2N+1)} \text{ and } \mathbb{E}\tau_N = \frac{N+2}{2(2N+1)}. \tag{2.7}$$

Surprisingly, the node occupancies are independent of p_s. Also, notice the particle-hole symmetry, i.e., $\mathbb{E}\tau_i = 1 - \mathbb{E}\tau_{N+1-i}$. Thus, the average number of occupied relays is

$$\sum_{i=0}^{N} \mathbb{E}\tau_i = 1 + N/2. \tag{2.8}$$

In a system with an odd number of relays, the middle relay has an occupancy of exactly $1/2$. Figure 2.6 shows the occupancies $\mathbb{E}\tau_i$ for a multihop network with $N = 10$ relay nodes. Also observe that the node occupancies monotonically

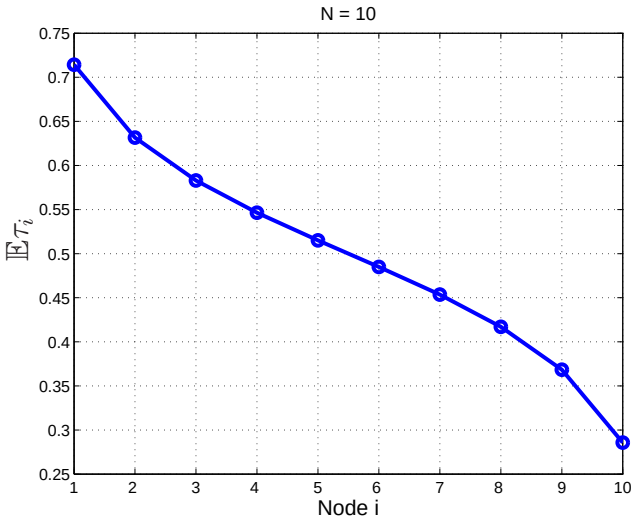

Figure 2.6. The steady state occupancy of each relay node for a r-TDMA-based multihop network with $N = 10$ relays. Notice the particle-hole symmetry, i.e., $\mathbb{E}\tau_i = 1 - \mathbb{E}\tau_{N+1-i}$.

decrease with proximity to the destination node. In other words, node 1 is the bottleneck node. This can be explained by noting that the destination is always willing to accept packets; thus the N^{th} relay node can empty its buffer at the highest rate. However, the $N-1^{\text{th}}$ relay needs the N^{th} relay to be empty to transmit its packet, so the likelihood that it will be occupied is higher when compared to node N, and so on.

2.6.1.3 Steady State Throughput

We now derive the throughput of the line network at steady state, defined as the average number of packets successfully delivered (to the destination) in a unit step of time.

Theorem 1. *For the r-TDMA-based line network with N nodes, the throughput at steady state is*

$$T = \frac{p_s(N+2)}{2(N+1)(2N+1)}. \tag{2.9}$$

Proof: At any instant of time, node N's buffer contains a packet w.p. τ_N; furthermore, it is picked for transmission w.p. $1/(N+1)$, and the transmission is successful w.p. p_s. Thus, the throughput of the line network is simply

$$T = p_s \mathbb{E}\tau_N/(N+1). \tag{2.10}$$

Using (2.6) in (2.10), we obtain the desired result. □

The system throughput at steady state is proportional to the link reliability and upper bounded by $p_s/4$, but decreases with increase in the system size: $T \sim p_s/(4N)$ for[5] $N \gg 1$. Also, since the reliability of the network is 100%, the rate of

[5]The notation $f(n) \sim g(n)$ means that the ratio $f(n)/g(n)$ approaches 1 asymptotically (as $n \to \infty$).

packets across each link is the same, and equal to (2.9). Noting that the probability that node i has a packet and node $i+1$ none is $\mathbb{P}(\tau_i = 1, \tau_{i+1} = 1) = \mathbb{E}[\tau_i(1-\tau_{i+1})]$, T may also be obtained using any of the $N+1$ equivalent expressions

$$T = p_s \mathbb{E}[\tau_i(1 - \tau_{i+1})]/(N+1), \tag{2.11}$$

which is equivalent to (2.9).

2.6.1.4 Average End-to-End Delay at Steady State

Corollary 2. *For the wireless multihop network with N relays running the r-TDMA scheme, the average delay experienced by a packet at node i is*

$$\mathbb{E}D_i = \frac{2(N+1)(2N+1)\mathbb{E}\tau_i}{(N+2)p_s}, \quad 0 \leq i \leq N, \tag{2.12}$$

and consequently, the average in-network end-to-end delay is

$$\mathbb{E}D_{e2e} = \sum_{i=0}^{N} \mathbb{E}D_i = \frac{2N^2 + 3N + 1}{p_s}. \tag{2.13}$$

Proof: Recall that the rate of packet flow across each node is equal to T, and that the average number of packets at node i, $0 \leq i \leq N$ is $\mathbb{E}\tau_i$. From Little's theorem [52], the average delay at node i is simply $\mathbb{E}\tau_i/T$. □

We see that the average end-to-end delay is proportional to the node occupancies and inversely proportional to the link reliability. Also, it is interesting to note that the product of throughput and delay is $1 + N/2$, which is independent of p_s.

For large N, we immediately see from (2.13) that

$$\mathbb{E}D_{\text{e2e}} \sim 2N^2/p_s. \tag{2.14}$$

The average end-to-end delay grows quadratically with the number of relay nodes N.

2.6.1.5 Delay Distributions

In this subsection, we analytically derive the pmfs of the steady state delays incurred by packets at each node along the linear flow, i.e., we evaluate $\mathbb{P}(D_i = k)$, $k \geq 1$, $0 \leq i \leq N$ in closed-form.

To this end, suppose that a packet arrives at a node i in an arbitrary time slot t (at steady state). The three events that need to occur in the following order for the packet to be able to hop to node $i+1$ successfully are:

(1) Node $i+1$ has an empty buffer.

(2) Node i is picked for transmission.

(3) Node i's transmission is successful.

While (2) occurs w.p. $1/(N+1)$, (3) happens (independently of (2)) w.p. p_s. Thus, at time t, if node $i+1$'s buffer is empty, the delay experienced by the packet at node i is simply geometrically distributed with mean $(N+1)/p_s$, i.e.,

$$\mathbb{P}(D_i = k) = \frac{p_s}{N+1}\left(1 - \frac{p_s}{N+1}\right)^{k-1}.$$

If instead, there is another packet present in node $i+1$'s buffer, however, no packet at node $i+2$'s buffer, the probability that the delay at the i^{th} node is k time slots is equal to the probability that a single successful transmission (of the packet at

node $i+1$) occurs within $k-1$ slots, and then the packet at node i hops in the k^{th} time slot. Extending this argument, if j nodes adjacent to node i have a packet, and the $j+1^{\text{th}}$ adjacent node has none, i.e., if

$$(\tau_{i+1}, \ldots, \tau_{i+j}, \tau_{i+j+1}) = (\underbrace{1, \cdots, 1}_{j \text{ ones}}, 0), \quad j \geq 0,$$

then the packet at node i will successfully hop to node $i+1$ in exactly k time steps if j packets (those at nodes $i+j, i+j-1, \ldots, i+1$ in that order) hop within $k-1$ time slots, and then, the packet present at node i hops (in the k^{th} time slot).

Let $e_{i,j}$ denote the event that given a packet arrives at node i (at some time t), j nodes adjacent to it are occupied. We now compute $\Delta_{i,j}^{(N)} := \mathbb{P}(e_{i,j})$. We have

$$\begin{aligned}
&\mathbb{P}(\tau_{i+1}[t] = 1, \ldots, \tau_{i+j}[t] = 1, \tau_{i+j+1}[t] = 0 \mid {}^{\text{packet arrives}}_{\text{at node } i}) \\
&= \frac{\mathbb{P}(\tau_{i+1}[t] = 1, \ldots, \tau_{i+j}[t] = 1, \tau_{i+j+1}[t] = 0, {}^{\text{packet arrives}}_{\text{at node } i})}{\mathbb{P}(\text{packet arrives at node } i)} \\
&= P(\tau_{i-1}[t-1] = 1, \tau_i[t-1] = 0, \tau_{i+1}[t-1] = 1, \ldots \\
&\qquad \ldots, \tau_{i+j}[t-1] = 1, \tau_{i+j+1}[t-1] = 0) \\
&\qquad \times \frac{1}{P(\tau_{i-1}[t-1] = 1, \tau_i[t-1] = 0)} \\
&\qquad \times \frac{\mathbb{P}(\text{the packet at node } i-1 \text{ hops to node } i)}{\mathbb{P}(\text{the packet at node } i-1 \text{ hops to node } i)}.
\end{aligned}$$

Using the MPA formalism, we may write at steady state,

$$\begin{aligned}
\Delta_{i,j}^{(N)} &= \frac{\langle W | C^{i-2} D E D^j E C^{N-i-j-1} | V \rangle}{\langle W | C^{i-2} D E C^{N-i} | V \rangle} \\
&\overset{(a)}{=} \frac{\langle W | C^{i-1} D^{j-1} C^{N-i-j} | V \rangle}{p_s \langle W | C^{N-1} | V \rangle},
\end{aligned} \tag{2.15}$$

where in (a), we have used (2.5a) thrice (twice in the numerator term and once

in the denominator term).

The evaluation of $\Delta_{i,j}^{(N)}$ is relatively straightforward for small values of j. For instance,

$$\begin{aligned}\Delta_{i,0}^{(N)} &= \frac{\langle W|C^{i-2}DEEC^{N-i-1}|V\rangle}{\langle W|C^{i-2}DEC^{N-i}|V\rangle} \\ &= \frac{\langle W|C^{i-1}EC^{N-i-1}|V\rangle}{\langle W|C^{N-1}|V\rangle} \\ &= 1-\mathbb{E}\tau_i^{(N-1)}, \end{aligned} \tag{2.16}$$

and

$$\begin{aligned}\Delta_{i,1}^{(N)} &= \frac{\langle W|C^{i-2}DEDEC^{N-i-2}|V\rangle}{\langle W|C^{i-2}DEC^{N-i}|V\rangle} \\ &= \frac{\langle W|C^{N-2}|V\rangle}{\langle W|C^{N-1}|V\rangle} \\ &= \eta(N-2)/\eta(N-1) \end{aligned} \tag{2.17}$$

In order to compute $\Delta_{i,j}^{(N)}$ for higher values of j, we use the following lemmas.

Lemma 1. *The following relationship holds for $j \geq 2$:*

$$\Delta_{i,j}^{(N)} = \Delta_{i,j-1}^{(N)} - \Delta_{i,j-2}^{(N-1)}\eta(N-2)/\eta(N-1). \tag{2.18}$$

Proof: Using the fact that $C = D + E$, we obtain

$$\begin{aligned}
\Delta_{i,j}^{(N)} &= \frac{\langle W|C^{i-1}D^{j-2}(C-E)C^{N-i-j}|V\rangle}{\langle W|C^{N-1}|V\rangle} \\
&= \frac{\langle W|C^{i-1}D^{j-2}C^{N-i-j+1}|V\rangle}{\langle W|C^{N-1}|V\rangle} \\
&- \frac{\langle W|C^{i-1}D^{j-3}DEC^{N-i-j}|V\rangle}{\langle W|C^{N-1}|V\rangle} \\
&\overset{(a)}{=} \Delta_{i,j-1}^{(N)} - \frac{\langle W|C^{i}D^{j-3}C^{N-i-j+1}|V\rangle}{p_s\langle W|C^{N-1}|V\rangle} \\
&= \Delta_{i,j-1}^{(N)} - \Delta_{i,j-2}^{(N-1)}\frac{\langle W|C^{N-2}|V\rangle}{p_s\langle W|C^{N-1}|V\rangle},
\end{aligned}$$

which is equivalent to (2.18), upon using property (2.5b). Here, (a) is derived using (2.15) and (2.5a). □

Lemma 2. *For $j \geq 2$, we have*

$$\begin{aligned}
\Delta_{i,j}^{(N)} &= \sum_{k=0}^{\lfloor \frac{j-1}{2} \rfloor} (-1)^k \frac{\eta(N-k-2)}{\eta(N-1)} \times \\
&\left[\binom{j-k-2}{k}\mathbb{E}\tau_i^{(N-k-2)} + \binom{j-k-2}{k-1}\right],
\end{aligned} \tag{2.19}$$

where $\mathbb{E}\tau_i^{(N)}$ denotes the occupancy of node i in the flow with N relays.

Proof: The proof involves induction. Using (2.16) and (2.17) in (2.18), we obtain for the case $j = 2$,

$$\Delta_{i,2}^{(N)} = \mathbb{E}\tau_i^{(N-2)}\frac{\eta(N-2)}{\eta(N-1)},$$

which satisfies (2.19). Similarly, using (2.18) for $j = 3$, we have

$$\Delta_{i,3}^{(N)} = \mathbb{E}\tau_i^{(N-2)}\frac{\eta(N-2)}{\eta(N-1)} - \frac{\eta(N-3)}{\eta(N-1)},$$

which conforms with (2.19).

Suppose that (2.19) is valid for the cases $j = m, m-1$, $m > 2$. Now, consider the case $j = m+1$. From (2.18), we have

$$
\begin{aligned}
\Delta_{i,m+1}^{(N)} &= \Delta_{i,m}^{(N)} - \Delta_{i,m-1}^{(N-1)} \eta(N-2)/\eta(N-1) \\
&= \sum_{k=0}^{\lfloor \frac{m-1}{2} \rfloor} (-1)^k \frac{\eta(N-k-2)}{\eta(N-1)} \times \\
&\quad \left[\binom{m-k-2}{k} \mathbb{E}\tau_i^{(N-k-2)} + \binom{m-k-2}{k-1} \right] \\
&\quad - \frac{\eta(N-2)}{\eta(N-1)} \sum_{k=0}^{\lfloor \frac{m-2}{2} \rfloor} (-1)^k \frac{\eta(N-k-3)}{\eta(N-2)} \times \\
&\quad \left[\binom{m-k-3}{k} \mathbb{E}\tau_i^{(N-k-3)} + \binom{m-k-3}{k-1} \right] \\
&= \binom{m-2}{0} \frac{\eta(N-2)}{\eta(N-1)} \mathbb{E}\tau_i^{(N-2)} + \sum_{k=1}^{\lfloor \frac{m-1}{2} \rfloor} (-1)^k \\
&\quad \frac{\eta(N-k-2)}{\eta(N-1)} \left[\binom{m-k-2}{k} \mathbb{E}\tau_i^{(N-k-2)} + \right. \\
&\quad \left. \binom{m-k-2}{k-1} \right] + \sum_{k=1}^{\lfloor \frac{m-2}{2} \rfloor + 1} (-1)^k \frac{\eta(N-k-2)}{\eta(N-1)} \\
&\quad \left[\binom{m-k-2}{k-1} \mathbb{E}\tau_i^{(N-k-2)} + \binom{m-k-2}{k-2} \right] \\
&= \binom{m-2}{0} \frac{\eta(N-2)}{\eta(N-1)} \mathbb{E}\tau_i^{(N-2)} + \sum_{k=1}^{\lfloor \frac{m-1}{2} \rfloor} (-1)^k \\
&\quad \frac{\eta(N-k-2)}{\eta(N-1)} \left[\left[\binom{m-k-2}{k} + \binom{m-k-2}{k-1} \right] \right. \\
&\quad \left. \mathbb{E}\tau_i^{(N-k-2)} + \left[\binom{m-k-2}{k-1} + \binom{m-k-2}{k-2} \right] \right] \\
&\quad + (-1)^{m/2} \frac{\eta\left(N - m/2 - 2\right)}{\eta(N-1)} 1[m \text{ is even}],
\end{aligned}
$$

where the last term involves an indicator function since it occurs only when $\lfloor (m-2)/2 \rfloor + 1 \neq \lfloor (m-1)/2 \rfloor$, i.e., when m is even. Using the identity

$$\binom{r}{s} + \binom{r}{s-1} \equiv \binom{r+1}{s}, \tag{2.20}$$

we obtain

$$\begin{aligned} \Delta_{i,m+1}^{(N)} &= \sum_{k=0}^{\lfloor m/2 \rfloor} (-1)^k \frac{\eta(N-k-2)}{\eta(N-1)} \times \\ &\quad \left[\binom{m-k-1}{k} \mathbb{E}\tau_i^{(N-k-2)} + \binom{m-k-1}{k-1} \right]. \end{aligned} \tag{2.21}$$

We see that (2.19) is valid for the case $j = m+1$ as well. By induction, the lemma holds. □

Theorem 3. *The pmf of the packet delay at node i, $0 \leq i \leq N$ is given by*

$$\mathbb{P}(D_i = k) = \sum_{j=0}^{N-i} \Delta_{i,j}^{(N)} \binom{k-1}{j} \chi^{j+1} (1-\chi)^{k-1-j}, \tag{2.22}$$

where $\chi = p_s/(N+1)$.

Proof: The conditional probability $\mathbb{P}(D_i = k \mid e_{i,j})$ is the probability that j packets (present at nodes $i+1, \ldots i+j$) hop out successfully in $k-1$ time slots, and then, the packet at node i is transmitted successfully only in the k^{th} time slot. Hence,

$$\mathbb{P}(D_i = k \mid e_{i,j}) = \binom{k-1}{j} \chi^j (1-\chi)^{k-1-j} \times \chi.$$

Summing up the joint pmf $\mathbb{P}(D_i = k, e_{i,j})$ over all the possible values of j ($0 \leq$

$j \leq N - i$) yields the desired result, i.e.,

$$\mathbb{P}(D_i = k) = \sum_{j=0}^{N-i} \mathbb{P}(e_{i,j})\mathbb{P}(D_i = k \mid e_{i,j}), \quad k > 0,$$

which is equivalent to (2.22). □

Figure 2.7 plots the delay pmfs at each node in a line network with $N = 3$. Note that apart from the delay at the final relay, none of the other delays are geometrically distributed, i.e., they are not memoryless. Also note that $D_0 \geq 2$. This may be explained by the fact that whenever a packet hops out of the source node (node 0), another packet arrives at the head of the source. Thus, the packet at node 0 has to wait for at least one time slot (for the packet at node 1 to hop out) before attempting to hop.

2.6.1.6 Joint Delay Distributions

Since the flow of packets in a wireless multihop network is relayed across multiple links, the delays experienced by a packet across hops are correlated. As mentioned earlier, the study of delay correlations has often been neglected in prior work; it is, however, crucial for the design of smarter retransmission and flow control algorithms.

For instance, suppose it is known that the conditional delay probability $\mathbb{P}(D_{i+1} = j \mid D_i = k)$ is high for some specific value $j = \ell$, i.e., given that a packet stayed at node i for k slots, it is likely to be present in node $i + 1$'s buffer for ℓ slots. Node $i+1$ can then decide to hold back the transmission of a packet for $\ell - 1$ slots, thus reducing the number of unnecessary transmissions. Knowing the spatial delay correlations also helps determine the variance of the end-to-end delay.

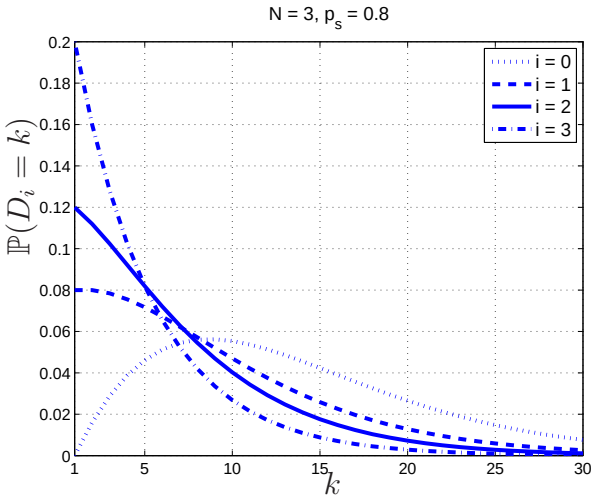

Figure 2.7. The pmf of the delay incurred by packets at various nodes in the line network with $N = 3$. For this plot, all link reliabilities are taken to be equal to $p_s = 0.8$.

We begin by stating the following simple lemma.

Lemma 3. *In a wireless line network with N nodes, D_N is independent of all the other hop delays. As a special case, when $N = 1$, D_0 and D_1 are independent.*

Proof: Irrespective of the delay experienced by a packet at any arbitrary node, it can hop from node N to the destination (node $N+1$) if node N is picked, and its transmission is successful. Thus, D_N follows a geometric distribution with mean $(N+1)/p_s$ and is independent of all other delays. □

We next compute $\mathbb{P}(D_{i+1} = \ell, D_i = k)$, i.e., the probability that a packet will stay at nodes i and $i+1$ for k and ℓ slots respectively at steady state? The same procedure may be extended (with extra care) to evaluate the joint pmfs of the delays at nodes farther apart.

To this end, let e_{i,j_1,j_2} denote the event that given a packet arrives at node i,

we have

$$(\tau_{i+1}, \ldots, \tau_{i+j_1}, \tau_{i+j_1+1}, \tau_{i+j_1+2} \ldots, \tau_{i+j_1+j_2+1}, \tau_{i+j_1+j_2+2}) = (\underbrace{1, \ldots, 1}_{j_1 \text{ ones}}, 0, \underbrace{1, \ldots, 1}_{j_2 \text{ ones}}, 0).$$

We first evaluate $\kappa^{(N)}_{i,j_1,j_2} := \mathbb{P}(e_{i,j_1,j_2})$. Using the same idea as in (2.15), we may write

$$\kappa^{(N)}_{i,j_1,j_2} = \frac{\langle W|C^{i-2}DED^{j_1}ED^{j_2}EC^{N-i-j_1-j_2-2}|V\rangle}{\langle W|C^{i-2}DEC^{N-i}|V\rangle} = \frac{\langle W|C^{i-1}D^{j_1}ED^{j_2-1}C^{N-i-j_1-j_2-1}|V\rangle}{p_s\langle W|C^{N-1}|V\rangle}.$$

Simplifying further, we get

$$\begin{aligned}\kappa^{(N)}_{i,j_1,j_2} &\overset{(a)}{=} \frac{\langle W|C^{i-1}D^{j_1-1}CD^{j_2-1}C^{N-i-j_1-j_2-1}|V\rangle}{p_s^2\langle W|C^{N-1}|V\rangle} \\ &\overset{(b)}{=} \frac{\eta(N-2)}{\eta(N-1)}\left[\frac{\langle W|C^{i-1}D^{j_1+j_2-1}C^{N-i-j_1-j_2-1}|V\rangle}{p_s\langle W|C^{N-2}|V\rangle} + \frac{\langle W|C^{i-1}D^{j_1-1}ED^{j_2-1}C^{N-i-j_1-j_2-1}|V\rangle}{p_s\langle W|C^{N-2}|V\rangle}\right] \\ &= \frac{\eta(N-2)}{\eta(N-1)}\left[\Delta^{(N-1)}_{i,j_1+j_2} + \kappa^{(N-1)}_{i,j_1-1,j_2}\right]. \end{aligned} \tag{2.23}$$

To derive (a), we used (2.5a) for the term in the numerator, and to derive (b), we used the identity $C = D + E$.

We obtain closed-form expressions for $\kappa^{(N)}_{i,j_1,j_2}$ considering the following two cases.

Case 1: $j_1 = 0$. From (2.23), we obtain

$$\begin{aligned}\kappa_{i,0,j_2}^{(N)} &= \frac{\langle W|C^{i-1}ED^{j_2}EC^{N-i-j_2-1}|V\rangle}{\langle W|C^{N-1}|V\rangle} \\ &= \frac{\langle W|C^{i}D^{j_2}EC^{N-i-j_2-1}|V\rangle}{p_s\langle W|C^{N-1}|V\rangle} - \frac{\langle W|C^{i-1}D^{j_2+1}EC^{N-i-j_2-1}|V\rangle}{p_s\langle W|C^{N-1}|V\rangle} \\ &= \Delta_{i+1,j_2}^{(N)} - \Delta_{i,j_2+1}^{(N)}. \end{aligned} \tag{2.24}$$

Case 2: $j_1 > 0$. Using the recursive equation (2.23), we obtain

$$\kappa_{i,j_1,j_2}^{(N)} = \frac{\eta(N-j_1-1)}{\eta(N-1)}\left(\Delta_{i+1,j_1+j_2}^{(N-j_1)} + \sum_{s=2}^{j_1}\Delta_{i,s+j_2}^{(N-j_1-1+s)}\right).$$

The following theorem establishes the joint pmfs between delays across adjacent hops in the network.

Theorem 4. *The joint pmf of the delays at nodes i and $i+1$ is given by*

$$\begin{aligned}\mathbb{P}(D_{i+1}=\ell, D_i = k) &= \sum_{j_1=0}^{s_1}\sum_{j_2=0}^{s_2}\sum_{j=j_1}^{2j_1+j_2}\kappa_{i,j_1,j_2}^{(N)}\binom{k-1}{j} \\ &\quad\times\binom{\ell-1}{2j_1+j_2-j}\chi^{2j_1+j_2+2}(1-\chi)^{k+\ell-2-2j_1-j_2} \\ &\quad+\sum_{j_1=0}^{s_3}\sum_{j=j_1}^{2j_1-1}\kappa_{i,j_1,j_2}^{(N)}\binom{k-1}{j}\binom{\ell-1}{2j_1-1-j}\chi^{2j_1+1} \\ &\quad\times(1-\chi)^{k+\ell-1-2j_1}, \end{aligned} \tag{2.25}$$

where $\chi = p_s/(N+1)$, $s_1 = \min\{k-1, N-i-1\}$, $s_2 = \min\{k+\ell-2j_1-2, N-i-1-j_1\}$, and $s_3 = \min\{k-1,(k+\ell-1)/2\}$.

Proof: We condition on the event e_{i,j_1,j_2}, which happens w.p. $\kappa_{i,j_1,j_2}^{(N)} := \mathbb{P}(e_{i,j_1,j_2})$. For clarity, we treat the following two cases separately.

Case 1: $0 \le j_1 \le N-i-1$. Since $D_i = k$ by assumption, at least j_1 packet hops

(for the ones at nodes $i + j_1, \ldots i + 1$, in that order) occur within $k - 1$ slots. In addition, $D_{i+1} = \ell$, thus the packets at nodes $i + 1, \ldots i + j_1$ hop out twice, which also means that j_2 other packet hops (from nodes $i + j_1 + 2, \ldots, i + j_1 + j_2 + 1$ to their respective adjacent nodes) occur, all within $k + \ell - 2$ slots. The flow length of N nodes also places a constraint on the possible values that j_1 and j_2 can take. Thus, the following hold:

(i) $j_1 \leq k - 1$.

(ii) $2j_1 + j_2 \leq k + \ell - 2$.

(iii) $i + j_1 + j_2 + 1 \leq N$.

Equivalently, we have

- $0 \leq j_1 \leq \min\{k - 1, N - i - 1\}$, and
- $0 \leq j_2 \leq \min\{k + \ell - 2j_1 - 2, N - i - 1 - j_1\}$.

The conditional joint pmf $\mathbb{P}(D_{i+1} = \ell, D_i = k \mid e_{i,j_i,j_2})$ is equal to the sum of the probabilities of having j successful packet hops, $j_1 \leq j < 2j_i + j_2$, occurring in $k - 1$ time slots, then the packet at node i hopping successfully to node $i + 1$ in the k^{th} time slot, then $2j_1 + j_2 - j$ successful transmissions occurring in $\ell - 1$ slots, and finally, the packet at node $i + 1$ hopping to node $i + 2$ in the $k + \ell$ th time slot.

Case 2: $j_1 = N - i$. For this case, when a packet arrives at node i, the configuration of the nodes $i + 1, \ldots, N$ is simply $(\tau_{i+1}, \ldots \tau_N) = (1, \ldots, 1)$. As in Case 1, at least j_1 packet hops (for the ones at nodes $i + j_1, \ldots i + 1$, in that order) occur within $k - 1$ slots. However, once the packet at node N is delivered to the destination, it does not hop further. Thus, $D_{i+1} = \ell$ would mean that $2j_1 - 1$ (and

not $2j_1$) successful transmissions must occur in $k+\ell-2$ time slots. The following constraints hold:

(i) $j_1 \leq k-1$.

(ii) $2j_1 - 1 \leq k+\ell-2$.

Putting together (i) and (ii), $0 \leq j_1 \leq \min\{k-1, (k+\ell-1)/2\}$.

The conditional joint pmf $\mathbb{P}(D_{i+1} = \ell, D_i = k \mid e_{i,j_i,j_2})$ is obtained by adding up the probabilities of having j successful packet hops, $j_1 \leq j < 2j_i - 1$, occurring in $k-1$ time slots, and the packet at node i hopping successfully to node $i+1$ in the k^{th} time slot, then $2j_1 - 1 - j$ successful transmissions occurring in $\ell - 1$ slots, and lastly, the packet at node $i+1$ hopping to node $i+2$ in the $k+\ell$ th time slot.

Summing up $\mathbb{P}(D_{i+1} = \ell, D_i = k, e_{i,j_i,j_2})$ over all possible values of j_1 and j_2 considering both the cases yields the joint pmf, which is given in (2.25). □

The conditional delay pmf may be obtained by using (2.25) together with (2.22). Figure 2.8 plots the conditional delay pmfs $\mathbb{P}(D_1 = \ell \mid D_0 = k)$ in a line network with $N = 3$ and $p_s = 0.8$, for several values of ℓ and k.

2.6.1.7 Empirical Results

Evaluating the joint pmfs between delays across nodes lying farther apart can be performed by essentially following the aforementioned procedure, but it gets computationally intensive and unwieldy. Instead, we resort to simulation and present the behavior of the *spatial delay correlation coefficients*. The correlation coefficient between delays at nodes i and j is defined as

$$\rho_{i,j} = \frac{\mathbb{E}\left[(D_i - \mathbb{E}D_i)\,(D_j - \mathbb{E}D_j)\right]}{\sigma_{D_i}\sigma_{D_j}},$$

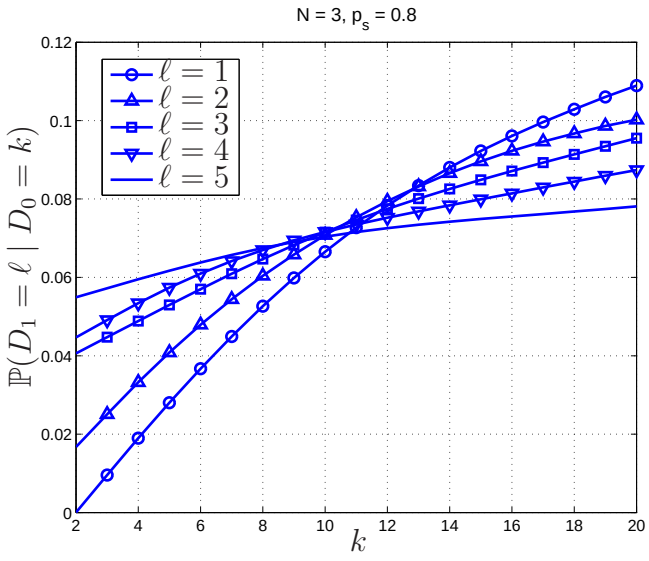

Figure 2.8. The conditional delay pmfs $\mathbb{P}(D_1 = \ell \mid D_0 = k)$ for several values of ℓ and k.

where σ_{D_i} and σ_{D_j} represent the standard deviations of the delays at node i and j, respectively.

Figure 2.9 plots the empirical values of correlation coefficients across one-, two- and three-hop neighbors in an r-TDMA-based wireless network with $N = 10$ relays and $p_s = 0.8$. Observe that all the delay correlation coefficients are non-positive. This can be explained by noting that if the transmission of a packet is delayed at any node, the adjacent nodes' buffers get emptied so that the packet traverses faster across them. Likewise, if the waiting time of a packet at any particular node is small, the neighboring relay node buffers are still occupied and therefore it takes longer for the packet to get transported across the system. Also, delays across hops closer to the destination, and delays across nodes farther apart are relatively lightly correlated compared to the corresponding values near the source

node. In fact, $\forall i$, $\rho_{i,N} = 0$, since D_N is independent of all other delays (which is also a consequence of Lemma 3).

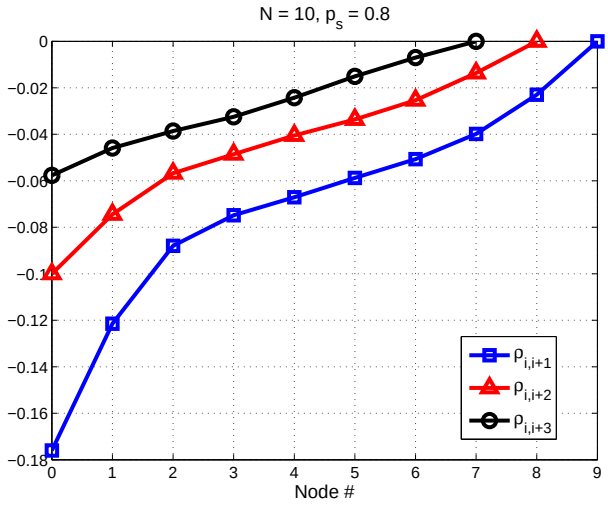

Figure 2.9. The correlation coefficients $\rho_{i,i+1}$, $\rho_{i,i+2}$ and $\rho_{i,i+3}$ for $p_s = 0.8$ in a multihop r-TDMA-based system with $N = 10$ relays. The delay correlations across nodes farther apart and closer to the destination are seen to be relatively light.

2.6.1.8 The Short-hop versus Long-hop Routing Problem

We now present a simple application of our results: the short-hop versus long-hop routing problem [53] in long ($N \gg 1$) regular r-TDMA-based wireless networks. Specifically, we determine if it is beneficial to route over many short hops or a smaller number of longer hops. The metrics we use for comparison are the

average end-to-end delay and throughput.

To this end, let us suppose that communication occurs only across nodes that are in general, m hops ($1 \leq m \leq N$) apart. Manipulating (2.3), it is straightforward to see that

$$p_s = \exp\left(-\Theta N_0 (md)^\gamma\right).$$

We now determine the optimum spacing between the communicating hops, m_{opt}, that minimizes the average end-to-end delay for this general line network. Since there are N/m relays now, we have from (2.14) (assuming that N is a multiple of m),

$$\mathbb{E}D_{e2e} \sim 2(N/m)^2/p_s = 2N^2 \exp\left(\Theta N_0 (md)^\gamma\right)/m^2, \tag{2.26}$$

Upon differentiating (2.26), we obtain[6]

$$m_{\text{opt}} = \frac{1}{d}\left(\frac{2}{\Theta N_0 \gamma}\right)^{1/\gamma}, \tag{2.27}$$

which is independent of N.

The values of m_{opt} (2.27) for several values of γ and Θ is plotted in Figure 2.10. Depending on the value of the SNR threshold, routing needs to be performed over longer or shorter hops in order to keep the packet delay minimal.

Likewise, let m'_{opt} denote the optimum value of the spacing between hops for which the network throughput is maximized. We can express the throughput for the N/m-relay system as

$$T \sim p_s/\left(4N/m\right) = m \exp\left(-\Theta N_0 (md)^\gamma\right)/4N, \tag{2.28}$$

[6]We allow m to assume any real value here. In practice, m_{opt} will be rounded up or down to an integer.

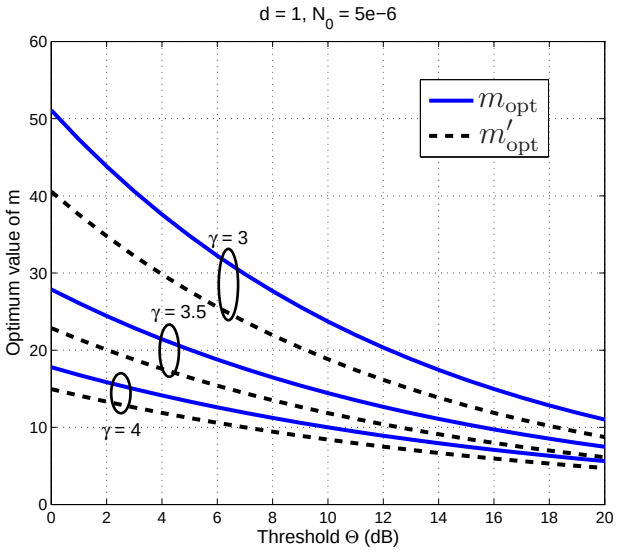

Figure 2.10. Delay-optimum hop spacing m_{opt} (2.27) and throughput-optimum hop spacing m'_{opt} (2.29) versus Θ for different values of the path loss exponent.

which is maximized at

$$m'_{\text{opt}} = \frac{1}{d}\left(\frac{1}{\Theta N_0 \gamma}\right)^{1/\gamma}. \tag{2.29}$$

We see that $m_{\text{opt}}/m'_{\text{opt}} = 2^{1/\gamma}$. The values of m'_{opt} are also depicted in Figure 2.10.

2.6.2 Throughput and Delay Analysis for the Slotted ALOHA-based Line Network

In this section, we employ existing results from the TASEP particle model with parallel update to analytically derive the buffer occupancies, throughput and average end-to-end delay[7] for the slotted ALOHA-based network at steady state.

[7]Computing the complete delay distribution and its correlations analytically is quite a formidable task, and is not presented in this thesis.

Additionally, we apply our findings to determine the optimum contention parameter that minimizes the average end-to-end delay in long wireless line networks.

2.6.2.1 Steady State Buffer Occupancies

Suppose that the link reliabilities[8] are each equal to p_s. Also, let q denote the contention probability, i.e., in each time slot, nodes having a packet independently transmit w.p. q or stay idle w.p. $1-q$. We can take the effective hopping probability in the corresponding parallel TASEP model to be $p = qp_s$. Then, the steady state occupancies are given by [54, Eqn. 10.16]

$$\mathbb{E}\tau_i = \frac{(1-qp_s)\sum_{n=0}^{N-i} B(N-n)B(n) + qp_sB(N)}{B(N+1) + qp_sB(N)}, \tag{2.30}$$

where $B(0) = 1$, and

$$B(k) = \sum_{j=0}^{k-1} \frac{1}{k}\binom{k}{j}\binom{k}{j+1}(1-qp_s)^j, \quad k > 0.$$

The steady state occupancies depend nontrivially on p (and hence, on q and p_s) as depicted in Figure 2.11. Also, owing to the particle-hole symmetry, we have $\mathbb{E}\tau_{\lceil (N+1)/2 \rceil} = \mathbb{E}\tau_{\lfloor (N+1)/2 \rfloor}$, and $\sum_{i=0}^{N} \mathbb{E}\tau_i = 1 + N/2$. For the special case $p = 1$, i.e., $q = p_s = 1$, the steady state configuration of each node alternates between ones and zeros, and the occupancy of each relay node is exactly $1/2$.
When $N \gg 1$, $\mathbb{E}\tau_1 = \left(2p - 1 + \sqrt{1-p}\right)/2p$ and $\mathbb{E}\tau_N = \left(1 - \sqrt{1-p}\right)/2p$ [54]. Also, the occupancy in the bulk is approximately equal to $1/2$, i.e., $\mathbb{E}\tau_i \approx 1/2$ for $1 < i < N$. Again, we see that the node occupancies monotonically decrease with proximity to the destination node.

[8] In general, the link reliability p_s is a function of the contention probability q, since the interference in the network depends on q. This will be discussed in Subsection 2.6.2.4.

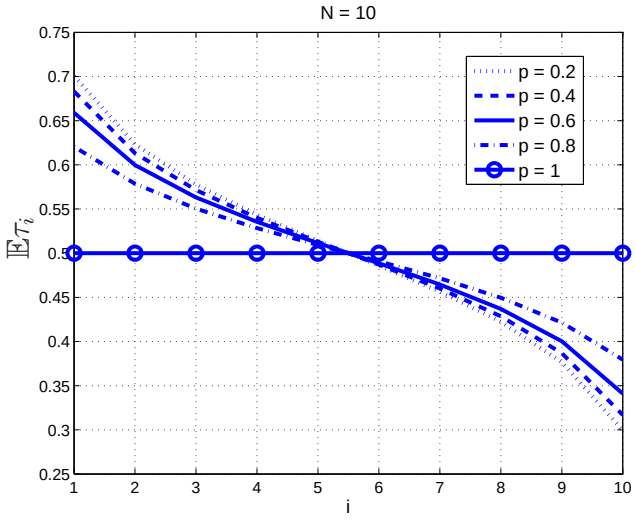

Figure 2.11. The occupancies for the parallel TASEP particle flow model for several values of p. Unlike the r-TDMA case (see Figure 2.6), $\mathbb{E}\tau_i$ depends on p.

2.6.2.2 Steady State Throughput

The following theorem quantifies the throughput and mean end-to-end delay across a typical flow in the network in closed-form.

Theorem 5. *For an ALOHA-based line network, the steady state throughput is*

$$T = \frac{qB(N)}{B(N+1) + qp_sB(N)}. \tag{2.31}$$

Proof: The proof is very similar to that of Theorem 1. Indeed, at any instant of time (in steady state), relay node N's buffer has a packet w.p. $\mathbb{E}\tau_N$; furthermore, it transmits w.p. q, and the transmission succeeds w.p. p_s. Thus, the throughput is simply given by $T = qp_s\mathbb{E}\tau_N$, which is identical to (2.31). (3.25) follows from Little's theorem. □

For $N \gg 1$, the network throughput at steady state is

$$T \sim \left(1 - \sqrt{1 - qp_s}\right) \Big/ 2. \tag{2.32}$$

2.6.2.3 Average Steady State Delay

Corollary 6. *For the ALOHA-based wireless line network with link reliability p_s, the average steady state delay D_i of a packet at node i is*

$$\mathbb{E}D_i = \mathbb{E}\tau_i/(qp_s\mathbb{E}\tau_N), \quad 0 \le i \le N. \tag{2.33}$$

Consequently, the average end-to-end delay is

$$\mathbb{E}D_{e2e} = \frac{1}{qp_s\mathbb{E}\tau_N}\sum_{i=1}^{N}\mathbb{E}\tau_i = \frac{N+2}{2qp_s\mathbb{E}\tau_N}. \tag{2.34}$$

Proof: The proof is identical to the one used to derive the delay across the r-TDMA-based network (see Corollary 2), and follows directly from Little's theorem [52]. □

For large N, we have

$$\mathbb{E}D_{\text{e2e}} \sim \frac{N+2}{1 - \sqrt{1 - qp_s}}. \tag{2.35}$$

As in the r-TDMA-based network, $T \times \mathbb{E}D_{\text{e2e}} = 1 + N/2$ here. For the special case $q = p_s = 1$, every alternate node transmits successfully in each time slot; the throughput is equal to 1/2, and the delay at each hop is 2.

2.6.2.4 Optimizing the Contention Probability in Long ALOHA-based Line Networks

Consider a long ($N \gg 1$) ALOHA-based wireless line network employing the modified transmission scheme. For small q, nodes hold on to packets for a long time before transmitting them, which results in a long delay. Likewise, for high q, the interference in the network is high and the delay is large. In this subsection, we study the interesting question of how to choose the optimum q that minimizes the end-to-end delay at steady state. An alternative problem is choose the value of q that maximizes the steady state throughput.

We assume that the system is interference-limited, thus $p_s = \Pr[\text{SIR} > \Theta]$. Now, from [55], the success probability p_s for the considered line network model is well-approximated by[9]

$$p_s \approx \exp(-qc/2), \tag{2.36}$$

where $c = \pi\Theta^{1/\gamma} \big/ \sqrt{\gamma/2} - 1$.
Using (2.36) in (2.35), we obtain

$$\mathbb{E}D_{\text{e2e}} \propto \left(1 - \sqrt{1 - q\exp(-qc/2)}\right)^{-1}. \tag{2.37}$$

Differentiating (2.37) and noting that $0 \leq q \leq 1$, the optimum value of the contention parameter that minimizes the average end-to-end delay is obtained as

$$q_{\text{opt}} = \min\{1, 2/c\}. \tag{2.38}$$

[9]Note that this is independent of the node separation d.

From (2.32), we see that $T \propto 1 - \sqrt{1 - q\exp(-qc/2)}$, thus q_{opt} maximizes the steady state throughput as well. Figure 2.12 plots analytical values of q_{opt} (2.38) versus the SIR threshold Θ, for several values of γ (dashed lines). It also shows empirical values of q_{opt} obtained via simulation (solid lines), which are seen to match the analytical values closely.

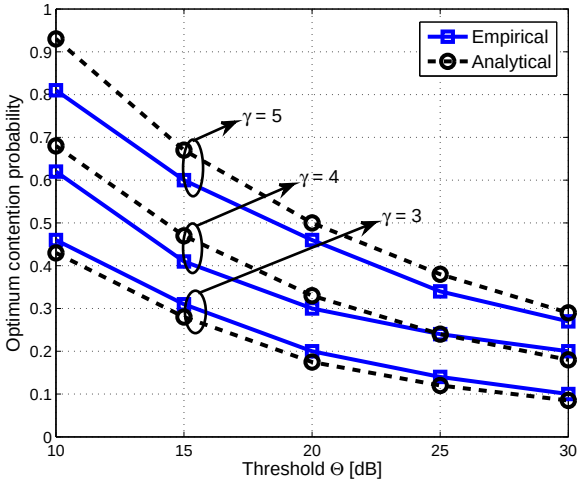

Figure 2.12. The analytical (dashed lines) and empirical (solid lines) values of the optimum contention parameter q_{opt} that minimizes the end-to-end delay (as well as maximizes the steady state throughput) versus Θ for different values of γ, in a long ($N \gg 1$) regular ALOHA-based wireless network.

2.7 Summary and Concluding Remarks

We propose a modified transmission policy for wireless networks that helps regulate the flow of packets in a completely decentralized manner. Using known results from statistical mechanics, in particular, the TASEP particle flow model, we characterize the steady state end-to-end delay and throughput performances of multihop line networks running the r-TDMA and slotted ALOHA MAC schemes. We also extend the results derived to long networks and provide applications to important wireless networking problems. This chapter is intended to provide insight into the dynamics of packet transport in multihop wireless networks.

The TASEP particle-flow model permits the application of statistical mechanics to wireless networking. It helps provide closed-form expressions for the average end-to-end delay and throughput of the multihop line network and has the advantage of obviating the cumbersome queueing theory-based analysis. Furthermore, the results obtained are scalable with the number of nodes and thus can provide helpful insights into the design of wireless networks. We wish to promote TASEPs as a powerful tool to analyze the performance of multihop networks and hope that this introductory work instigates interest in solving other relevant wireless networking problems employing ideas from statistical mechanics.

CHAPTER 3

A SYSTEM OF MULTIHOP WIRELESS LINE NETWORKS

3.1 Introduction

Having studied the multihop wireless line network, we consider in this chapter a more complex network model: a two-dimensional multihop network comprising several source-destination pairs, each communicating wirelessly in a multihop fashion. The network may thus be observed as consisting of many multihop wireless line network flows (or routes). Considering the modified transmission policy (proposed in the Chapter 2) for each flow in the network, we characterize the throughput and end-to-end delay performances of a typical flow for this 2-D wireless network for the two different channel access mechanisms, r-TDMA and ALOHA. Our study also offers valuable insights from a system design stand-point such as determining the optimum density of transmitters or the optimal number of hops along a flow that maximizes the system's throughput performance. We corroborate our theoretical analyses via simulations.

The rest of this chapter is organized as follows. Section 3.2 describes the system and channel models. Section 3.3 reviews prior work in this area, and highlights our contributions. Section 3.4 investigates the design and analysis of r-TDMA-based wireless networks, while 3.5 studies ALOHA-based wireless networks. Section 3.6 discusses the issues of having relays serving multiple routes. Section 3.7 provides

some simulation results to corroborate the theory. Section 3.8 characterizes the throughput-delay tradeoff for each MAC scheme in the network, and Section 3.9 concludes the chapter.

3.2 System Model

3.2.1 Network Geometry

We consider a wireless network comprising an infinite number of source nodes, each of which initiates a (in general, multihop) flow of packets to a certain (destination) node lasting over an infinite duration of time. This framework is suitable for modeling general multihop networks since the aggregate traffic in such a network can always be decomposed into several multihop flows. The distribution of source nodes is assumed to be a homogeneous Poisson point process (PPP)[1] on the infinite plane $\mathbb{R}^2$ with density δ. Additionally, the network consists of a countably infinite population of other nodes (potential relays and destinations) arranged as a homogeneous PPP with density $1-\delta$. Thus, the total density of the network is (without loss of generality) equal to unity. For each source node, the destination node is chosen at a random direction, and at a finite distance.

3.2.2 Routing Strategy

Across each flow, we then take that packets are then routed in a general manner as follows[2]. Each node that receives a packet relays it to its n^{th}-nearest neighbor

[1]For the resulting so-called "Poisson network" of density δ, the number of nodes in any given set V of Lebesgue measure $|V|$ is Poisson with mean $\delta|V|$, and the numbers of nodes in disjoint sets are independent. The PPP is a well accepted model for nodal distribution (in particular when nodes are randomly deployed in large numbers) also owing to its analytical tractability, and helps obtain some useful insights in real-world networks.

[2]For implementation, each source needs to know its own location and the direction towards its intended destination.

($n \geq 1$) in a sector of angle $\phi \in [0, \pi]$, i.e., the next-hop node is the n^{th}-nearest neighbor that lies within $\pm\phi/2$ of the axis to the destination. Figure 3.1 illustrates the case of nearest-neighbor routing ($n = 1$).

A sample realization of the system model comprising several source-destination pairs is shown in Figure 3.2 with $\delta = 0.05$ and $\phi = \pi/2$. In the figure, each destination node is taken to be located 5 nearest-neighbor ($n = 1$) hops away from its corresponding source, at a random direction.

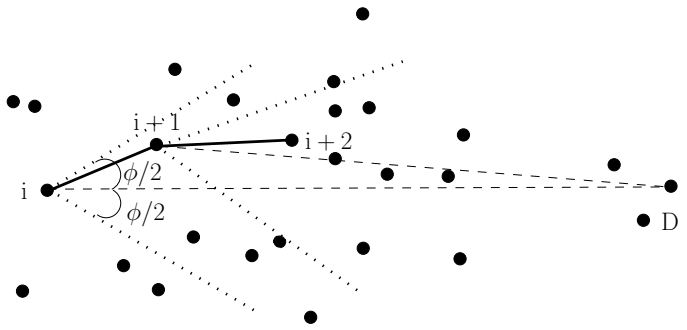

Figure 3.1. Illustration of nearest-neighbor routing in a sector of angle $\pm\phi/2$ along the axis to the destination for an arbitrary flow. The packet is routed from node i (for some i) to node $i + 1$, which then relays it to node $i + 2$. We denote the argument to the destination by the random variable Ψ. The thick solid lines along the axes to the destination represent the *progress* (to be defined later) of packets across the links $i \to i + 1$ and $i + 1 \to i + 2$.

Note that in this setup, the same common relay node may be a part of multiple flows, in particular when δ is not small.

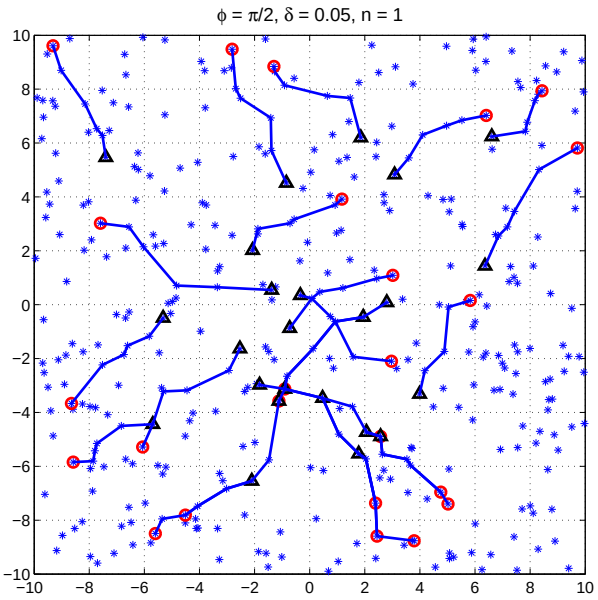

Figure 3.2. A sample realization of the system model with $\delta = 0.05$ and $\phi = \pi/2$. The triangles depict the sources, while the circles represent destinations. The thick solid lines mark the flows in the network. In this illustration, each destination is assumed to be located 5 nearest-neighbor ($n = 1$) hops away from its corresponding source node, along a randomly chosen direction.

3.2.3 Channel Model

We consider the case where all nodes use the same frequency band such that simultaneous transmissions cause interference between links. Furthermore, we assume that the transmit power at each transmitting node is equal to unity. Also, we model the attenuation in each link as the product of a large-scale path loss with exponent γ and a block i.i.d. Rayleigh fading component. Now, let $\Phi = \{x_i\}$ denote the set of transmitters in an arbitrary time slot. Then, the total received

power at location y on the plane is

$$I_\Phi(y) = \sum_{x \in \Phi} G_{xy} g(x - y),$$

where G_{xy} denotes the (power) fading gain of the wireless link between x and y, and $g(z) = \|z\|^{-\gamma}$. We take the noise power to be negligible compared to the interference and define the transmission of a packet from a node located at x to another located at y to be successful if and only if the instantaneous signal-to-interference-ratio (SIR) at y is greater than a threshold Θ, i.e., the probability of a successful transmission across the link $x \to y$ (denoted by p_s) equals

$$p_s = \Pr\left(\frac{G_{xy}\|x - y\|^{-\gamma}}{I_{\Phi \setminus \{x\}}(y)} > \Theta\right). \tag{3.1}$$

All the results in this chapter are obtained by averaging over all possible realizations of the channels and the underlying point processes.

3.2.4 MAC Schemes and the Transmission Policy

We assume a slotted system and analyze the same (those analyzed in Section 2.6) two MAC schemes *for each flow in the system*: r-TDMA and ALOHA. However, unlike in Chapter 2, we take that only the nodes *having a packet* may be chosen for transmission (rather than being chosen from the set of all nodes in that particular flow, including those that may not have a packet to transmit).

Also, we assume the transmission policy described in Section 2.3 *for each flow* in the network. Accordingly, each relay node have a buffer size of unity (for each flow it is associated with), and incoming transmissions are not accepted by relays

if their buffer (corresponding to that flow) already contains a packet.

3.2.5 Performance Metrics

Again, we are interested in the performance of the multihop network in its *steady state* (as $t \to \infty$). Specifically, in this work, we focus on two important end-to-end metrics: the (spatial) throughput density and the mean end-to-end delay, each evaluated for a typical flow at steady state.

In the remainder of the chapter, we suppose that each source-destination pair in the network is separated by N hops. Since the distribution of nodes is homogeneous, it is sufficient to simply analyze a "typical" flow in the system. Thus, in the rest of this chapter, we focus only on a representative flow occurring across N relays. Furthermore, we take that the source nodes are backlogged, i.e., they always have packets to transmit.

The metrics of interest are formally defined as follows.

- The throughput of the typical flow, $T(N)$, is defined as the average number of packets successfully delivered (to the destination) in unit time.

  The (spatial) **throughput density**, $\rho_T(N)$, is then defined as the mean number of packets successfully delivered (in unit time) per unit surface area. Since the density of destination nodes[3] is δ, $\rho_T(N) = \delta T(N)$.

- The **mean end-to-end delay**, $D(N)$, is defined as the average number of time slots it takes for the packet at the head of the source node[4] to successfully hop to the destination.

[3]For each source node, there exists a corresponding destination node.

[4]Note that we consider only the *in-network* delay (and neglect the queueing delay at the source) since the source nodes are always backlogged.

3.3 Related Work

While wireless networks with single-hop flows are fairly well understood, there has been limited contribution in the study of interference-limited multihop networks. For analytical tractability, previous work on Poisson multihop networks considered only a single link of a typical route (with the implicit assumption that the source-destination distance being infinitely large) and focused on metrics such as energy consumption [56], transmission range [57], spatial density of progress [58; 59], or the transmission capacity [60]. Furthermore, prior work assumed that all nodes in the network are backlogged, i.e., they always have packets to transmit. In recent papers [61]-[63], a problem of similar flavor as the one in this chapter was studied, wherein the authors considered a random multihop network and employed tools from basic queueing theory to determine the number of relays and their placements such that the mean network delay is minimized. However, the authors make the idealized assumption that the relays are always located along the source-destination axis, instead of being arranged as a PPP.

In this work, we characterize the performance of multihop networks assuming a more realistic system model than the ones employed earlier. The unified approach used here also has the following advantages. First, it allows for a rigorous and clean analysis. In contrast to prior work, we only consider the nodes that have packets as potential transmitters. Second, since we consider relays with unit buffer sizes, we only need to concern ourselves with access and retransmission delays, and no queueing analysis (which is often cumbersome) is required. Third, all our results are scalable with respect to the number of hops per route (or equivalently the source-destination separation) and help provide useful insights into the design of wireless networks.

3.4 Analysis and Design of r-TDMA-based Wireless Networks

In this section, we analyze the delay and throughput performance of r-TDMA-based multihop networks employing ideas from stochastic geometry and the random sequential TASEP literature. Our analysis helps provide some useful insights into system design such as choosing the optimal density of source nodes or the number of hops along a route that maximizes the spatial density of throughput. We begin by presenting the following lemma.

Lemma 4 (Corollary 3, [64])**.** *In a PPP with density λ, the probability density of the distance R_n from any node to its n^{th}-nearest-neighbor in a sector of angle ϕ is*

$$p_{R_n}(r) = r^{2n-1}\left(\frac{\lambda\phi}{2}\right)^n \frac{2}{(n-1)!}e^{-\lambda r^2\phi/2}, \quad r \in \mathbb{R}^+. \tag{3.2}$$

Furthermore, we have

$$\mathbb{E}[R_n] = \sqrt{\frac{2}{\lambda\phi}}\frac{\Gamma(n+1/2)}{\Gamma(n)} \approx \sqrt{\frac{2}{\lambda\phi}}\sqrt{n-1+\frac{\pi}{4}}. \tag{3.3}$$

The approximation may be obtained by using the series expansion of the Γ function, and is a generalization of [56, Eqn. 19]. For n large, $\mathbb{E}[R_n] \approx \sqrt{2n/\lambda\phi}$.

3.4.1 Packet Success Probability

We next measure the packet success probabilities defined as the probability of a successful packet transmission. The following proposition evaluates the packet success probability for the transmission across a typical link[5], i.e., between an arbitrary node and its n^{th}-nearest-neighbor in the r-TDMA-based network.

[5]Basically, any link along a typical route is said to be a typical link. Since the nodal arrangement is homogeneous, the packet success probability across every typical link in the network is the same.

Proposition 7. *For the r-TDMA-based multihop network, the probability of a successful transmission* $p_s = \mathbb{P}[SIR > \Theta]$ *from any node to its* n^{th}*-nearest-neighbor in a sector* ϕ *is*

$$p_s = \left(\frac{(1-\delta)\phi}{(1-\delta)\phi + 2\delta c} \right)^n, \tag{3.4}$$

where $c = \pi\Gamma(1+2/\gamma)\Gamma(1-2/\gamma)\Theta^{2/\gamma}$.

Proof: Recall that for the r-TDMA MAC scheme, only a randomly chosen node having a packet transmits in each flow. Thus, the set of interferers in any time slot[6] forms a homogeneous PPP with density δ. From [58, Corollary 3.2], the success probability $p_s(r)$ across any link of length r in a Poisson network equals

$$p_s(r) = e^{-\delta c r^2}, \tag{3.5}$$

with c given above.

Given that the relay node density is $1-\delta$, we may put together (3.2) (with $\lambda = 1-\delta$) and (3.5) to obtain the success probability of a packet transmission across n^{th} nearest-neighbors as

$$\begin{aligned} p_s &= \left(\frac{(1-\delta)\phi}{2} \right)^n \frac{2\int_0^\infty e^{-((1-\delta)\phi/2+\delta c)r^2} r^{2n-1} \mathrm{d}r}{(n-1)!} \\ &= \left(\frac{(1-\delta)\phi}{(1-\delta)\phi + 2\delta c} \right)^n \frac{\int_0^\infty e^{-t} t^{n-1} \mathrm{d}t}{(n-1)!}, \end{aligned} \tag{3.6}$$

where the latter equality is obtained by a simple change of variables $t = ((1-\delta)\phi/2+\delta c)r^2$. Noting that the integral evaluates to $\Gamma(n) = (n-1)!$, (3.6) simplifies to (3.4). □

[6] We neglect the temporal correlation of the interference.

3.4.2 Steady State Throughput and Average End-to-end Delay

The following theorem uses the occupancies to characterize the throughput and end-to-end delay for a typical flow in the r-TDMA-based multihop network.

Theorem 8. *For an r-TDMA-based flow across N relays, the throughput at steady state is*

$$T(N) = \frac{p_s}{2N+1}, \tag{3.7}$$

while the average end-to-end delay is

$$D(N) = \frac{2N^2+5N+2}{2p_s}, \tag{3.8}$$

where p_s is as given in (3.4).

Proof: The proof very closely follows that of Theorem 1. Along the same lines, consider first that an arbitrary node is picked for transmission with probability $1/(N+1)$, as in the random sequential TASEP. At any instant of time, relay node N's buffer contains a packet w.p. $\mathbb{E}\tau_N$; furthermore, it is picked for transmission (w.p. $1/(N+1)$), and the transmission is successful w.p. p_s. Then, the throughput across the flow is

$$T(N) = p_s \mathbb{E}\tau_N/(N+1), \tag{3.9}$$

where $\mathbb{E}\tau_N$ is given by (2.7).

Now, instead of picking any of the $N+1$ nodes randomly, if one only chooses among the nodes having a packet, the throughput is improved by a factor of

$(N+1)/\sum_{i=0}^{N}\mathbb{E}\tau_i = 2(N+1)/(N+2)$, i.e.,

$$T(N) = \frac{2p_s\mathbb{E}\tau_N}{N+2} = \frac{p_s}{2N+1}. \tag{3.10}$$

Recall that at steady state, the average number of packets in the flow is $\sum_{i=0}^{N}\mathbb{E}\tau_i = 1 + N/2$ (2.8). By Little's theorem [52], $D = \sum_{i=0}^{N}\mathbb{E}\tau_i/T$, which equals (3.8). □

Putting together Proposition 7 and Theorem 1, we obtain the throughput for a N-hop r-TDMA-based route wherein routing is performed across n^{th}-nearest neighbors in a sector ϕ as

$$T(N) = \left(\frac{(1-\delta)\phi}{(1-\delta)\phi + 2\delta c}\right)^n \frac{1}{2N+1}. \tag{3.11}$$

In Section 3.7, we verify the correctness of (3.11) via simulations.

We remark that even though the r-TDMA scheme dictates only a single transmission per flow, in principle, intra-route spatial reuse can also be incorporated into the model. Indeed, suppose that in each time slot, for every node i that gains the right to access the channel, several nodes $\ldots, i-m, i, i+m, \ldots$ are also allowed to transmit, where m is chosen such that simultaneous transmissions occurring at nodes m hops apart still does not cause intra-flow interference. While several (approximately N/m) nodes harness the same space, the density of interferers from other flows' transmissions also (approximately) increases to $m\delta$. Manipulating (3.11), we see that the throughput across a typical flow becomes

$$\begin{aligned} T(N) &\approx \left(\frac{(1-m\delta)\phi}{(1-m\delta)\phi + 2m\delta c}\right)^n \frac{N}{m(2N+1)} \\ &\sim \left(\frac{(1-m\delta)\phi}{(1-m\delta)\phi + 2m\delta c}\right)^n \frac{1}{2m}. \end{aligned} \tag{3.12}$$

Depending on the values of δ and Θ, employing spatial reuse may turn out to be beneficial or not.

We next provide some useful insights from a system design stand-point such as determining the optimal fraction of sources and the optimum number of hops between the source and destination such that the throughput density of the network is maximized. For clarity, we treat the cases $n = 1$ and $n > 1$ separately.

3.4.3 Nearest-neighbor Routing

Assume that the source-destination distance can be traversed in $N+1$ nearest-neighbor hops (or equivalently, across N relays). For the case $n = 1$, the throughput density is (using (3.11))

$$\rho_T(N) = \frac{1}{2N+1}\frac{(1-\delta)\delta\phi}{(1-\delta)\phi + 2\delta c}. \tag{3.13}$$

Clearly, for small δ, the throughput density is small. As δ increases, the density of flows increases as well, thus the throughput performance of the network improves. However, as δ gets very large, the interference in the network becomes high, and the link reliabilities begin to drop, resulting in a decreased throughput density. Evidently, there exists an optimum value of δ that maximizes the throughput density of the network.

Differentiating (3.13) w.r.t. δ and equating to 0 yields

$$(\phi - 2c)\delta^2 - 2\phi\delta + \phi = 0.$$

Noting that $0 \leq \delta \leq 1$, we see that ρ_T is maximized at

$$\delta_{\text{opt}} = \frac{\phi - \sqrt{2\phi c}}{\phi - 2c}, \tag{3.14}$$

irrespective of the value of N.

Figure 3.3 plots the throughput density-maximizing values of δ versus the threshold Θ for the network adopting nearest-neighbor routing and the r-TDMA MAC scheme for several values of the path loss exponent (PLE) γ. As expected intuitively, the higher the threshold Θ and/or smaller the PLE γ, the smaller is the packet success probability p_s, thus the smaller is the optimum fraction of sources δ_{opt}.

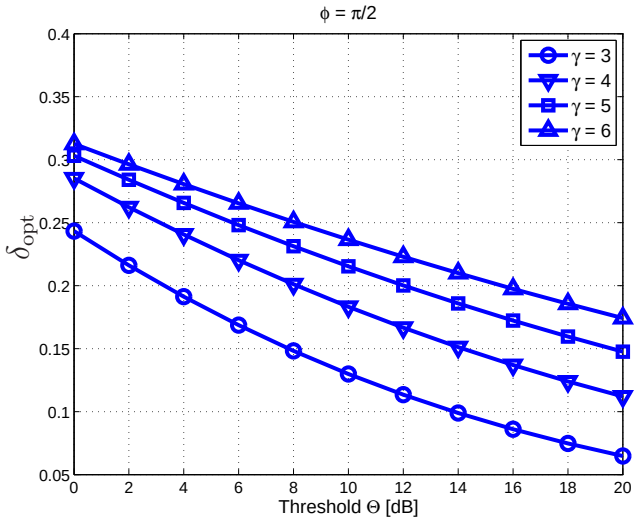

Figure 3.3. The optimum values of δ (3.14) that maximize the throughput density in the r-TDMA-based network employing the nearest-neighbor routing strategy for several Θ and γ values.

3.4.4 n^{th}-nearest-neighbor Routing ($n > 1$)

Supposing now that each relay that receives a packet forwards it to its n^{th}-nearest neighbors ($n > 1$). For a fair comparison of the routing schemes for different n, we take the total average progress[7] made by the packet to be the same for every value of n.

Now, recall that for the case $n = 1$, the mean progress[8] of the packet over $N + 1$ hops is

$$\Delta = (N+1)\mathbb{E}[R_1 \cos(\Psi)] = (N+1)\mathbb{E}[R_1]\mathbb{E}[\cos\Psi], \tag{3.15}$$

where Ψ is the argument of the destination node (see Figure 3.1). Since Ψ is uniformly distributed on $[-\phi/2, \phi/2]$, we have

$$\mathbb{E}[\cos\Psi] = \int_{-\phi/2}^{\phi/2} \frac{1}{\phi}\cos\psi \mathrm{d}\psi = \frac{2}{\phi}\sin\left(\frac{\phi}{2}\right). \tag{3.16}$$

Substituting for (3.3) and (3.16) in (3.15), we obtain the average total progress of packets (from the source to the destination) as

$$\Delta = \frac{(N+1)\sqrt{2\pi}\sin(\phi/2)}{\sqrt{(1-\delta)}\phi^{3/2}}.$$

For the general case of n^{th} nearest-neighbor routing ($n > 1$), the per-hop progress in this case is $\mathbb{E}[R_n]\mathbb{E}[\cos\Psi]$. Thus, the number of hops N' required to

[7]The progress of a packet across any link is defined as the effective distance travelled by it along the axis to the destination (see Figure 3.1). The total progress is the sum of the progresses across all the links from the source to the destination.

[8]The expectation is taken over several different realizations of the underlying PPP.

achieve the same average (total) progress is approximately

$$N' = (N+1)\mathbb{E}[R_1]/\mathbb{E}[R_n] \sim N/\sqrt{n}, \tag{3.17}$$

using (3.3). Thus, for a flow employing n^{th}-nearest neighbor routing, the number of relays in the flow is approximately $N/\sqrt{n}$.

The throughput density in the general case then becomes

$$\rho_T(N) = \frac{\delta\sqrt{n}}{2N+\sqrt{n}} \left(\frac{(1-\delta)\phi}{(1-\delta)\phi + 2\delta c} \right)^n. \tag{3.18}$$

Following the same steps as earlier, the throughput density-maximizing (optimal) value of δ is obtained as

$$\delta_{\text{opt}} = \frac{(n-1)c + \phi - \sqrt{(n-1)^2c^2 + 2n\phi c}}{(\phi - 2c)}, \tag{3.19}$$

which is also independent of N. The values of δ_{opt} versus the routing parameter n are plotted in Figure 3.4 for different values of the PLE γ.

Another critical design issue in wireless networks is determining the optimum routing parameter n. Indeed, as argued in [53], a smaller hop length does not necessarily relate to an improved network performance. Differentiating (3.18) with respect to n, and equating to 0, we obtain

$$\left(2n + \frac{n^{3/2}}{N}\right) \ln\left(1 + \frac{2\delta c}{(1-\delta)\phi}\right) - 1 = 0. \tag{3.20}$$

The throughput density-maximizing routing parameter n_{opt} may be evaluated numerically. Figure 3.5 shows optimum values of the routing parameter n_{opt} (rounded off to the nearest integer) that maximize the throughput density in

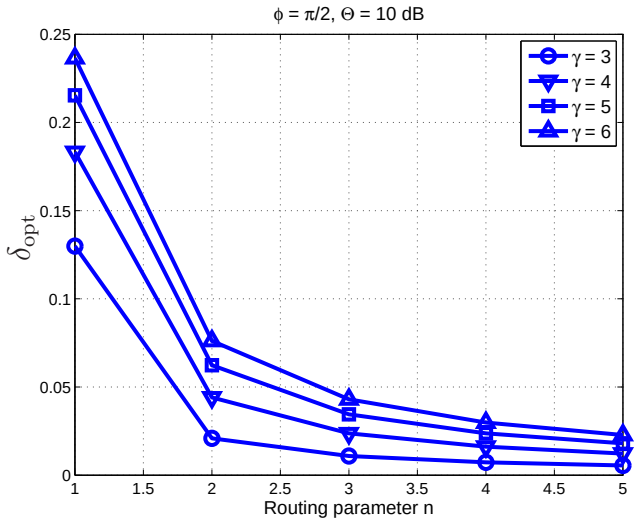

Figure 3.4. The optimum values of δ (3.19) that maximize the throughput density in the r-TDMA-based network employing the n^{th}-nearest-neighbor routing scheme for different values of Θ and γ.

the network for several values of Θ and γ.

3.5 Analysis and Design of ALOHA-based Wireless Networks

In this subsection, we analyze the end-to-end delay and throughput performances for the multihop network model considered with ALOHA. For our analysis, we use known results from the parallel TASEP literature [54].

3.5.1 Node Buffer Occupancies

Recall from (2.30) that the occupancies of nodes along a typical ALOHA-based flow are

$$\mathbb{E}\tau_i = \frac{(1-qp_s)\sum_{n=0}^{N-i} B(N-n)B(n) + qp_sB(N)}{B(N+1) + qp_sB(N)}, \tag{3.21}$$

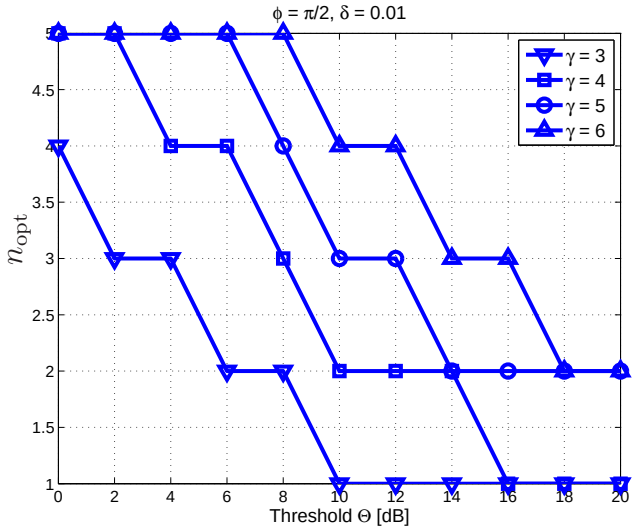

Figure 3.5. The optimum values of n (3.20) that maximize the throughput density in a r-TDMA-based network with $N = 4$ nodes versus the SIR threshold for successful transmissions, Θ.

where $B(0) = 1$, and

$$B(k) = \sum_{j=0}^{k-1} \frac{1}{k} \binom{k}{j} \binom{k}{j+1} (1 - qp_s)^j, \quad k > 0.$$

3.5.2 Packet Success Probability

We next measure the packet success probability for a typical link in the ALOHA-based network. Recall that the average number of packets (at steady state) in a flow with N relays is $1 + N/2$. With δ being the density of source nodes (or flows) and q the ALOHA contention probability, it follows that the

density of interferers for the ALOHA-based network is at most[9]

$$\lambda_{\mathrm{I}} \lessapprox \delta q \left(1 + N/2\right). \tag{3.22}$$

Even though transmissions in the network are completely uncoordinated, the interference is actually spatially and temporally correlated owing to the presence of common randomness in the locations of nodes [65]. However, for analytical tractability, we make the relaxed assumption that the set of interfering nodes forms a PPP with density λ_{I}, which is quite accurate at small q [65].

We then have the following proposition concerning the packet success probability over a typical link between a node and its n^{th}-nearest-neighbor in the ALOHA-based network.

Proposition 9. *For the ALOHA-based flow across N relays, the packet success probability p_s from any node to its n^{th}-nearest-neighbor in a sector of angle ϕ is*

$$p_s = \left(\frac{(1-\delta)\phi}{(1-\delta)\phi + 2\lambda_I c}\right)^n. \tag{3.23}$$

where λ_I is given by (3.22)*, and $c = \pi\Gamma(1+2/\gamma)\Gamma(1-2/\gamma)\Theta^{2/\gamma}$.*

Proof: The proof is equivalent to the one for Proposition 7 with the density of interferers in this case being λ_{I} (instead of δ, for the r-TDMA-based network). □

[9]This term is actually an upper bound, owing to the existence of relay nodes having multiple packets in their buffers (corresponding to several flows). The bound is tight for small q (when the density of interferers is small), or small δ (when the flows in the network themselves are sparse).

3.5.3 Steady State Throughput and Average End-to-end Delay

Recall (2.31) - the throughput across a typical flow at steady state is

$$T(N) = \frac{qB(N)}{B(N+1) + qp_sB(N)}. \tag{3.24}$$

Also, by Little's theorem [52], the end-to-end delay along a typical flow in the system is

$$D(N) = \frac{1 + N/2}{T(N)}. \tag{3.25}$$

3.5.4 Throughput Density

Putting together (3.22), (3.23) and (3.24), we obtain a bound on the throughput density for the ALOHA-based network as

$$\rho_{\mathrm{T}}(N) \gtrapprox \frac{\delta qB(N)\left(\frac{(1-\delta)\phi}{(1-\delta)\phi+2\delta q\left(1+N/(2\sqrt{n})\right)c}\right)^n}{B(N+1) + qB(N)\left(\frac{(1-\delta)\phi}{(1-\delta)\phi+2\delta q\left(1+N/(2\sqrt{n})\right)c}\right)^n}. \tag{3.26}$$

The above equation helps provide useful insights into network design. For instance, the throughput density-maximizing values of δ or n may be computed numerically using (3.26).

3.6 Common Relays Serving Multiple Flows

Note that in our analyses, we have neglected the occurrence of the event E, wherein an arbitrarily chosen relay serves multiple routes at the same time. It is important to consider E in the analysis because if it happens often, the density of interferers would be smaller. Also, the occurrence of E would mean that the average number of successful packet receptions in any time slot is reduced (as-

suming that typical values of Θ are > 1) since each relay can successfully receive at most one packet (corresponding to the transmitter with the strongest channel to that relay). Moreover, event E may lead to a 'transmit bottleneck', where relays end up with multiple packets in their buffer and the transmission scheduling algorithms may then get complicated. However, we argue in the following that ignoring the occurrence of E is not critical and that our analyses are still quite accurate. We also later verify this argument via simulation results in Section 3.7.

We begin by approximating the arrangement of flows in the network as a *Poisson line segment process* [66], according to which the mid-segment points form a PPP of density δ, and take that all the nodes involved in the flows are located on the corresponding line segments. Also, the segments are uniformly randomly oriented, and the lengths of the line segments are finite and random, drawn according to a certain distribution function $F_L(l)$. As per [66, Eqn. 14], the density of intersecting points, λ_i, is given by $\lambda_i = (\delta \mathbb{E}L)^2/\pi$. When δ is small, this is already much smaller than unity (which is the total density of the considered network). For instance, taking $\delta = 0.05$ and $\mathbb{E}L = 5$ yields $\lambda_i = 0.02 \ll 1$. Now, the density of relay nodes serving multiple flows is smaller than λ_i, since the points of intersection of the line segments do not always correspond to common relay nodes' locations. Furthermore, the probability that two nodes corresponding to two intersecting flows transmit to the same (common) relay in the same time slot for either MAC schemes (r-TDMA or ALOHA) is even smaller - given that a node in the first flow transmits a packet to that (common) relay, the probability that another node (along the second flow) also transmits to it in the same time slot[10] is simply its access probability. Thus, the occurrence of E is quite rare.

[10]The probability of $k \geq 2$ nodes transmitting to that common relay in the same time slot is $1/N^k$, and decays fast to 0 with increasing k.

A few ways to circumvent the consideration of E are as follows. First, we may assume $\delta \ll 1$, for which relays serving multiple flows are rare (as we have seen above using ideas from the theory of Poisson line segment processes), and the expression concerning the density of interferers is quite accurate. Second, the MAC scheme may be modified such that relays having multiple packets may schedule them in a sequential fashion. This however leads to an increased end-to-end delay (and a decreased throughput) since packets stay in queues longer. Third, the routing protocol may be revised such that packets are not routed through relays that already support another flow. Modeling the interference (and in turn, the success probabilities) is tricky in this case though, since the set of interferers no longer forms a PPP.

3.7 Simulation Results

We now provide simulation results to illustrate the theoretical results. All the results are obtained using MATLAB. The simulated multihop network comprises nodes arranged as a PPP with unit density on a 50×50 square. Thus, on average, there exist $2,500$ nodes in the network. We also choose the following values for the system parameters: the source density $\delta = 0.01$, the SIR threshold $\Theta = 10$ dB, the routing angle $\phi = \pi/2$, the PLE $\gamma = 4$, and the fading to be i.i.d. Rayleigh with unit mean. The throughput of each flow is measured as the rate of packets delivered to the destination, and its steady state value is computed by considering only those packets delivered during the time slots $3,000$ through $5,000$. In order to avoid border effects, we collect the metrics only for those routes completely lying in the inner square of dimensions 40×40. We obtain results from 100 different realizations of the point process, which is found to be sufficient to obtain

good statistical confidence. Figure 3.6 plots the steady state throughput density in both the r-TDMA- and ALOHA-based for $N = 4$. In both cases, we observe that the empirical and analytical values match closely for a wide range of system parameters, thus corroborating the theory.

3.8 Throughput-Delay Tradeoff

It is interesting to study the achievable tradeoff between the throughput and delay across a typical flow for both the MAC schemes. For the r-TDMA-based network, we may use (3.7) and (3.8) to see that the ratio $D(N)/T(N)$ is a cubic function of N.

As expected, the ALOHA-based network obtains a much better tradeoff since it incorporates spatial reuse. Figure 3.7 plots the ratio D/T versus N (using (2.31) and (3.25)) for the ALOHA-based network for some values of the effective link reliability $p = qp_s$. It is seen that D/T is (approximately) a linear function of N; this is verified by the dashed lines that are also shown in the figure.

We now show that the ALOHA-based network achieves the same tradeoff scaling that is obtained for the optimal operation of a wireless network flow. To this end, consider a wireless flow across N relay nodes. It is always possible to choose the *optimal spatial-reuse parameter* m, which is the minimum number of hops separating any two transmitters i and j such that both their transmissions are successful, i.e., at each receiver node, the condition SINR $> \Theta$ holds. The optimal scheduling scheme thus is to have every m^{th} node transmit simultaneously[11]. Indeed, for this case, all transmissions are successful; the network end-to-end delay is minimal, and equal to $N + 1$ time slots. Also, the throughput attains its max-

[11] A centralized scheduler is, however, required to perform this operation.

imum value (of $1/m$). Thus, the optimal throughput-delay scaling for a wireless network flow is obtained as $D \propto NT$.

The optimal scheduling that minimizes the end-to-end delay (and maximizes the throughput) in a flow with $N = 10$ relays is illustrated in Figure 3.8, for $m = 3$. This MAC scheme can be implemented by simply having all nodes with packets transmit; it can be viewed as ALOHA with transmit probability 1.

In the above scenario, all the transmissions are successful. However, in the presence of fading, unequal spacing between the nodes, or interference from other networks, transmissions can fail, and the ALOHA scheme with contention parameter 1 may perform sub-optimally. Nevertheless, this example illustrates that for efficient network operation, it is necessary that the transmitting nodes not be too closely located. In fact, for half-duplex nodes, m needs to be always kept ≥ 2. Also, since adjacent nodes cannot both transmit successfully at the same time, it is not necessary to have $K > 1$ as packets are never stacked; unit-sized buffers ($K = 1$) are sufficient for optimal network operation.

3.9 Summary

We consider a planar Poisson network comprising infinite packet flows from an infinite number of sources to their corresponding destinations. Using concepts and tools from both stochastic geometry and statistical mechanics, in particular, the TASEP particle flow model, we analytically characterize the system throughput for two different channel access schemes. We also provide valuable insights from a network design stand-point such as choosing the optimum density of transmitters and the number of hops in each route in the network such that the spatial throughput density is maximized.

We would also like to remark that we use the same (constant) number of hops N in each flow for analytical tractability, in particular to obtain closed-form expressions for the optimal network design parameters n_{opt} and δ_{opt}. The results in this chapter may however be generalized to the case wherein the lengths of the flows are different. Indeed, we may simply treat N to be a random variable with a certain distribution or a flow-specific value (that way, all destinations are at random distances from their corresponding sources); the throughput density would then simply have to be averaged w.r.t. the distribution of N.

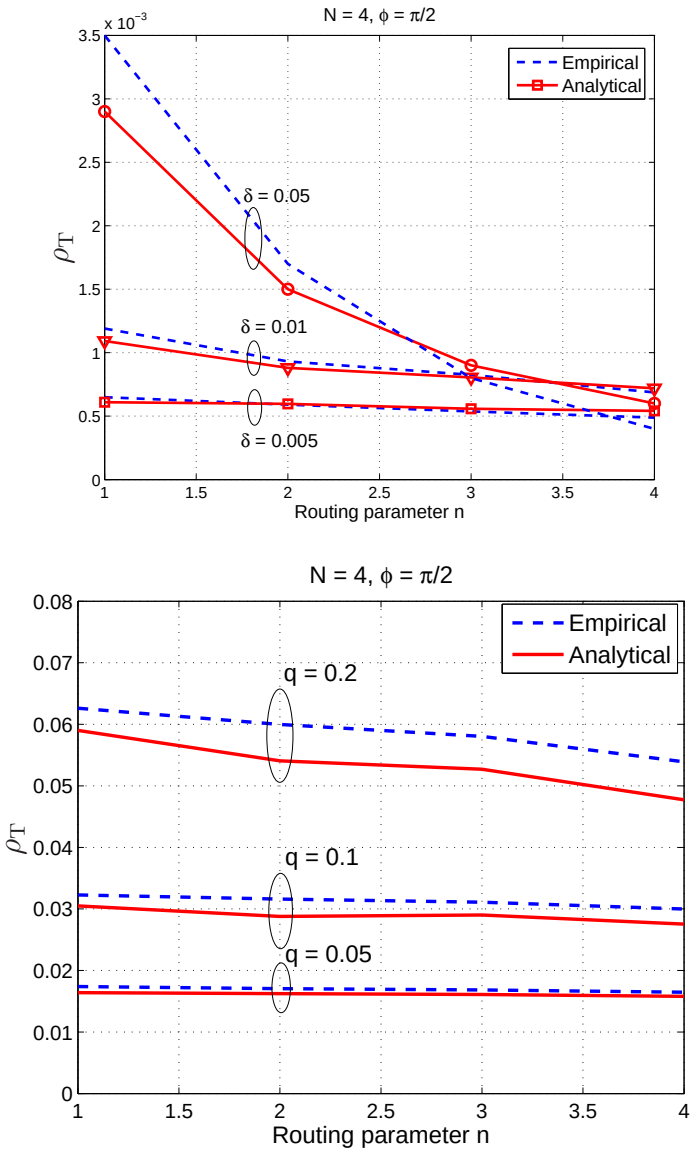

Figure 3.6: Theoretical and simulation-based plots for ρ_{T} versus the routing parameter n for r-TDMA-based (left) and ALOHA-based (right) networks. The empirical and analytical values are seen to match closely for a wide range of system parameters, validating our analysis.

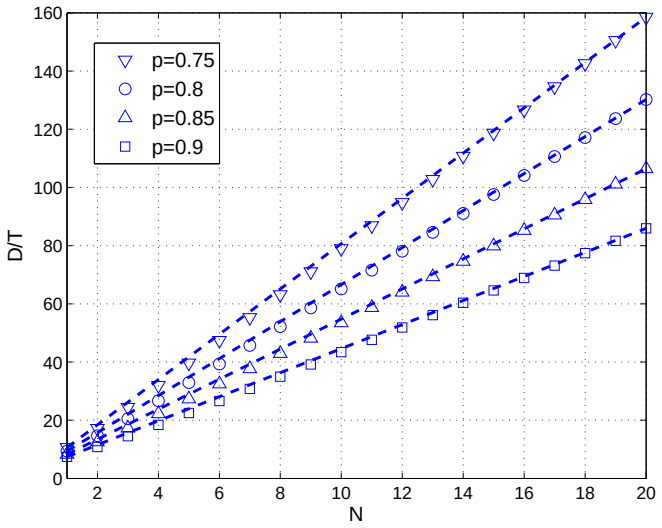

Figure 3.7. The plot of D/T versus N for the ALOHA-based network for some values of the link reliability p. The (dashed) lines $D/(NT)$ illustrate that $D \propto NT$ (approximately).

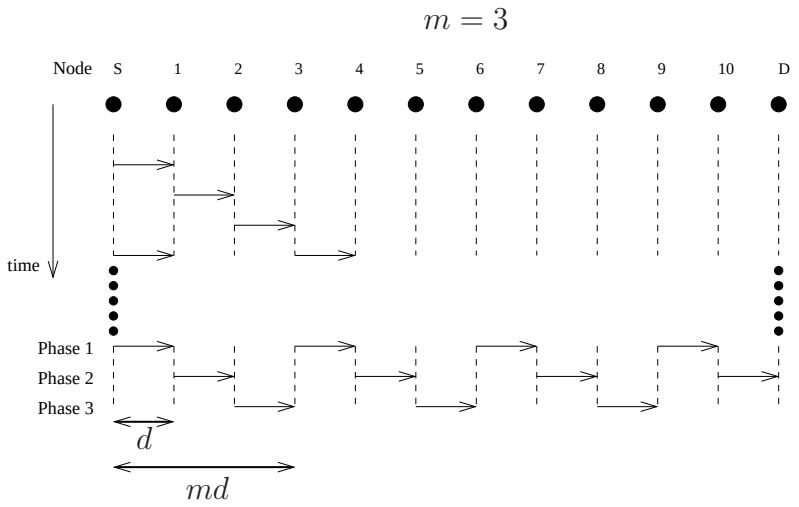

Figure 3.8. The optimal scheduling assignment (in the absence of fading) for a multihop flow with 10 relay nodes for $m = 3$. Here, d is the spacing between adjacent relays. In the steady state (long-time limit), there are three unique transmission phases, in each of which nodes three hops apart transmit simultaneously. The system achieves a throughput of 1/3 and an end-to-end delay of 11 time slots for each packet.

CHAPTER 4

MULTIHOP WIRELESS NETWORKS WITH COMPLEX TOPOLOGIES

4.1 Introduction

So far, we have considered simple multihop networks comprising a single path from every source to its corresponding destination. In general, however, the network topology is more complex than just having the source-destination pair located in a collinear fashion. Indeed, since these networks are formed on-the-fly, the same (common) relay node may form part of several routes, resulting in merging and splitting of routes in the system. Examples of network structures other than the line include tree, mesh, star and bus.

In this chapter, we consider more complex wireless network models comprising intersecting flows, and propose the partial mean-field approximation (PMFA), an elegant technique that helps tightly approximate the throughput (and end-to-end delay) performance of the system. We also demonstrate via a simple example that the PMFA procedure is quite general in that it may be used to accurately evaluate the performance of multihop networks with arbitrary topologies.

The organization of this chapter is as follows. Section 4.2 provides an overview of related literature. Section 4.3 outlines the system and channel model. Section 4.4 analyzes the throughput performances of networks with several different topologies comprising relays that serve multiple routes. It also introduces the

PMFA, a framework that is quite useful towards analyzing networks with complex topologies. Section 4.5 concludes the chapter.

4.2 Related Work

Most earlier attempts at analyzing multihop networks have neglected the correlations in the system for tractability. An approximation commonly used in this regard is *Kleinrock's Independence Assumption* [52]. Accordingly, for a densely connected network involving Poisson arrivals and uniform loading among source-destination pairs, the queues at each link in the network behave independently regardless of the interaction of traffic across different links. Kleinrock's approximation has been used to characterize the delay performance of wireless systems (see for example [68; 69]). Under general scenarios, however, this approximation may be very loose; the correlations in the system cannot be neglected.

Much of the prior work on the performance analysis of multihop networks has also focused on very small networks, (e.g., two-relay [45] or three-relay networks [67]). Their results, however, do not directly extend to larger networks. More recently, discrete-time queueing theory has been applied to the study of end-to-end delay [43] and throughput [70] performances of multihop networks. The authors however focus specifically on a linear multihop network model fed with a single flow, and do not consider intersecting flows. To the best of our knowledge, this is the first attempt at studying the throughput performances of multihop networks with arbitrary topologies.

4.3 System Model

We consider an multihop network comprising a set of source nodes intent to deliver packets to a set of destinations over an infinite duration of time in a multihop fashion. We study several different network topologies in this chapter; the specifics of each topology will be described in its corresponding analysis subsection. Time is slotted to the duration of a packet, and packet transmissions occur at slot boundaries. No power control is employed, and the transmit power at each node is taken to be unity. We take r-TDMA to be the channel access scheme.

4.4 Throughput Analysis of Networks with Arbitrary Topologies

4.4.1 Two Two-hop Flows via a Common Relay

We begin by considering the network model depicted in Figure 4.1. It comprises two source nodes S_1 and S_2 (each numbered 0 with respect to (w.r.t) its corresponding flow) intending to deliver packets to destinations D_1 and D_2 (each numbered 2) respectively, each via a common relay node R (numbered 1). Here, we take that the relay node has a buffer size of two since it accommodates two flows. Furthermore, the r-TDMA dictates that in any time slot, only one of the three nodes (S_1, S_2 or R) is (uniformly) randomly picked (w.p. 1/3) for transmission. Let p_s denote the reliability of each link. Whenever R is picked, any one of the following event occurs:

1) If the relay's buffer has no packet, it obviously does not transmit anything.

2) If the relay's buffer contains only one packet (intended for either of the destinations), that packet is transmitted.

3) If the relay's buffer has two packets (to be forwarded to both the destinations), it transmits either the packet intended for D_1 w.p. ω or the packet meant for D_2 w.p. $1-\omega$. Note that priority-based routing may be modeled by setting $\omega = 1$ (prioritizing the first flow) or $\omega = 0$ (for the second flow). $\omega = 0.5$ models having equal priorities for the flows.

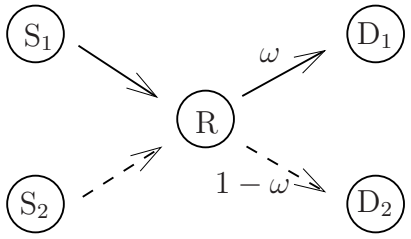

Figure 4.1. The two flows $S_1 \rightarrow R \rightarrow D_1$ and $S_2 \rightarrow R \rightarrow D_2$, each occurring via the relay node R are represented by solid and dashed arrows respectively. When the relay node contains two packets, it routes either the packet meant for D_1 w.p. ω or the one for D_2 w.p. $1-\omega$. The probability of a successful transmission across all links is p_s.

For notational convenience, let $\tau_j^{[i]}$ represent the steady state configurations for the buffers across the two flows, $i = \{1, 2\}$, for each of the three nodes involved in each flow, numbered $j = \{0, 1, 2\}$. By definition, $\tau_0^{[1]} = \tau_0^{[2]} = 1$ and $\tau_2^{[1]} = \tau_2^{[2]} = 0$. We shall now derive the steady state throughput, $T^{[1]}$, for the first flow; $T^{[2]}$ may simply be obtained by replacing ω by $1-\omega$.

Using the fact that for each flow, the throughput across each link is the same (2.11), we get from 1) - 3),

$$\mathbb{E}\left[1-\tau_1^{[1]}\right]=\mathbb{E}\left[\tau_1^{[1]}\left(1-(1-\omega)\,\tau_1^{[2]}\right)\right], \tag{i}$$

and

$$\mathbb{E}\left[1-\tau_1^{[2]}\right]=\mathbb{E}\left[\tau_1^{[2]}\left(1-\omega\tau_1^{[1]}\right)\right] \tag{ii}$$

for the first and second flows, respectively. In order to solve the above equations analytically, we can use the *mean-field approximation* (MFA) [26], according to which all the correlations between the buffer occupancies are neglected. Mathematically, the MFA takes that

$$\mathbb{E}\left[\tau_i^{[j]}\tau_k^{[l]}\right]=\mathbb{E}\tau_i^{[j]}\mathbb{E}\tau_k^{[l]},$$

for all (valid) node pairs (i,k) and flow pairs (j,l).

For this example in particular, we assume that $\mathbb{E}\left[\tau_1^{[1]}\tau_1^{[2]}\right]=\mathbb{E}\tau_1^{[1]}\mathbb{E}\tau_1^{[2]}$. Employing the MFA and the simplified notation $\mathbb{E}\tau_1^{[1]}=x$, $\mathbb{E}\tau_1^{[2]}=y$ in (i) and (ii), we obtain

$$\begin{aligned} 1-x &= x-(1-\omega)xy \\ 1-y &= y-\omega xy. \end{aligned}$$

Solving the above equations simultaneously, we obtain the only meaningful solution as

$$x=\frac{2\omega+3-\sqrt{4\omega^2-4\omega+9}}{4q}.$$

Since the channel access probability for each node in the system is 1/3, we see that the throughput for the flow $S_1 \rightarrow R \rightarrow D_1$ is given by

$$T^{[1]}(\omega) = \frac{p_s \mathbb{E}\tau_1^{[1]}}{3} = \frac{p_s \left(2\omega - 3 + \sqrt{4\omega^2 - 4\omega + 9}\right)}{12\omega}. \tag{4.1}$$

When $\omega = 1$, i.e., when the first flow is always given priority over the second flow, $T^{[1]}(1) = p_s/6$. On the other hand, when $\omega = 0$, we use the L´ Hôpital rule to see that $T^{[1]}(0) = p_s/9$. When both flows are prioritized equally, $T^{[1]}(0.5) = T^{[2]}(0.5) = p_s(\sqrt{2} - 1)/3$. The achievable set of throughput for the first flow, $T^{[1]}$ is plotted in Figure 4.2 for different values of p_s. For comparison, we have also shown empirical results, which match the theoretical ones (4.1) closely, in particular when p_s is small.

4.4.2 Two Three-hop Flows via a Common Relay

We next consider the case where again, the two source nodes S_1 and S_2 intend to deliver packets to different destinations D_1 and D_2 respectively. Here, however, we take that in each flow, packets traverse two hops each, one of which is the common relay. Evidently, the common relay may be the node numbered 1 or node one numbered 2 (see Figure 4.3). The channel access probability for each node is 1/5.

4.4.2.1 Common Relay: Node 1

We first analyze the case wherein the common relay is the node numbered 1. Since the throughput across each link is the same (for each flow), we obtain at

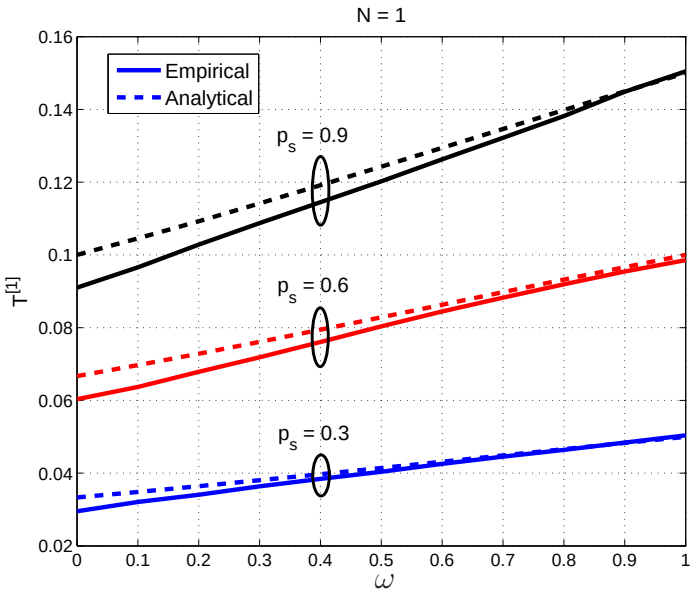

Figure 4.2. Steady state throughput across the first flow, $T^{[1]}$ versus ω for several values of the link success probability p_s. The results obtained numerically (dashed lines) closely approximate the empirical results (solid lines).

steady state,

$$1 - \mathbb{E}\tau_1^{[1]} = \mathbb{E}\left[\tau_1^{[1]}\left(1 - (1-\omega)\,\tau_1^{[2]}\right)\left(1 - \tau_2^{[1]}\right)\right] = \mathbb{E}\tau_2^{[1]},$$

and

$$1 - \mathbb{E}\tau_1^{[2]} = \mathbb{E}\left[\tau_1^{[2]}\left(1 - \omega\tau_1^{[1]}\right)\left(1 - \tau_2^{[2]}\right)\right] = \mathbb{E}\tau_2^{[2]},$$

Evidently, when $\omega = 1$, the second flow (the one without the priority) does not affect the throughput across the first flow. Following (2.6), $\mathbb{E}\tau_2^{[1]} = 2/5$; $T^{[1]}(1) = p_s\mathbb{E}\tau_2^{[1]}/5 = 0.08p_s$.

For general ω, we may use the MFA to analytically evaluate the throughput.

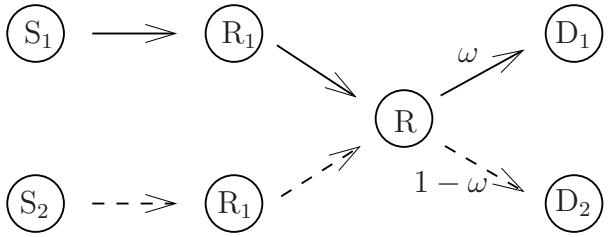

Figure 4.3. The two three-hop flows $S_1 \to R_1 \to R \to D_1$ and $S_2 \to R_2 \to R \to D_2$, each occurring via the relay R are represented by solid and dashed lines respectively. In this case, the common relay is the node numbered 2.

Indeed, setting $\mathbb{E}\tau_1^{[1]} = x$, $\mathbb{E}\tau_1^{[2]} = y$, $\mathbb{E}\tau_2^{[1]} = u$ and $\mathbb{E}\tau_2^{[2]} = v$, we obtain the following set of 4 equations:

$$\begin{aligned} 1-x &= u \\ u &= x(1-u)(1-(1-\omega)y) \\ 1-y &= v \\ v &= y(1-v)(1-\omega x), \end{aligned}$$

which may be solved numerically. It is easily seen that when $\omega = 0$, the first flow does not affect the throughput across the second flow. From (2.6), $\mathbb{E}\tau_1^{[2]} = 3/5$, so that

$$\mathbb{E}\tau_1^{[1]} = \frac{9-\sqrt{65}}{4} \approx 0.234,$$

and $T^{[1]}(0) = \mathbb{E}\tau_1^{[1]} p_s/5 \approx 0.047 p_s$.

4.4.2.2 Common Relay: Node 2

We now consider the case when the common relay is the node numbered 1. For this scenario, we have

$$1 - \mathbb{E}\tau_1^{[1]} = \mathbb{E}\left[\tau_1^{[1]}\left(1 - \tau_2^{[1]}\right)\right] = \mathbb{E}\left[\tau_2^{[1]}\left(1 - (1-\omega)\,\tau_2^{[2]}\right)\right],$$

and

$$1 - \mathbb{E}\tau_1^{[2]} = \mathbb{E}\left[\tau_1^{[2]}\left(1 - \tau_2^{[2]}\right)\right] = \mathbb{E}\left[\tau_2^{[2]}\left(1 - \omega\tau_2^{[1]}\right)\right].$$

Using similar arguments as earlier, we obtain $T^{[1]}(1) = 0.08p_s$. When $\omega = 0$, $\mathbb{E}\tau_2^{[2]} = 3/5$, and employing the MFA, we have $T^{[1]}(0) = (11 - \sqrt{85})/30 \approx 0.06p_s$.

The above analysis suggests that the throughput across the flow is higher when the bottleneck node is closer to the destination (also see Figure 4.4). This is explained by the fact that the node occupancies monotonically decrease with proximity to the destination.

4.4.3 Multiple Flows via a Common Relay

Next, we consider a network topology comprising multiple (> 2) flows passing through a common relay (see Figure 4.5). Here the source nodes S_1,S_2,...,S_n attempt to deliver packets to their corresponding destinations D_1,D_2,...,D_n, through a common relay node R (that has a buffer size of n). We also take that routing is priority-based with packets intended for D_1 having the highest priority and those meant for D_n the lowest. Thus, the relay node transmits the packet meant for node k, $1 \leq k \leq n$, only when it does not have other packets corresponding to the destination nodes D_j, $j < k$ in its buffer.

Since the throughput of each flow is conserved, we obtain the following set of

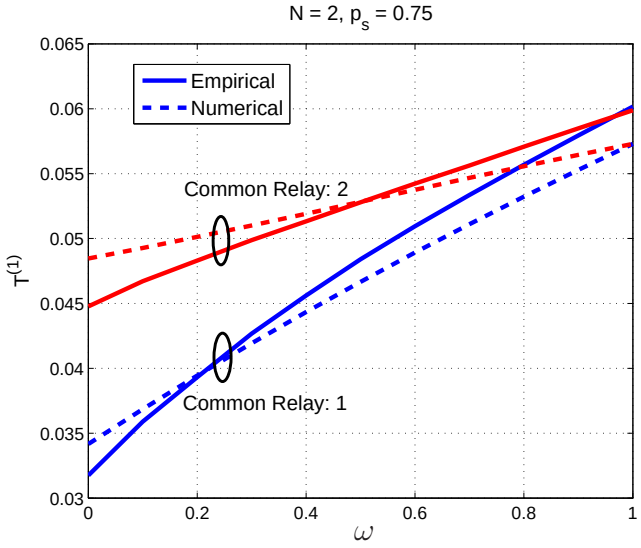

Figure 4.4. Steady state throughput across the first flow, $T^{[1]}$ versus ω for $p_s = 0.75$ for different locations of the common relay node. The results obtained numerically (dashed lines) closely approximate the empirical results (solid lines).

equations:

$$\begin{aligned} 1 - \mathbb{E}\tau_1^{[1]} &= \mathbb{E}\tau_1^{[1]} \\ 1 - \mathbb{E}\tau_1^{[2]} &= \left(1 - \mathbb{E}\tau_1^{[1]}\right) \mathbb{E}\tau_1^{[2]} \\ &\vdots \\ 1 - \mathbb{E}\tau_1^{[n]} &= \prod_{i=1}^{n-1} \left(1 - \mathbb{E}\tau_1^{[i]}\right) \mathbb{E}\tau_1^{[n]} \end{aligned}$$

Solving the above set of equations using the MFA yields $\mathbb{E}\tau_1^{[k]} = k/(k+1)$, $1 \leq k \leq n$. In this case, the channel access probability for each node is $1/(n+1)$, so that

$$T^{[k]} = \frac{1 - \mathbb{E}\tau_1^{[k]}}{n+1} = \frac{1}{(k+1)(n+1)}, \quad 1 \leq k \leq n. \tag{4.2}$$

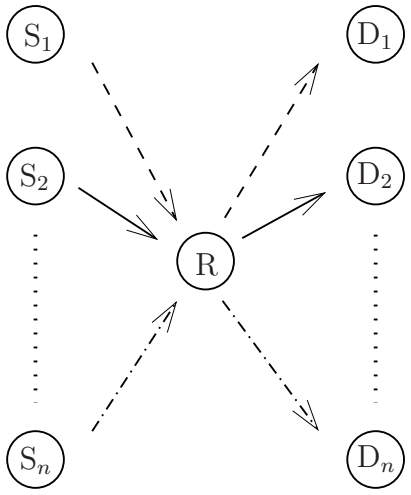

Figure 4.5. n flows $S_1 \to D_1$, $S_2 \to D_2$, ..., $S_n \to D_n$ passing through a common relay node R. When routing, packets intended for D_1 are taken to have the highest priority, and those meant for D_n, the lowest.

4.4.4 The Partial Mean-Field Approximation

While the MFA tightly approximates the throughput performance of networks comprising short flows, it can get loose, in particular when the flows in the network traverse several nodes, since it neglects the correlations between all the node occupancies. In this subsection, we present the partial mean-field approximation (PMFA), which (as we shall see later) is more accurate than the MFA. Later, in Subsection 4.4.5, we illustrate (via a simple example) how to employ the PMFA framework to evaluate the throughput performance of a network with an arbitrary topology.

We begin by considering a scenario where two general multihop flows (of arbitrary lengths) both pass through a common relay node. Suppose that source node S_1 delivers data to D_1 in a multihop fashion via N_1 nodes, while S_2 forwards

packets to D_2 via N_2 relays, each via a common relay node R (see Figure 4.6). We take that R is numbered $1 \leq n_1 \leq N_1$ w.r.t. the first flow, and $1 \leq n_2 \leq N_2$ w.r.t. the second flow.

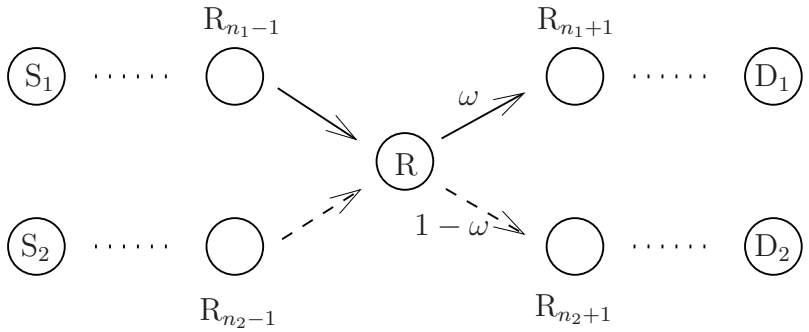

Figure 4.6. Two multihop flows $S_1 \rightarrow D_1$ and $S_2 \rightarrow D_2$ across N_1 and N_2 nodes each occur via a common relay node R. The common relay is numbered n_1 and n_2 w.r.t. the first and second flows respectively.

In principle, the MFA may be used to compute the steady state throughput of each flow. Indeed, we get for the first flow

$$\begin{aligned} 1-\mathbb{E}\tau_1^{[1]} &= \mathbb{E}\left[\tau_1^{[1]}\left(1-\tau_2^{[1]}\right)\right] = \dots \\ &= \mathbb{E}\left[\tau_{n_1}^{[1]}\left(1-\tau_{n_1+1}^{[1]}\right)\left(1-(1-\omega)\,\tau_{n_2}^{[2]}\right)\right] \\ &= \dots = \mathbb{E}\left[\tau_{N_1-1}^{[1]}\left(1-\tau_{N_1}^{[1]}\right)\right] = \mathbb{E}\tau_{N_1}^{[1]}, \end{aligned}$$

and the second flow

$$\begin{aligned} 1-\mathbb{E}\tau_1^{[2]} &= \mathbb{E}\left[\tau_1^{[2]}\left(1-\tau_2^{[2]}\right)\right] = \ldots \\ &= \mathbb{E}\left[\tau_{n_2}^{[2]}\left(1-\tau_{n_2+1}^{[2]}\right)\left(1-\omega\tau_{n_1}^{[1]}\right)\right] \\ &= \ldots = \mathbb{E}\left[\tau_{N_2-1}^{[2]}\left(1-\tau_{N_2}^{[2]}\right)\right] = \mathbb{E}\tau_{N_2}^{[2]}. \end{aligned}$$

Employing the MFA, the above set of N_1+N_2 equations may be solved for the N_1+N_2 buffer occupancies, and consequently, the throughput of the networks at steady state for any $0 \leq \omega \leq 1$. However, as aforementioned, the MFA neglects all the correlations between the node occupancies.

We now present a tighter approximation, which we term the partial mean-field approximation (PMFA), wherein the correlations between the occupancies of nodes involved in intersections alone are neglected[1]. The basic idea behind PMFA is to "cut" the network flow into constituent linear flows, and to use the fact that the throughput across each cut (or linear segment) in the flow is the same. To this end, we present the following lemma.

Lemma 5. *Consider an r-TDMA-based multihop network with N nodes (the channel access probability for each node is $1/(N+1)$). Let p_s denote the packet success probability across each link in the network. The throughput across a cut in the network comprising n nodes with influx and outflux rates and hopping probability α, β and p_s respectively (see Figure 2.5) is given by*

$$T(\alpha,\beta,n) = \begin{cases} p_s/(N+1) \times \min\{\alpha,\beta\} & n=0 \\ p_s/(N+1) \times \frac{Z(\alpha,\beta,n-1)}{Z(\alpha,\beta,n)} & n \geq 1, \end{cases}$$

[1]The PMFA gives exact performance results in networks without intersections, i.e., for a linear flow of packets. The MFA, on the other hand, is fairly inaccurate [37].

where $Z(\alpha, \beta, 0) = 1$ *and*

$$Z(\alpha, \beta, n) = \sum_{i=1}^{n} \frac{i(2n-1-i)!}{n!(n-i)!} \frac{(1/\beta)^{i+1} - (1/\alpha)^{i+1}}{1/\beta - 1/\alpha}, n \geq 1.$$

Proof: Proving the case $n = 0$ is straightforward; the rate of packet flow across the cut is the minimum of the influx and outflux rates, multiplied by the channel access and success probabilities ($1/(N+1)$ and p_s respectively).
For the case $n \geq 1$, the throughput across the flow is (2.10)

$$T(\alpha, \beta, n) = \frac{p_s \mathbb{E}\tau_n}{N+1} = \frac{p_s}{N+1} \frac{\langle W|C^{N-1}|V\rangle}{\langle WC^N|V\rangle}.$$

From [37, Eqn. 39], the lemma is established. □

We now show how to use the PMFA framework to evaluate the throughput for the multihop network shown in Figure 4.6. First, we cut each flow across S → D at the common relay node R to form two line network flows. Thus, the flow $S_1 \rightarrow D_1$ is split into flows $S_1 \rightarrow R_{n_1}$ and $R_{n_1} \rightarrow D_1$. Now, the flow $S_1 \rightarrow R_{n_1}$ may be modeled as a line network flow across $n_1 - 1$ relay nodes (considering R_{n_1} as the destination node for that flow); it has an influx rate of 1 and an effective outflux rate of $\beta_{\text{eff}}^{(1)} = 1 - \mathbb{E}\tau_{n_1}^{[1]}$. Likewise, for the latter flow spanning $N_1 - n_1$ relays (through nodes R_{n_1} to D_1), the effective influx rate is $\alpha_{\text{eff}}^{(1)} = \mathbb{E}\left[\tau_{n_1}^{[1]}\left(1 - (1-\omega)\tau_{n_2}^{[2]}\right)\right]$, and the outflux rate is 1. Since the throughput across each cut is the same, we have

$$T(1, \beta_{\text{eff}}^{(1)}, n_1) = T(\alpha_{\text{eff}}^{(1)}, 1, N_1 - n_1). \quad \text{(i)}$$

Similarly, considering the second flow, we obtain

$$T(1, \beta_{\text{eff}}^{(2)}, n_2) = T(\alpha_{\text{eff}}^{(2)}, 1, N_2 - n_2), \tag{ii}$$

where $\beta_{\text{eff}}^{(2)} = 1 - \mathbb{E}\tau_{n_2}^{[2]}$ and $\alpha_{\text{eff}}^{(2)} = \mathbb{E}\left[\tau_{n_2}^{[2]}\left(1 - \omega\tau_{n_1}^{[1]}\right)\right]$.

One may then use (i) and (ii) in conjunction with Lemma (5) to solve for the two unknowns $\mathbb{E}\tau_{n_1}^{[1]}$ and $\mathbb{E}\tau_{n_2}^{[2]}$, and subsequently evaluate the throughputs across the two flows.

4.4.5 A Toy Example

We now describe how to use the PMFA to approximate the throughput performance of networks with arbitrary topologies. As intuitively expected, the PMFA method outperforms the MFA method. For the purpose of illustration, we consider a simple example comprising two six-hop flows across two common relays (see Figure 4.7). The packet routing priorities for the first flow $S_1 \rightarrow D_1$ at the common relay nodes R_1 and R_5 are ω_1 and ω_2 respectively. We evaluate the throughput only for the first flow; the computation of the throughput of the second flow is quite similar.

The main idea to use is that for each flow, the throughput into a common relay node equals the throughput out of it. Accordingly, we make some "cuts" along the multihop flow, and equate the throughputs across the constituent linear flows. For the toy example shown in Figure 4.7, we make two cuts I and II along the flow.

Now, for notational convenience, let $\mathbb{E}\tau_1^{[1]} = x$, $\mathbb{E}\tau_5^{[1]} = y$, $\mathbb{E}\tau_1^{[2]} = z$ and $\mathbb{E}\tau_5^{[2]} = w$. Since the rate of packet flow across each cut is the same, we obtain for

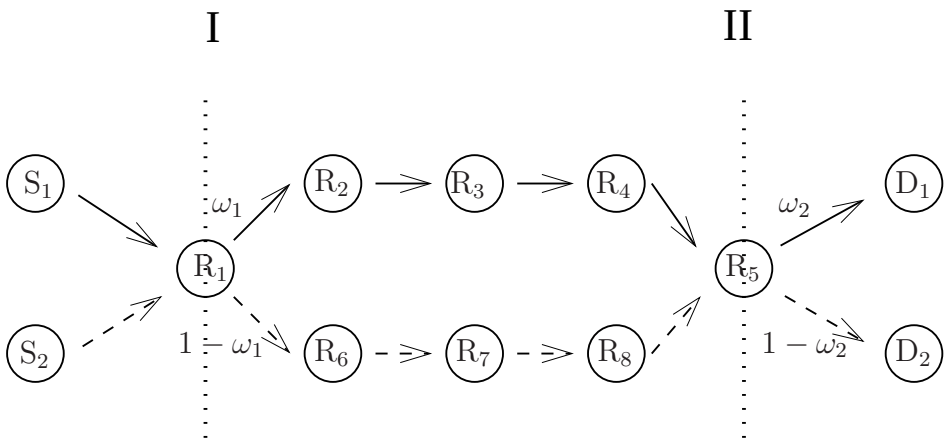

Figure 4.7. A toy example consisting of two multihop flows $S_1 \rightarrow D_1$ and $S_2 \rightarrow D_2$. The packet routing priorities at the common relay nodes R_1 and R_5 are ω_1 and ω_2 respectively. The dotted lines I and II represent two cuts along the flow.

the two flows, $S_1 \rightarrow D_1$ and $S_2 \rightarrow D_2$,

$$\begin{aligned} T(1, 1-x, 1) &= T(x(1-(1-\omega_1)z), 1-y, 3), \\ T(1, 1-x, 1) &= T(y(1-(1-\omega_2)w), 1, 1) \end{aligned}$$

and

$$\begin{aligned} T(1, 1-z, 1) &= T(z(1-\omega_1 x), 1-w, 3), \\ T(1, 1-z, 1) &= T(w(1-\omega_2 y), 1, 1) \end{aligned}$$

respectively. The above 4 equations may be solved to obtain the unknowns x, y, z and w. The channel access probability for each node is 1/10; the steady state steady state throughput is $T^{[1]} = p_s(1-x)/10$.

Alternatively, one may use the MFA to evaluate the throughput across the first flow at steady state. For simplicity of notation, let $\mathbb{E}\tau_1^{[1]} = x_1$, $\mathbb{E}\tau_2^{[1]} = x_2$, $\mathbb{E}\tau_3^{[1]} = x_3$, $\mathbb{E}\tau_4^{[1]} = x_4$, $\mathbb{E}\tau_5^{[1]} = x_5$, $\mathbb{E}\tau_1^{[2]} = x_6$, $\mathbb{E}\tau_2^{[2]} = x_7$, $\mathbb{E}\tau_3^{[2]} = x_8$, $\mathbb{E}\tau_4^{[2]} = x_9$ and $\mathbb{E}\tau_5^{[2]} = x_{10}$. We obtain the following 10 equations:

$$\begin{aligned}
1 - x_1 &= x_1(1 - x_2)(1 - (1 - \omega_1)x_6) \\
1 - x_1 &= x_2(1 - x_3) \\
1 - x_1 &= x_3(1 - x_4) \\
1 - x_1 &= x_4(1 - x_5) \\
1 - x_1 &= x_5(1 - (1 - \omega_2)x_{10}) \\
1 - x_6 &= x_6(1 - x_7)(1 - \omega_1 x_1) \\
1 - x_6 &= x_7(1 - x_8) \\
1 - x_6 &= x_8(1 - x_9) \\
1 - x_6 &= x_9(1 - x_{10}) \\
1 - x_6 &= x_{10}(1 - \omega_2 x_5),
\end{aligned}$$

which may be solved numerically to obtain the steady state occupancies for any ω_1, ω_2. Again, we have $T^{[1]} = (1 - x_1)p_s/10$. Compared to the PMFA method, the MFA approach, however, neglects correlations between the occupancies of all pairs of nodes, and in particular, between the occupancies of nodes R_2, R_3 and R_4.

Figure 4.8 plots the (steady state) throughput $T^{[1]}$ across the first flow versus ω_1 for $\omega_2 = 0.5$, obtained upon using both the MFA and PMFA approaches, as well as simulation results. The plots show that the throughput evaluation from the PMFA framework closely matches the empirical result and is more accurate

compared to the results yielded by the MFA approach, in particular, for high ω_1.

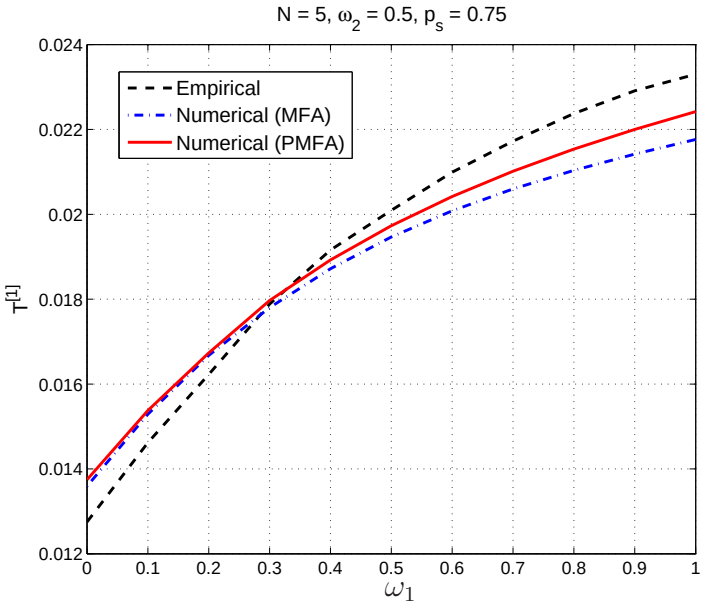

Figure 4.8. Steady state throughput across the first flow, $T^{[1]}$ versus ω_1 for $\omega_2 = 0.5$ and $p_s = 0.75$. The results obtained numerically using the PMFA framework (solid line) closely approximate the empirical results, and is more accurate than the MFA approach (dashed line).

4.5 Summary

In this chapter, we have employed ideas from the TASEP literature to study multihop networks with random access. Specifically, we have introduced the PMFA framework, a more accurate version of the MFA, which helps (tightly)

quantify the throughput performances of multihop network models with arbitrary topologies.

CHAPTER 5

THROUGHPUT-DELAY-RELIABILITY TRADEOFFS IN MULTIHOP NETWORKS

5.1 Introduction

Performance goals in wireless networks often conflict with one another. For instance, it is hardly possible to guarantee a high rate of transmission, i.e., throughput (or a small end-to-end delay) in conjunction with highly reliable packet delivery, due to the random transmission errors caused by the unpredictable behavior of the wireless channel. In particular, when the link qualities in the system are poor, packets require to be retransmitted several times across hops in order to assure reliable end-to-end delivery. This, however, leads to queueing of packets at the relay nodes, resulting in an unreasonably large average end-to-end delay, as well as a low rate of transmission. Evidently, there exist tradeoffs between the throughput, the end-to-end delay and reliability of multihop networks.

So far in this thesis, we have considered networks with unit reliability (guaranteed delivery). In scenarios where reliable delivery of packets is not very critical, a viable solution to balance end-to-end delay and reliability is to have the nodes forcibly drop a small fraction of packets. That way, even though the network reliability is reduced slightly, the queueing delay of packets can be lessened considerably. In order to determine the optimal operating point of the system and

effectively study the achievable quality of service offered by the network, it is important to analyze the throughput-delay-reliability (TDR) tradeoffs, which is the primary focus of this chapter.

We consider a multihop wireless network consisting of several source-destination pairs communicating with each other employing the slotted ALOHA channel access mechanism, and present an analytical framework that helps quantify the TDR performances of the system. We find that while in the noise-limited regime, dropping a small fraction of packets in the network leads to a smaller end-to-end delay at the cost of reduced throughput, in the interference-limited scenario, dropping a few packets in the network can help mitigate the interference in the network leading to an increased throughput. We also present some empirical (simulation-based) results which closely match the values obtained analytically.

5.1.1 Related Work

Scaling laws governing the tradeoff between throughput and delay in wireless networks comprising several users are a fairly well-investigated topic [71], [72]. More recently, the effect of dropping packets on the delay and throughput performance of single-hop wireless networks has been studied [47]. However, little work exists towards characterizing TDR tradeoffs in the context of multihop wireless network flows comprising a finite number of relays.

In [73], the authors evaluate the delay-reliability tradeoff in a wireless line network for a bounded delay packet dropping strategy employing queueing theory. However, their analysis neglects the dependence of the link success probabilities on the packet dropping event. In [74], the author uses the notion of transmission capacity to characterize the TDR tradeoffs in wireless networks employing a packet

dropping scheme based on limited retransmissions. However, it is assumed that all nodes in the network are backlogged, i.e, always have packets to transmit.

In this work, we use some ideas from the literature on statistical mechanics, in particular the totally asymmetric simple exclusion process, a particle flow model, and the mean-field approximation (MFA). Employing these tools, we present a simple framework to analyze multihop networks, which also has the advantage of obviating the often-unwieldy queueing theory-based analysis (that is typically used to study multihop networks). To the best of our knowledge, this is the first attempt at quantifying the TDR performances of ALOHA-based multihop wireless networks, all together, whilst explicitly taking into consideration the nodes' buffer states and the effect of dropping packets on the interference in the network.

The rest of this chapter is organized as follows. Section 5.2 describes the considered multihop network model, and also outlines the channel access, routing and buffering schemes considered in this chapter. Section 5.3 studies the TDR tradeoffs in multihop networks, treating the noise-limited and interference-limited regimes separately. Section 5.4 concludes the chapter.

5.2 System Model

We consider the same system model as described in Section 3.2. Just to recap, the multihop network comprised of an infinite number of source nodes, each of which intends to establish a (in general, multihop) flow of packets to a certain destination node lasting over an infinite duration of time. The distribution of source nodes is assumed to be a homogeneous Poisson point process (PPP) on the infinite plane $\mathbb{R}^2$ with density δ. Additionally, the network consists of a countably infinite population of other nodes (potential relays and destinations) arranged as

a homogeneous PPP with density $1-\delta$. Thus, the total density of the network is (without loss of generality) equal to unity. For each source node, the destination node is chosen at a random orientation, and at a random finite distance.

As described in Chapter 3, the probability of a successful transmission at the receiver at y is given by

$$p_s = \mathbb{P}\left(\frac{G_{x_j y}\|x_j - y\|^{-\gamma}}{N_0 + I_{\Phi\setminus\{x_j\}}(y)} \geq \Theta\right), \tag{5.1}$$

where N_0 denotes the noise (AWGN) variance.

We remark that since the distribution of nodes is homogeneous, it is sufficient to analyze a "typical" flow in the system. All the results in this chapter are obtained for an "average" network, that is the one obtained upon averaging over all possible realizations of the channels and the underlying point processes.

5.2.1 MAC Scheme: slotted ALOHA

We assume that transmissions in the network are completely uncoordinated; the transmission scheme is slotted ALOHA. Accordingly, in each time slot, every node *having a packet* independently transmits with some (contention) probability q or remains idle w.p. $1-q$.

5.2.2 Performance Metrics

We are interested in the performance of the multihop network in its *steady state* (as $t \to \infty$). The performance of the system is characterized based on three end-to-end metrics, throughput, mean end-to-end delay and reliability, each evaluated for a typical flow at steady state. They are formally defined as follows.

- The per-flow **throughput** T, is defined as the average number of packets

successfully delivered (to the destination) in unit time, along a typical flow in the network.

- The **mean end-to-end delay**, D, is defined as the average number of time slots it takes for the packet at the head of the source node[1] to successfully hop to the destination.

- The **end-to-end reliability** R is defined as the fraction of packets generated at the source that are eventually successfully delivered. By definition, $0 \leq R \leq 1$.

5.3 TDR Characterization for the ALOHA-based Wireless Network

In this section, we introduce a framework based on mean-field theory that we will employ to characterize the TDR tradeoffs for the considered multihop network model. For analytical tractability, we neglect the interactions between flows that occur via common relays[2]. We treat the noise-limited and interference-limited regimes separately.

5.3.1 The Noise-limited Regime

We first consider the scenario where the noise power in the network is much stronger than the interference. This occurs, for instance, when the source density δ is small, or when the path loss exponent γ is large. Transmission success events

[1]Note that we consider only the *in-network* delay since the source nodes are always backlogged.

[2]In other words, it is not possible for the same common relay node transmit or receive multiple packets (corresponding to different flows) simultaneously. This assumption is quite reasonable for small values of the contention parameter q or small δ (when the flows in the network themselves are sparse).

across links are independent of the configurations of other nodes in the network and occur w.p. $p_s = \mathbb{P}(\text{SNR} \geq \Theta)$.

5.3.1.1 Case 1: $R = 1$

We first consider the case with perfect reliability: all packets along each flow are retransmitted until they are successfully received. As described earlier (see Section 2.6.2.1),

$$\mathbb{E}\tau_i = \frac{(1-qp_s)\sum_{n=0}^{N-i} B(N-n)B(n) + qp_sB(N)}{B(N+1) + qp_sB(N)}, \tag{5.2}$$

where $B(0) = 1$, and

$$B(k) = \sum_{j=0}^{k-1} \frac{1}{k}\binom{k}{j}\binom{k}{j+1}(1-qp_s)^j, \quad k > 0.$$

Recalling (3.24) and (3.25) respectively, we have the steady state throughput at full reliability ($R = 1$) for an ALOHA-based line flow along N relays to be

$$T = \frac{qp_sB(N)}{B(N+1) + qp_sB(N)}, \tag{5.3}$$

while the average end-to-end delay is given by

$$D = (1 + N/2)/T. \tag{5.4}$$

Evidently, $T \to 0$ while $D \to \infty$ as $p_s \to 0$. Also, as $N \to \infty$, $T \to \left(1 - \sqrt{1-qp_s}\right)/2$ (2.32). It is interesting to note that irrespective of the values of q and p_s, the product of throughput and average delay for the $R = 1$ case is equal to the constant $1 + N/2$.

Figure 5.1 plots a portion of the TDR region for the slotted ALOHA-based flow with $R = 1$ and $q = 0.2$, for different values of N; they are essentially hyperbolas along the $R = 1$ axis. For each value of N, the curves are obtained by plotting the throughput (5.3) and delay (5.4) for different values of p_s.

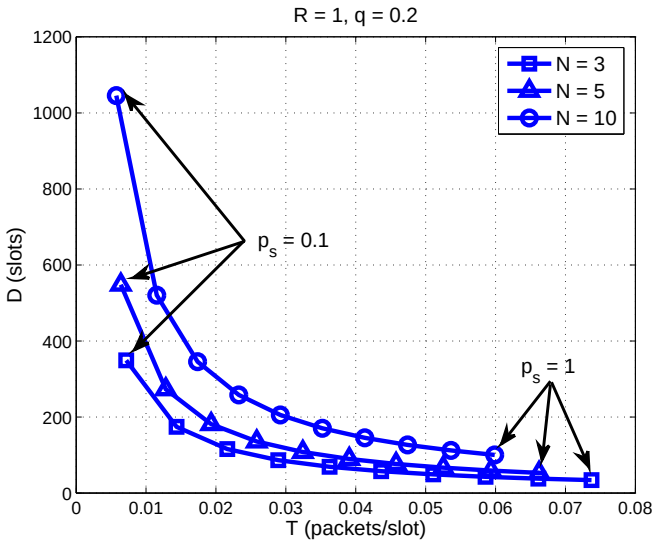

Figure 5.1. A portion of the region (for $p_s = \{0.1, \ldots, 1\}$) depicting the mean end-to-end delay versus the throughput for the ALOHA-based network, along the $R = 1$ axis. For each value of N, the TD curve is a hyperbola.

5.3.1.2 Case 2: $R < 1$

For the case with 100% reliability, the delay and throughput performances of the network are very poor, in particular when the link reliability p_s is small. In

order to achieve favorable TDR tradeoffs, relay nodes may instead choose to drop a small fraction of packets. In the rest of this chapter, we consider a *stochastic packet dropping scheme* which is straightforward to implement in a distributed fashion (with zero overhead). Accordingly, at every time slot, each node having a packet decides to drop the packet in its buffer or not stochastically (based on the toss outcome of a biased coin).

In this subsection, we evaluate the throughput, delay and reliability performances of the ALOHA-based network in the noise-limited regime. We show that dropping a small fraction of packets helps lessen the end-to-end delay (due to reduced queueing); however, it also results in a decreased flow throughput. We now provide a mean-field theory-based analytical framework for analyzing the TDR region of the wireless network.

Let ξ denote the packet dropping probability (or the bias of the tossed coins). In an arbitrary time slot $t \rightarrow t+1$, the following events can alter the configuration of node i.

1. If node i, $0 \leq i \leq N$ has a packet in its buffer,

   - it decides to drop its packet w.p. ξ.
   - it decides to transmit its packet w.p. $(1-\xi)q$ (product of the packet-retention and the contention probabilities), and the packet hops to node $i+1$ (if its buffer is empty) w.p. p_s.

2. If node $i-1$ $(1 \leq i \leq N+1)$ has a packet in its buffer, it chooses to transmit (w.p. $(1-\xi)q$), and its packet hops to node i (provided its buffer is empty) w.p. p_s.

In case 1), we have $\tau_i[t] = 1$ and $\tau_i[t+1] = 0$. Likewise, the occurrence of 2)

implies that $\tau_i[t] = 0$ while $\tau_i[t+1] = 1$.

Following 1) and 2), the evolution of the node configurations, τ_i for $1 \leq i \leq N$ takes the form

$$\begin{aligned} \Delta\tau_i[t] &= -\xi_i\tau_i - (1-\xi_i)q_i\tau_i(1-\tau_{i+1}[t])p_{s,i} \\ &\quad +(1-\xi_{i-1})q_{i-1}\tau_{i-1}[t](1-\tau_i[t])p_{s,i-1}, \end{aligned} \tag{5.5}$$

where $\Delta\tau_i[t] = \tau_i[t+1] - \tau_i[t]$, and $\{\xi_i,\, \xi_{i-1}\}$, $\{q_i,\, q_{i-1}\}$, and $\{p_{s,i},\, p_{s,i-1}\}$ are all independent Bernoulli random variable pairs with means ξ, q and p_s respectively. At steady state, $\mathbb{P}(\lim_{t\to\infty}\tau_i[t] = 1)$ becomes temporally stationary. In other words, $\mathbb{E}\lim_{t\to\infty}\Delta\tau_i[t] = 0$. From (5.5), this means that the set of equations,

$$-\xi\mathbb{E}\tau_i - (1-\xi)qp_s\left[\mathbb{E}\left[\tau_i(1-\tau_{i+1})\right] - \mathbb{E}\left[\tau_{i-1}(1-\tau_i)\right]\right] = 0,$$

$1 \leq i \leq N$, has a solution. To solve for the node occupancies, we employ the *MPA*[3], according to which the occupancies of the nodes are assumed to be uncorrelated[4], i.e., $\forall i, j, \mathbb{E}[\tau_i\tau_j] = \mathbb{E}\tau_i\mathbb{E}\tau_j$. Then, for $1 \leq i \leq N$, (5.5) simplifies to

$$p_s(1-\xi)q\big[\mathbb{E}\tau_{i-1}(1-\mathbb{E}\tau_i) - \mathbb{E}\tau_i(1-\mathbb{E}\tau_{i+1})\big] - \xi\mathbb{E}\tau_i = 0. \tag{5.6}$$

The steady state occupancies of nodes, $\mathbb{E}\tau_i$, $1 \leq i \leq N$ are evaluated by simultaneously solving this set of N non-linear equations, and may be performed numerically.

Figure 5.2 plots the numerically evaluated occupancies of the nodes in the

[3]The MPA is tight at small values of the 'effective' link reliability qp_s, and gets looser with increasing values of that product term [26].

[4]Since $\tau_i, \tau_j \in \{0, 1\}$, this also means that the node configurations are independent as $\mathbb{P}(\tau_i = 1, \tau_j = 1) = \mathbb{E}[\tau_i\tau_j] = \mathbb{E}\tau\mathbb{E}\tau_j = \mathbb{P}(\tau_i = 1)\mathbb{P}(\tau_j = 1)$.

ALOHA-based flow, for some values of the packet dropping probability ξ. As expected, observe that the node occupancies decrease with increasing ξ. The empirical (simulation-based) values are also shown, and they closely match the values obtained numerically.

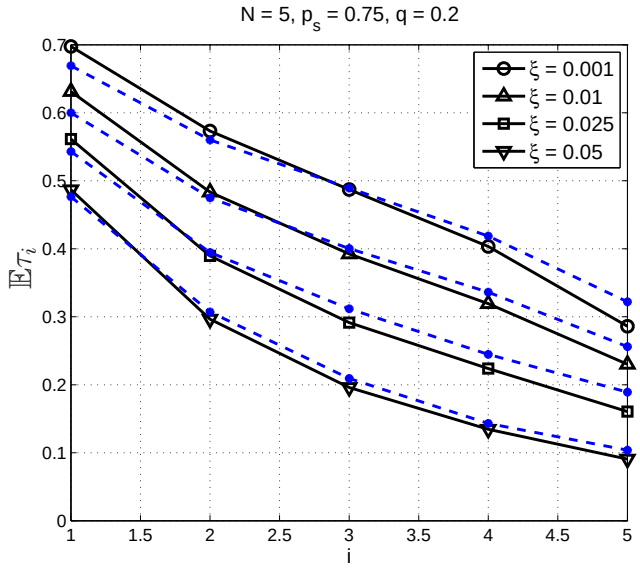

Figure 5.2. Values of the node occupancies (solid lines) for several values of ξ with $N = 5$ relays, obtained upon numerically solving the set of equations (5.6). Values obtained empirically (dashed lines) are also plotted, and are seen to closely match the values obtained numerically.

Asymptotics: When the number of nodes in the flow is large ($N \gg 1$), the set of non-linear equations (5.6) may be solved in closed form by explicitly considering the *quasi-continuum limit*. Accordingly, we fix the total length of the line network

to a constant l, and take the lattice spacing constant to be $\epsilon = l/N$. Thus, for $N \gg 1$, $\epsilon \ll 1$, and the rescaled nodal position variable $x_i = il/N = i\epsilon$, $1 \leq i \leq N$ (hence, $1/N \leq x_i \leq 1$) is quasi-continuous. Without loss of generality, we may take the constant $l = 1$.

From the Taylor series expansion for $\mathbb{E}\tau_{i-1}$ and $\mathbb{E}\tau_{i+1}$ in powers of ϵ, we obtain

$$\mathbb{E}\tau_{i\pm1} = \mathbb{E}\tau_i \pm \epsilon\partial\mathbb{E}\tau_i/\partial x_i + O(\epsilon^2). \tag{5.7}$$

Employing (5.7) in (5.6) and neglecting terms with quadratic or higher orders in ϵ, we obtain

$$\partial\mathbb{E}\tau_i\,(2 - 1/\mathbb{E}\tau_i) \approx K\partial x_i, \quad 1 \leq i \leq N,$$

where $K = \xi/\left((1-\xi)qp_s\epsilon\right)$. Integrating both sides, we get

$$2\mathbb{E}\tau_i - \ln\mathbb{E}\tau_i \approx \frac{\xi i}{(1-\xi)qp_s\epsilon} + C_i, \tag{5.8}$$

for some constants C_i, $1 \leq i \leq N$.

Note that setting $\xi = 0$ emulates the case wherein packets are never dropped ($R = 1$). Setting $\xi = 0$, we may write

$$C_i = 2\Delta_i - \ln\Delta_i, \quad 1 \leq i \leq N,$$

where we have from (5.2),

$$\Delta_i = \frac{(1-qp_s)\sum_{n=0}^{N-i} B(N-n)B(n) + qp_sB(N)}{B(N+1) + qp_sB(N)}.$$

Now, the solution to (5.8) is expressible in terms of the Lambert W function

[75] as

$$\mathbb{E}\tau_i \approx -\frac{1}{2}\mathcal{W}\left(-2\exp\left(-\frac{\xi i}{(1-\xi)qp_s} - C_i\right)\right), \tag{5.9}$$

where $\mathcal{W}(z)$ denotes the value of the Lambert W function at z. The Lambert W function, however, is a multi-valued function with two real branches, $\mathcal{W}_0$ and $\mathcal{W}_{-1}$. The branches merge at $z = -1/e$ where the Lambert W function takes the value -1 [75]. To evaluate (5.9), we need to choose the right branch of the Lambert W function. To this end, recall that the node occupancies monotonically decrease with proximity to the destination node (Section 2.6.1.2).

Let $\psi_i = -2\exp\left(-\left(K_i x + C_i\right)\right)$. Evidently, ψ_i is always negative and $\psi_i \uparrow 0$ as $i \to \infty$. Now, for $z < 0$, $\mathcal{W}_0(z)$ is an increasing function of z, while $\mathcal{W}_1(z)$ decreases with increasing z [75]. Noting that $\mathbb{E}\tau_i$ is be a decreasing function of i, it is possible to show after some manipulations that

$$\mathbb{E}\tau_i = \begin{cases} -1/2\mathcal{W}_{-1}(\psi_i) & \text{if } i \leq i^* \\ -1/2\mathcal{W}_0(\psi_i) & \text{if } i > i^*, \end{cases} \tag{5.10}$$

where i^* is the smallest value of i that satisfies $\phi_i < \phi_{i+1}$, i.e.,

$$i^* = \arg\min_i \psi_i.$$

Figure 5.3 depicts the analytically obtained values of $\mathbb{E}\tau_i$ in a long network ($N = 20$) (5.10) for several values of the packet dropping probability ξ.

End-to-end Delay, Throughput and Reliability: We now derive analytical expressions for the throughput, end-to-end delay and reliability in terms of the steady state node occupancies, for the general case ($R < 1$).

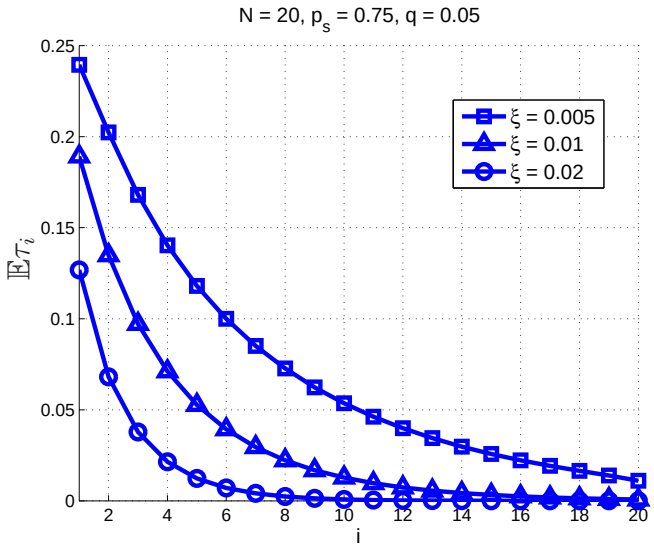

Figure 5.3. Analytical approximation of the occupancies of nodes (5.9) in a long ($N = 20$) flow with $p_s = 0.75$ and $q = 0.05$.

Proposition 10. *For a (typical) ALOHA-based flow along N relay nodes, we have the following.*

(a) The steady-state throughput is

$$T = qp_s\mathbb{E}\tau_N. \tag{5.11}$$

(b) The delay experienced by a packet at the i^{th} node, $0 \leq i \leq N$, follows a geometric distribution with parameter

$$s_i = qp_s(1 - \mathbb{E}\tau_{i+1}). \tag{5.12}$$

Consequently, the mean end-to-end delay is

$$D = \sum_{i=0}^{N} \left(qp_s(1 - \mathbb{E}\tau_{i+1})\right)^{-1}. \tag{5.13}$$

(c) The end-to-end reliability of the network is

$$R = \prod_{i=0}^{N} \frac{s_i(1-\xi)}{s_i + \xi - s_i\xi}, \tag{5.14}$$

Proof: The proof of (a) is similar to the proof of Theorem 5. Indeed, as explained earlier, the probability that the packet at node N successfully hops to the destination in one time slot is $qp_s\mathbb{E}\tau_N$.

In order to prove (b), let us suppose that a packet arrives at an arbitrary node i, $0 \leq i \leq N$. The three events that need to occur in the following order for the packet to be able to hop to node $i+1$ successfully are:

(1) Node i transmits its packet.

(2) Node $i+1$ has an empty buffer.

(3) Node i's transmission is successful.

Since the node occupancies are assumed to be independent of each other (by the MPA), the probability of node $i+1$ having an empty buffer conditioned on the fact that a packet arrives at node i is still $1 - \mathbb{E}\tau_{i+1}$. The events (1), (2) and (3) are also clearly independent of each other, thus the probability that it hops successfully to $i+1$ in a time slot is

$$s_i = qp_s(1 - \mathbb{E}\tau_{i+1}).$$

Consequently, the delay experienced by a packet at node i is geometrically dis-

tributed with mean $1/s_i$.

We now derive (c), i.e., compute the fraction of packets successfully hopping from node i to $i+1$, $1 \leq i \leq N$. Suppose the packet stays at node i for n_i slots before hopping to node $i+1$. The reliability r_i across the link $i \rightarrow i+1$, is

$$r_i = (1-\xi)^{n_i} \tag{5.15}$$

From (5.12), we know that $n_i \sim \text{Geo}(s_i)$. Therefore, we get

$$r_i = \sum_{k=1}^{\infty} (1-s_i)^{k-1} s_i (1-\xi)^k = \frac{s_i(1-\xi)}{1-(1-s_i)(1-\xi)}.$$

The end-to-end reliability is simply $R = \prod_{i=0}^{N} r_i$, which is equivalent to (5.14). $\square$

Figure 5.4 depicts the achievable throughput, mean end-to-end delay and reliability values for a typical flow in the considered multihop network model for $p_s = [0.1, 0.2, \ldots, 0.9, 1]$, $q = 0.2$ and $N = 5$. The corresponding empirical values are also plotted (dashed lines), and are shown to closely match the analytical curves. We see that in the noise-limited regime, the average end-to-end delay may be reduced significantly by increasing the packet dropping probability. The trade-off is that increasing ξ also results in emptying some buffers in the network, thus the reliability and throughput performances of the multihop network deteriorate.

5.3.2 The Interference-limited Regime

Typically, the performance of multihop networks is limited not only by thermal noise but also by the interference in the network due to concurrent transmissions. We argue that in order to study this general case, it is sufficient to analyze the case where the system is purely interference-limited. Indeed, under the conditions of

Rayleigh fading, the success probability across a typical link in the PPP network is equal to the product of the Laplace transforms of noise and interference [58]. Since the Laplace transform of noise for any given value of Θ is independent of the occupancies of other nodes in the network (or equivalently, of the packet dropping process), the effective value of the link reliability (in the general case) is simply the link reliability for the interference-limited case scaled down by a constant factor. Thus, it is adequate to analyze the TDR performance for the interference-limited regime, and the results extend directly for the general scenario. In this section, we define the success probability (across a typical link) as $p_s = \mathbb{P}(\text{SIR} \geq \Theta)$, which critically depends on the occupancies of other nodes in the network.

5.3.2.1 Case 1: $R = 1$

We first consider the case with 100% reliability, i.e., all packets are retransmitted until successfully received. Recall from Subsubsection 5.3.1.1 that when $R = 1$, the product of throughput and mean end-to-end delay is equal to $1 + N/2$ (as a consequence of Little's theorem). Thus, the TD curve is a hyperbola along the $R = 1$ axis (equivalent to the plot in Figure 5.1).

5.3.2.2 Case 2: $R < 1$

Next, we consider the case where $R < 1$. Note that dropping a fraction of packets leads to a decreased intensity of interfering nodes in the network, thus the link reliabilities increase with increasing ξ. We now proceed to derive the success probability across a typical link.

To this end, suppose that the node occupancies for a typical flow at steady state are $(1, \mathbb{E}\tau_1, \ldots, \mathbb{E}\tau_N)$. The average number of potential interferers in each

flow is $1 + \sum_{i=1}^{N} \mathbb{E}\tau_i$. With δ being the density of source nodes (or flows) and q the ALOHA contention probability, it follows that the density of interferers is at most[5]

$$\lambda_{\mathrm{I}} \lessapprox \delta q \left(1 + \sum_{i=1}^{N} \mathbb{E}\tau_i \right). \tag{5.16}$$

Even though transmissions in the network are completely uncoordinated, the interference is actually spatially and temporally correlated owing to the presence of common randomness in the locations of nodes [65]. However, for analytical tractability, we make the relaxed assumption that the set of interfering nodes forms a PPP with density λ_{I}, which is actually quite reasonable at small q [65].

Substituting for λ_{I} in (3.23) using (5.16), we obtain the success probability across a typical link to be lower-bounded as

$$p_s \gtrapprox \left(\frac{(1-\delta)\phi}{(1-\delta)\phi + 2\delta q \left(1 + \sum_{i=1}^{N} \mathbb{E}\tau_i\right) c} \right)^n, \tag{5.17}$$

where the approximation is tight for small q.

The steady state occupancies of nodes, $\mathbb{E}\tau_i$, $1 \leq i \leq N$, may be obtained by simultaneously solving the set of N non-linear equations (5.6), where the value of p_s is as given by (5.17).

Figure 5.5 shows numerically obtained values (solid lines) of the node occupancies for $N = 5$, $n = 1$, $\phi = \pi/2$, $\gamma = 4$, $q = 0.2$ and $\Theta = 10$ dB, and several values of ξ. The corresponding empirical values (dashed lines) are also plotted, and they corroborate the values obtained numerically.

The throughput, delay and reliability performances of the multihop flow are

[5]This term is actually an upper bound, owing to the existence of relay nodes having multiple packets in its buffer (corresponding to several flows). The bound is tight for small q (when the density of interferers is small), or small δ (when the flows in the network themselves are sparse).

quantified using (5.11), (5.13) and (5.14) respectively, together with values of the node occupancies. Figure 5.6 depicts the TDR performances of the ALOHA-based line network versus ξ, in the interference-limited regime, for some values of the system parameters. We observe the following.

- When δ is small (for example, when $\delta = 0.05$), increasing the packet dropping probability ξ reduces the system throughput. However, as δ gets larger (for instance, when $\delta = 0.1$), dropping a few packets helps mitigate the interference, thus the link reliabilities increase, and the throughput across a typical flow improves (for example, at $\xi = 0.005$). As ξ increases further, the loss in throughput due to dropped packets exceeds the gain in throughput due to interference mitigation, and the throughput begins to fall. Indeed, there exists an optimum value of ξ that maximizes the throughput of the flow (which may be obtained numerically).

- As expected, with increasing ξ or decreasing δ, the mean end-to-end delay decreases; the reliability also suffers.

5.4 Summary

We considered a multihop wireless network consisting of several source-destination pairs communicating with each other in a completely uncoordinated manner. Employing the MPA, we presented a framework for computing the steady state node occupancies, and quantifying the network's TDR performance. As intuitively expected, we found that in the noise-limited regime, dropping a small fraction of packets in the network leads to a smaller end-to-end delay at the cost of reduced throughput, whereas, in the interference-limited scenario, dropping a few packets in the network can help mitigate the interference in the network leading to an in-

creased throughput. We also provided some empirical (simulation-based) results to corroborate the theory.

In conclusion, we view this work as an initial effort towards understanding the throughput, delay and reliability tradeoffs in multihop wireless networks. Extending the analysis in order to accommodate different source traffic models such as constant bit rate and Bernoulli, other MAC schemes such as CSMA and spatial TDMA, and more sophisticated packet dropping strategies such as those based on bounded delay and limited retransmissions are interesting directions for future work.

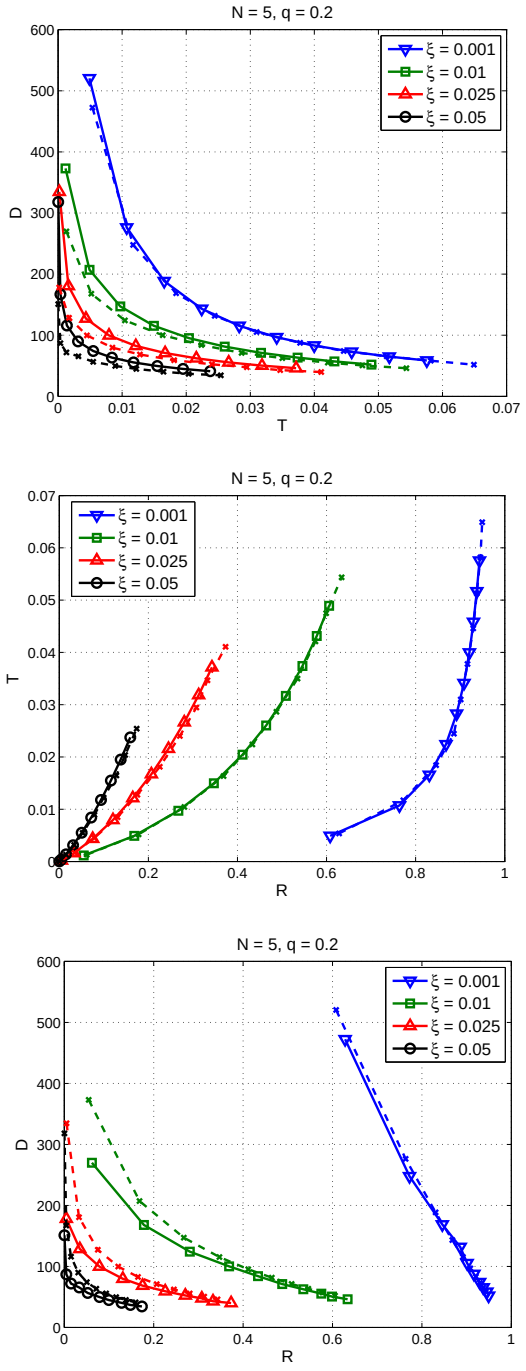

Figure 5.4: Analytically (solid lines) and empirically (dashed lines) obtained TDR Tradeoffs for an multihop network flow along $N = 5$ relays. In the noise-limited regime, increasing ξ helps reduce the end-to-end delay significantly, although the throughput and reliability performances worsen.

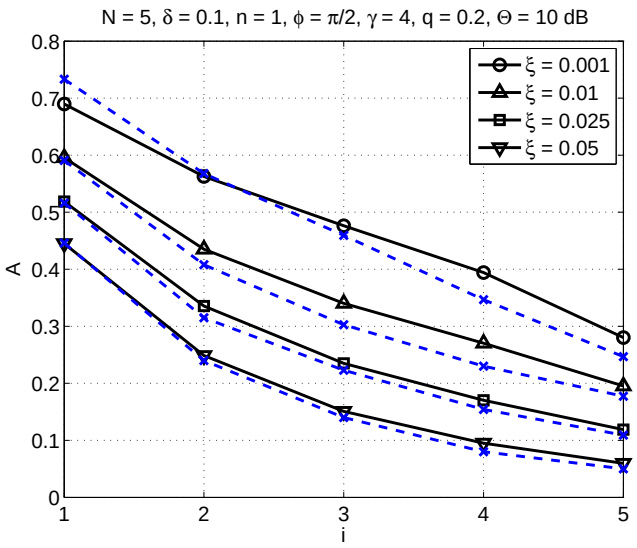

Figure 5.5. Values of $\mathbb{E}\tau_i$ obtained numerically (solid lines) using (5.6) for some system parameter values. The empirical values (dashed lines) are also plotted, and are seen to match the theoretical ones closely.

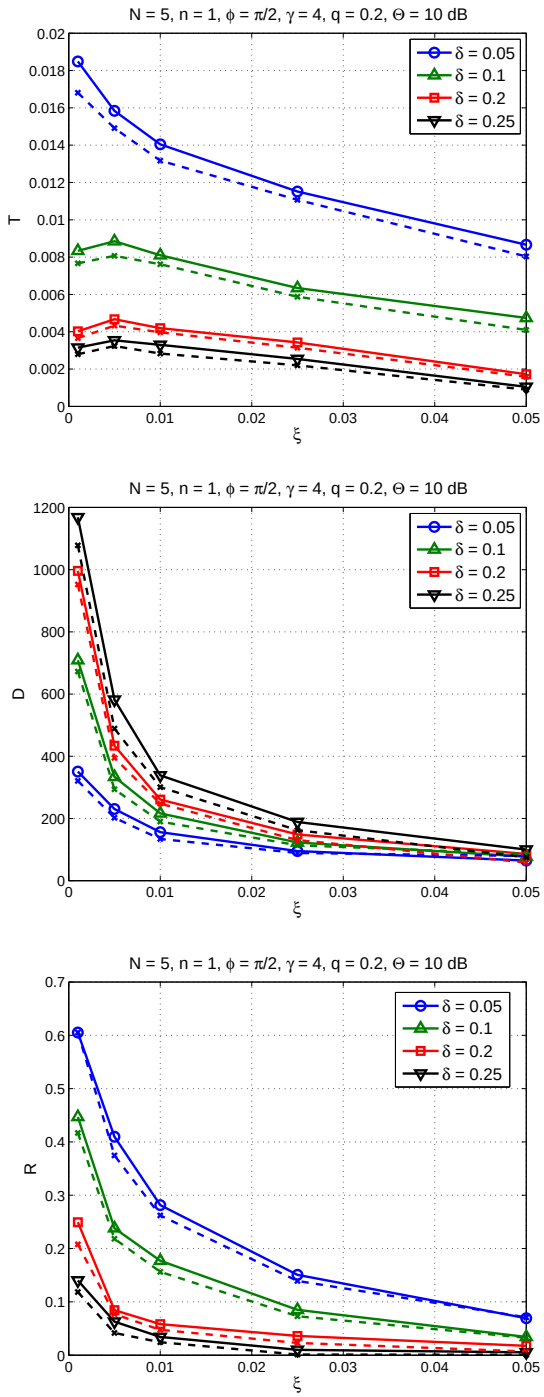

Figure 5.6: TDR performances of the ALOHA-based flow versus ξ, for $N = 5$, $n = 1$, $\phi = \pi/2$, $\gamma = 4$, $q = 0.2$ and $\Theta = 10$ dB. The empirical results (dashed lines) match the analytical ones(solid lines). Note that at high δ, dropping a small fraction of packets can actually help improve the system throughput.

BIBLIOGRAPHY

[1] C.-K. Toh, *Ad Hoc Mobile Wireless Networks: Protocols and Systems*, Prentice Hall, 2002.

[2] Y.-D. Lin and Y.-C. Hsu, "Multihop cellular: a new architecture for wireless communications," *IEEE INFOCOM*, Mar. 2000.

[3] J. G. Andrews, N. Jindal, M. Haenggi, R. Berry, D. Guo, M. Neely, S. Weber, S. Jafar and A. Yener, "Rethinking information theory for mobile ad hoc networks," *IEEE Communications Magazine*, Vol. 46, pp. 94-101, Dec. 2008.

[4] T. Cover and A. El Gamal, "Capacity theorems for the relay channel," *IEEE Transactions on Information Theory*, Vol. 25, No. 5, pp. 572-584, Sep. 1979.

[5] G. Kramer, M. Gastpar, and P. Gupta, "Cooperative strategies and capacity theorems for relay networks," *IEEE Transactions on Information Theory*, Vol. 51, No. 9, pp. 3037-3063, Sep. 2005.

[6] A. Goldsmith and S. B. Wicker, "Design challenges for energy-constrained ad hoc wireless networks," *IEEE Wireless Communications Magazine*, Vol. 9, No. 4, pp. 8-27, Aug. 2002.

[7] R. C. Alamino and D. Saad, "Statistical mechanics analysis of LDPC coding in MIMO Gaussian channels," *Journal of Physics A: Mathematical and Theoretical*, Vol. 40, No. 41, pp. 12259-12279, Oct 2007.

[8] K. Takeuchi and T. Tanaka, "Statistical-mechanics-based analysis of multiuser MIMO channels with linear dispersion codes," *Journal of Physics: Conference Series*, Vol. 95, Iss. 1, Jan. 2008.

[9] D. Guo and S. Verdu, "Randomly spread CDMA: Asymptotics via statistical physics," *IEEE Transactions on Information Theory*, Vol. 51, pp. 1261-1282, Apr. 2005.

[10] M. B. Hastings, "Statistical mechanics of interfering links," *Physics Review E*, Jul. 2005.

[11] M. Franceschetti and R. Meester, *Random Networks for Communication: From Statistical Physics to Information Systems*, Cambridge University Press, 2008.

[12] M. Haenggi, J. G. Andrews, F. Baccelli, O. Dousse, and M. Franceschetti, "Stochastic geometry and random graphs for the analysis and design of wireless networks," *IEEE Journal on Selected Areas in Communications*, Vol. 27, pp. 1029-1046, Sept. 2009.

[13] F. Baccelli and B. Blaszczyszyn, *Stochastic Geometry and Wireless Networks, Volume I and Volume II'*, NOW, 2009.

[14] M. Haenggi and R. K. Ganti, "Interference in large wireless networks," *Foundations and Trends in Networking*, Vol. 3, No. 2, pp. 127-248, 2008.

[15] J. G. Andrews, R. K. Ganti, M. Haenggi, N. Jindal, and S. Weber, "A primer on spatial modeling and analysis in wireless networks," *IEEE Communications Magazine*, Vol. 48, pp. 156-163, Nov. 2010.

[16] K. Stamatiou and M. Haenggi, "Delay characterization of multihop transmission in a Poisson field of interference," *IEEE/ACM Transactions on Networking*, 2011. Submitted.

[17] K. Stamatiou and M. Haenggi, "Random-access Poisson networks: stability and delay," *IEEE Communications Letters*, Vol. 14, pp. 1035-1037, Nov. 2010.

[18] J. G. Andrews, S. Weber, M. Kountouris, and M. Haenggi, "Random access transport capacity," *IEEE Transactions on Wireless Communications*, Vol. 9, pp. 2101-2111, Jun. 2010.

[19] M. Grossglauser and D. Tse, "Mobility increases the capacity of ad-hoc wireless networks," *IEEE/ACM Transactions on Networking*, Vol. 10, No. 4, pp. 477-486, Aug. 2002. *Ozgur* A. Ozgur, O. Leveque, and D. Tse, "Hierarchical cooperation achieves optimal capacity scaling in ad hoc networks," *IEEE Transactions on Information Theory*, Vol. 53, No. 10, pp. 3549-3572, Oct. 2007.

[20] F. Xue and P. R. Kumar, "Scaling laws for ad hoc wireless networks: an information theoretic approach," *Foundations and Trends in Networking*, Vol. 1, No. 2, pp. 145-270, 2006.

[21] S. Toumpis and A. J. Goldsmith, "Large wireless networks under fading, mobility, and delay constraints," *IEEE INFOCOM*, Mar. 2004.

[22] O. Leveque and I. E. Teletar, "Information-theoretic upper bounds on the capacity of large extended ad hoc wireless networks," *IEEE Transactions on Information Theory*, Vol. 51, No. 3, pp. 858-865, Mar. 2005. *Franceschetti2* M. Franceschetti, M. Migliore, and P. Minero, "The capacity of wireless networks: information-theoretic and physical limits," *IEEE Transactions on Information Theory*, Vol. 55, No. 8, pp. 3413-3424, Aug. 2009.

[23] U. Niesen, P. Gupta, and D. Shah, "On capacity scaling of arbitrary wireless networks," *IEEE Transactions on Information Theory*, Vol. 55, No. 9, pp. 3959-3982, Sep. 2009.

[24] L. Xie and P. R. Kumar, "A network information theory for wireless communication: scaling laws and optimal operation," *IEEE Transactions on Information Theory*, Vol. 50, No. 5, pp. 748-767, May 2004.

[25] S. B. Lowen and M. C. Teich, "Power-law shot noise," *IEEE Transactions on Information Theory*, Vol. 36, No. 6, pp. 1302-1318, Nov. 1990.

[26] N. Rajewsky, L. Santen, A. Schadschneider and M. Schreckenberg, "The asymmetric exclusion process: comparison of update procedures," *Journal of Statistical Physics*, Vol. 92, Nos. 1/2, pp. 151-194, Jul. 1998.

[27] S. Srinivasa and M. Haenggi, "The TASEP: a statistical mechanics tool to study the performance of wireless line networks," *IEEE International Conference on Computer Communication Networks*, Aug. 2010.

[28] S. Srinivasa and M. Haenggi, "A statistical mechanics-based framework to analyze ad hoc networks with random access," *IEEE Transactions on Mobile Computing*, 2011. Accepted.

[29] S. Srinivasa and M. Haenggi, "Combining stochastic geometry and statistical mechanics for the analysis and design of mesh networks," *Elsevier Ad Hoc Networks*, 2011. Accepted.

[30] S. Srinivasa and M. Haenggi, "Throughput-delay-reliability tradeoffs in multihop networks with random access," *Allerton Conference on Communication, Control and Computing*, Sep. 2010.

[31] I. F. Akyildiz, X. Wang and W. Wang, "Wireless mesh networks: a survey," *Computer Networks*, Vol. 47, Iss. 4, pp. 445-487, Mar. 2005.

[32] S. Xu and T. Saadawi, "Does the IEEE 802.11 MAC protocol work well in multihop wireless adhoc networks?," *IEEE Communications Magazine*, Vol. 36. Iss. 6, pp. 130-137, Jun. 2001.

[33] Z. Fu, P. Zerfos, H. Luo, S. Lu, L. Zhang and M. Gerla, "The impact of multihop wireless channel on TCP throughput and loss," *INFOCOM 2003*, Vol. 3, pp. 1744-1753, Mar./Apr. 2003.

[34] J. Li, C. Blake, D. S. J. De Couto, H. I. Lee, R. Morris, "Capacity of ad hoc wireless networks," *Proc. ACM International Conference on Mobile Computing and Networking*, pp. 61-69, Jul. 2001.

[35] L. Tassiulas, "Adaptive back-pressure congestion control based on local information," *IEEE Trans. on Automatic Control*, Vol. 40, No. 2, pp. 236-250, Feb. 1995.

[36] V. Gupta, "On the Effect of Transmission Delay on Estimation," submitted to *IEEE Transactions on Automatic Control*, Sep. 2009.

[37] B. Derrida, E. Domany and D. Mukamel, "An exact solution of a one-dimensional asymmetric exclusion model with open boundaries," *Journal of Statistical Physics*, Vol. 69, Nos. 3/4, pp. 667-687, Nov. 1992.

[38] G. Schütz and E. Domany, "Phase transitions in an exactly soluble one-dimensional exclusion process," *Journal of Statistical Physics*, Vol. 72, Nos. 1/2, pp. 4265-4277, Jul. 1993.

[39] K. Nagel and M. Schreckenberg, "A cellular automaton model for freeway traffic," *Journal de Physique I France*, Vol. 2, No. 12, pp. 2221-2229, Dec. 1992.

[40] B. Derrida, M. R. Evans, V. Hakim and V. Pasquier, "Exact solution of a 1D asymmetric exclusion model using a matrix formulation," *Journal of Physics A*, Vol. 26, No. 7, pp. 1493-1517, Apr. 1993.

[41] A. K. Elhakeem, R. Di Girolamo, I. B. Bdira, M. Talla, "Delay and throughput characteristics of TH, CDMA, TDMA, and hybrid networks for multipath faded data transmission channels," *IEEE Journal on Selected Areas in Communications*, Vol. 12, No. 4, pp. 622-637, May 1994.

[42] R. Nelson, L. Kleinrock, "Spatial TDMA: A collision-free multihop channel access protocol," *IEEE Transactions on Communications*, Vol. 33, No. 9, pp. 934-944, Sep. 1985.

[43] M. Xie and M. Haenggi, "Towards an end-to-end delay analysis of wireless multihop networks," *Elsevier Ad Hoc Networks*, Vol. 7, pp. 849-861, July 2009.

[44] N. Bisnik and A. A. Abouzeid, "Queuing network models for delay analysis of multihop wireless ad hoc networks," *Elsevier Ad Hoc Networks*, Vol. 7, Iss. 1, pp. 79-97, Jan. 2009.

[45] N. Ryoki, K. Kawahara, T. Ikenaga and Y. Oie, "Performance analysis of queue length distribution of tandem routers for QoS measurement," *Proc. IEEE Symposium on Applications and the Internet*, pp. 82-87, Jan./Feb. 2002.

[46] P. Gupta and P. R. Kumar, "The capacity of wireless networks," *IEEE Transactions on Information Theory*, Vol. 46, pp. 388-404, Mar. 2000.

[47] J. Abouei, A. Bayesteh, and A. K. Khandani, "Delay-throughput analysis in decentralized single-hop wireless networks," *IEEE ISIT*, June 2007.

[48] Y. Yang and T. S. P. Yum, "Delay distributions of slotted ALOHA and CSMA," *IEEE Transactions on Communications*, Vol. 51, No. 11, pp. 1846-1857, Nov. 2003.

[49] O. Dousse, "Revising buffering in CSMA/CA wireless multihop networks," *IEEE SECON*, June 2007.

[50] S. Bhadra and S. Shakkottai, "Looking at large networks: coding vs. queueing," *IEEE INFOCOM*, Apr. 2006.

[51] V. J. Venkataramanan, X. Lin, L. Ying and S. Shakkottai, "On scheduling for minimizing end-to-end buffer usage over multihop wireless networks," *IEEE INFOCOM*, Mar. 2010.

[52] L. Kleinrock, *Queueing Systems Volume I: Theory*, Wiley, 1975.

[53] M. Haenggi and D. Puccinelli, "Routing in ad hoc networks: a case for long hops," *IEEE Communications Magazine*, Vol. 43, pp. 93-101, Oct. 2005.

[54] M. R. Evans, N. Rajewsky and E. R. Speer, "Exact solution of a cellular automaton for traffic," *Journal of Statistical Physics*, Vol. 95, Nos. 1/2, 1999.

[55] M. Haenggi, "Outage, local throughput, and capacity of random wireless networks," *IEEE Transactions on Wireless Communications*, Vol. 8, pp. 4350-4359, Aug. 2009.

[56] M. Haenggi, "On routing in random Rayleigh fading networks," *IEEE Transactions on Wireless Communications*, Vol. 4, No. 4, pp. 1553-1562, Jul. 2005.

[57] E. S. Sousa and J. A. Silvester, "Optimum transmission ranges in a direct-sequence spread-spectrum multi-hop packet radio network," *IEEE Journal on Selected Areas in Communications*, Vol. 8, pp. 762-771, Jun. 1990.

[58] F. Baccelli, B. Błaszczyszyn and P. Mühlethaler, "An ALOHA protocol for multihop mobile wireless networks," *IEEE Transactions on Information Theory*, Vol. 52, No. 2, pp. 421-436, Feb. 2006.

[59] F. Baccelli, B. Błaszczyszyn and P. Mühlethaler, "Stochastic analysis of spatial and opportunistic ALOHA," *IEEE Journal on Selected Areas in Communications*, Vol. 27, Iss.7, pp. 1105-1119, Sep. 2009.

[60] S. P. Weber, J. G. Andrews, X. Yang and G. de Veciana, "Transmission capacity of wireless ad hoc networks with successive interference cancellation," *IEEE Transactions on Information Theory*, Vol. 53, No. 8, pp. 2799-2814, Aug. 2007.

[61] K. Stamatiou, F. Rossetto, M. Haenggi, T. Javidi, J. R. Zeidler and M. Zorzi, "A delay-minimizing routing strategy for wireless multihop networks," *Fifth Workshop on Spatial Stochastic Models for Wireless Networks (SpaSWiN)*, Jun. 2009.

[62] K. Stamatiou and M. Haenggi, "The delay-optimal number of hops in Poisson multi-hop networks," *IEEE Symposium of Information Theory (ISIT)*, Jun. 2010.

[63] K. Stamatiou and M. Haenggi, "Optimal spatial reuse in Poisson multi-hop networks," *IEEE Global Communications Conference (GLOBECOM)*, Dec. 2010.

[64] M. Haenggi, "On distances in uniformly random networks," *IEEE Transactions on Information Theory*, Vol. 51, pp. 3584-3586, Oct. 2005.

[65] R. K. Ganti and M. Haenggi, "Spatial and temporal correlation of the interference in ALOHA ad hoc networks," *IEEE Communication Letters*, Vol. 13, No. 9, pp. 631-633, Sep. 2009.

[66] P. Parker and R. Cowan, "Some properties of line segment processes," *Journal of Applied Probability*, Vol. 13, No. 1, pp. 96-107, Mar. 1976.

[67] H. Daduna and R. Szekli, "On the correlation of sojourn times in open networks of exponential multiserver queues," *Queueing Systems*, Vol. 34, Nos. 1-4, pp. 169-181, Mar 2000.

[68] L. Galluccio and S. Palazzo, "End-to-end delay and network lifetime analysis in a wireless sensor network performing data aggregation," *IEEE GLOBECOM*, 2009.

[69] T. Jun and C. Julien, "Delay analysis for symmetric nodes in mobile ad hoc networks," *4th ACM Workshop on Performance Monitoring and Measurement of Heterogeneous Wireless and Wired Networks*, Oct. 2009.

[70] M. Xie and M. Haenggi, "A Study of the correlations between channel and traffic statistics in multihop networks," *IEEE Transactions on Vehicular Technology*, Vol. 56, pp. 3550-3562, Nov. 2007.

[71] A. E. Gamal, J. Mammen, B. Prabhakar and D. Shah, "Optimal throughput-delay scaling in wireless networks: part I: the fluid model," *IEEE Transactions on Information Theory*, Vol. 52, No. 6, pp. 2568-2592, Jun. 2006.

[72] M. J. Neely and E. Modiano, "Capacity and delay tradeoffs for ad-hoc mobile networks," *IEEE Transactions on Information Theory*, Vol. 51, No. 6, pp. 1917-1937, Jun. 2005.

[73] M. Xie and M. Haenggi, "Delay-reliability tradeoff in wireless networked control systems," *Workshop on Networked Embedded Sensing and Control (NESC)*, Oct. 2005.

[74] R. Vaze, "Throughput-delay-reliability tradeoff in ad hoc networks," *Sixth Workshop on Spatial Stochastic Models for Wireless Networks (SpaSWiN)*, Jun. 2010.

[75] R. M. Corless, H. H. Gonnet, D. E. G. Hare, D. J. Jeffrey and D. E. Knuth, "On the Lambert W function," *Advances in Computational Mathematics*, Vol. 5, pp. 329-359, 1996.